Tracking apoptosis and efferocytosis *in vivo* via novel genetically encoded probes

Michael Howard Raymond

B.S., University of South Carolina, 2010

A dissertation presented to the Graduate Faculty of the University of Virginia in Candidacy for the Degree of Doctor of Philosophy

Department of Neuroscience

University of Virginia

Abstract

Apoptosis and efferocytosis are central to maintaining homeostasis and implicated in numerous pathological conditions. Elucidation of these processes during development and disease will help further define mechanism, cellular identity and dynamics in vivo. To date, the identification and characterization of apoptotic cell death and clearance of apoptotic bodies is limited to histological markers, co-localization imaging, synthetic dyes, and antibodies. The lack of tools to monitor apoptosis and phagocytosis in vivo highlight the need for development of genetically encoded reporters.

To meet this need, we developed a genetically encoded dual fluorescent reporter, denoted 'CharON' after the Greek mythical character who ferries the recently deceased across the river separating the living from the dead, that can concurrently track both emerging apoptotic cells and their efferocytic clearance by phagocytes. Through use of CharON transgenic Drosophila, we track and validate the key steps of efferocytosis in vivo, and for the first time directly measure coordinated clearance of apoptotic corpses in a living organism. Using CharON, we are able to discern novel challenges macrophages face during efferocytosis in vivo. For instance, when macrophages are confronted with a dense field of apoptotic corpses in vivo, macrophages adopt a strategy which prioritizes debris uptake over corpse acidification and degradation. As a result of this expedited clearance, individual macrophages display huge variation in corpse burden, with additional consequences. When challenged with a necrotic wound, macrophages with high apoptotic corpse burden are impaired in necrotic debris uptake, despite migrating to the wound site. Furthering this idea, enforcing phagocyte 'eating limits' via modeling suggests that macrophages benefit from 'unrestrained' uptake and variable corpse burden, as the alternative of 'equal distribution' drastically increases clearance time. These findings suggest that macrophages 'gamble' or make a functional compromise, wherein they maximize clearance of developmental / homeostatic apoptosis that is occurring immediately, while potentially jeopardizing the ability to resolve future tissue damage. Collectively, these live tracking studies advance and unveil new concepts in macrophage efferocytosis in vivo.

As a follow up to CharON, we develop a second reporter, termed 'CharOFF', which is tailored for both time-lapse imaging and flow cytometry-based analysis of efferocytosis. This novel probe can detect internalization and phagosome acidification, permitting us to dissect these steps at a cellular and population level. Using the CharOFF probe, we develop a 'One-Dish' co-culture efferocytosis assay, which features an inducible death system for on-demand induction of apoptotic targets. This system can report efferocytosis of several target cell types,

demonstrating the wide applicability of CharOFF. Finally, we develop a ‘One-Dish, Multi-Target’ system termed ‘Dubbel’ which is able to track single and multi-corpse engulfment events. Using Dubbel we uncover interesting trends with regards to macrophage ‘priming’, whereby engulfment of a corpse enhances the ability of a macrophage to eat a subsequent corpse. Findings from these studies provide a foundation for elucidating the response of efferocytes during single and multi-corpse engulfment. Collectively, these data provide novel insights into apoptosis and efferocytosis in vivo based on new genetically encoded probes.

To Allison, Mom and Dad.

Acknowledgements

This dissertation would not have been possible without the unwavering support from family, friends and mentors. I have been fortunate to be able to pursue my academic interests due to those who have provided help, insight, motivation and levity at every stage of the journey. As a result, this small outward dent in the sphere of expanding knowledge is dedicated to those who have believed in me every step of the way.

To Allison, this dissertation is dedicated to you. You are the glue that holds our world together. Through thick and thin, your love, compassion, friendship, strength and toleration of my puns and corny jokes knows no bounds. At the end of long days you help put things in perspective and see the path forward for what otherwise seem like insurmountable challenges. You are the strongest person I know, and witnessing your relentless work ethic, bravery, and effort towards whatever you set your mind to has had a profound influence on me. We have been on countless adventures together, from 19,341 foot mountain peaks to home projects, and I'm thrilled about the path ahead of us.

To my family: Mom and Dad, thank you for instilling a sense of curiosity, creativity and passion for the world and its wonders. You always challenged me to think for myself, have a fearless sense of independence and work hard for whatever you want to achieve. Beyond wisdom and encouragement, your unwavering, unconditional support and love throughout my life has been a source of strength. This work is a reflection of what was taught to me, and I hope it fills you with joy. Steve, thank you for being a mentor and more importantly a great big brother. You served as a source of inspiration and motivation for my academic pursuits, always setting a high bar. Our shared sense of humor, and inside jokes, are always a welcome distraction from the grind of academic life. I just know that one of our inventions will make its way out of R&D one day.

To my extended family: Rosie and Stan, thank you for being a constant source of support and wisdom for Allison and I. Your generous hospitality of smoked meats, homemade pickles and famous oatmeal chocolate chip cookies was always comforting. Thank you for being excellent grandparents to Murph and always taking great care of him, he always looks forward to his stays at the mountain lodge and has developed excellent garden critter security skills over the years.

To Pedro, thank you for being a close friend over the years and always putting our friendship first. I was fortunate to have been in the same graduate class as you, and I'm certain that my experience would have not been the same if this weren't the case. From our coffee

banter, fantasy football, Saab stories, Shenandoah hikes and detailed investigations into Slimmy, Murph and Ginny, we have grown closer. I am excited for you and Kate's new adventures in Philly, and I look forward to whatever the future has in store.

To Ravi, thank you for your advice and guidance over the years. You always provided a degree of freedom and independence in the lab which was most welcome for my personal development. Your invaluable curiosity, enthusiasm and knowledge of science has been a driving force and a quality which I will take with me.

To the Edinburgh crew: Andrew, thank you for being an excellent collaborator throughout the entire CharON project. I greatly appreciate you taking the time to get me up to speed on *Drosophila* and your patience throughout the process. I look forward to our future collaborations and wish you the best in your next steps. Will, thank you for taking a 'gamble' on the project, it has been a pleasure getting to know you and I hope that we can all meet up for a pint soon.

To members of the lab: Scott, thank you for being an excellent friend both in and out of the lab. From lobster lunches to canoeing adventures we have had a lot of fun and I hope that it continues. Lucas, your friendship and mentorship during your all-too-brief stay was greatly appreciated. I hope that we can get together in the future to share several toasts and recount the numerous lab memories. Lisa, thank you for all your day-to-day help, and for keeping the lab in working order. Kristen, Sho and Justin, thank you for helping me get started during my first few years in the lab. Your shared scientific and academic wisdom made my journey much less rocky. Gamze and Turan, thank you for your help and I wish you the best. To other members of the lab, thank you for your scientific input and support over the years, I will be sure to keep in touch.

To my thesis committee: Chris Deppmann,Tajie Harris, Sarah Kucenas, and Hui Zong. Thank you for always providing constructive feedback on my project and pushing me to challenge myself. I believe that my progress as a scientist and dissertation were better because of your collective guidance. I hope that we stay in touch.

Coordination, challenges, and compromises in macrophage efferocytosis 1

Abstract 2

Acknowledgements 5

List of Figures 10

List of Tables 12

List of Abbreviations 13

Chapter I 15
1.1 A Brief History of Cell Clearance 15
1.2 Setting the table: Beginnings of the efferocytic process 15
1.3 Dinner Bell is Ringing: Signals between apoptotic cells and phagocytes 17
1.4 Utensils for Eating: Signaling during efferocytosis 19
1.4.1 Fork, Spoon, Knife, Chopsticks: The variety of tools for eating 19
1.4.2 Not one more bite: Negative regulation of efferocytosis 22
Figure 1.1: Stop, Engulfment Time: Engulfment Receptors 25
1.4.3 Rest and Digest: Post-engagement signaling during efferocytosis 27
Figure 1.2: Many ways to dine 28
Figure 1.3: Down the hatch: Digesting the meal 28
Figure 1.4: Seconds, anyone?: Maintaining homeostatic balance during efferocytosis 31
1.5 Can You Smell What the Macrophage is Cooking? 33
1.6 Cell death and cell clearance in the CNS 36
1.6.1 Identity of CNS Phagocytes 36
1.6.2 Cell Clearance in CNS Pathologies 40
1.7 Cell Death and Cell Clearance In Drosophila 44
1.7.1 Background and Signaling 44
1.7.2 Macrophage Mediated Cell Clearance within the Ventral Nerve Cord 46
1.7.3 Glial Mediated Cell Clearance within the Drosophila CNS 47
1.8 Current tools for studying phagocytosis, apoptosis, and future design 48
1.8.1 Current Tools available for Apoptosis Detection 48
Table 1.1: In vitro and in vivo sensors of apoptosis 50
1.9 Current Tools available for Acidic Environment Detection 51
Table 1.2: In vitro and in vivo sensors of pH 52
1.9.1 Chemical labeling for phagocytosis assays 53
Table 1.3: Chemical probes used to study efferocytosis 54
1.11 Publications arising from my work under Dr. Ravichandran 55

Chapter II 57
2.1 Abstract 57
2.2 Introduction 58

2.3 Material and Methods 59
2.3.1 In vitro cell death assays 59
2.3.2 In vitro live cell imaging engulfment assays 59
2.3.3 Plasmid construction 59
2.3.4 CharON expressing transgenic Drosophila generation 60
2.3.5 Imaging of Drosophila embryos 60
2.3.6 Image analysis 60
2.3.7 Lentivirus production, purification, and transduction 62
2.3.8 Drosophila heatmap generation 62
2.3.9 General pHlorina genetic construction methods and materials 62
2.3.10 pHlorina protein engineering 63
2.3.11 Imaging of pHlorina in cell culture for calibration of pH dependency 64
2.3.12 pHlorina in vitro characterization 65
2.3.13 In Silico macrophage efferocytosis 65
2.4 Results 66
2.4.1 Generation of 'CharON' to concurrently track both apoptosis and efferocytosis 66
Figure 2.1: Evaluation and engineering of a pH-Stable apoptosis reporter and RFP pH sensor 68
2.4.2 CharON visualises in vivo efferocytosis 72
Figure 2.2: Caspase and pH Activated Reporter, Fluorescence ON (CharON) detects apoptosis and efferocytosis In Vitro and In Vivo. 74
2.4.3 Macrophages prioritize corpse uptake over degradation 76
Figure 2.3: A macrophage efferocytic program is orchestrated during development to ensure removal and degradation of CNS corpses. 79
2.4.4 Macrophage prioritization of uptake results in corpse burden heterogeneity 82
2.4.5 Macrophages compromise between apoptotic and necrotic corpse uptake in vivo 84
Figure 2.4: Macrophage efferocytic heterogeneity during development 85
Figure 2.5: Evaluation of Apoptosis Probes, pH-CaspGFP 88
Figure 2.6: Evaluation of pH-CaspGFP in THP-1 and pHlorina expression in mammalian cells 90
Figure 2.7: In vitro evaluation of pHlorina during efferocytosis and CharON Drosophila expression during embryonic development 92
Figure 2.8: CharON fluorescent signature during development, efferocytic event tracking in vivo and embryonic macrophage dispersal 94
Figure 2.9: Pioneer Macrophage dispersal and efferocytosis, efferocytic burden across embryonic stages and Drosophila wounding model 96
Figure 2.10: In silico modeling of efferocytic burden with consumption limits 98
Table 2.1: Sequences of pHlorina, CharON and UAS-CharON 100
2.5 Discussion 102

Chapter III 104
3.1 Abstract 104
3.2 Introduction 105

3.3 Materials and Methods 106
3.3.1 In vitro cell death assays 106
3.3.2 In vitro live cell imaging engulfment assays 106
3.3.3 In vitro flow cytometry engulfment assays 106
3.3.4 Plasmid construction 107
3.3.5 CharOFF expressing transgenic Drosophila generation 108
3.3.6 Lentivirus production, purification, and transduction 108
3.4 Results 110
3.4.1: Generation of CharOFF for detection of apoptosis and efferocytosis in vitro 110
Figure 3.1: Development and evaluation of CharOFF for detection of apoptosis and efferocytosis in vitro 112
Figure 3.2: Evaluation of RFP-based apoptosis sensors, CaspRFP, and CharOFF fluorescent signature during efferocytosis 115
3.4.2 Macrophage corpse-priming occurs in a time dependent manner 117
Figure 3.3: Macrophage corpse-priming enhances efferocytosis in a time dependent manner 118
Figure 3.4: Evaluation of miRFP720-SEP engulfment and itBID induction of apoptosis. 120
Figure 3.5: Flow cytometry gating strategy for CharOFF in vitro efferocytosis assays 122
Table 3.1: CharOFF, CharOFF-ic9, CharOFF-itBID sequences 124
3.5 Discussion 127
3.6 Future Directions 128
3.6.1 Generation of additional CharON and CharOFF transgenics 128
3.6.2 Application and analysis 129
3.6.3 Extending our understanding of efferocytic compromise and coordination 131
References 133

List of Figures

Chapter I

Figure 1.1: Stop, Engulfment Time: Engulfment Receptors
Figure 1.2: Many ways to dine: Intracellular signaling during efferocytosis
Figure 1.3: Down the hatch: Digesting the meal
Figure 1.4: Seconds, anyone?: Maintaining homeostatic balance during efferocytosis

Chapter II

Figure 2.1: Evaluation and engineering of a pH-Stable apoptosis reporter and RFP pH sensor
Figure 2.2: Caspase and pH Activated Reporter, Fluorescence ON (CharON) detects apoptosis and efferocytosis *In Vitro* and *In Vivo*
Figure 2.3: A macrophage efferocytic program is orchestrated during development to ensure removal and degradation of CNS corpses
Figure 2.4: Macrophage efferocytic heterogeneity during development.
Figure 2.5: Evaluation of Apoptosis Probes, pH-CaspGFP
Figure 2.6: Evaluation of pH-CaspGFP in THP-1 and pHlorina expression in mammalian cells
Figure 2.7: *In vitro* evaluation of pHlorina during efferocytosis and CharON *Drosophila* expression during embryonic development
Figure 2.8: CharON fluorescent signature during development, efferocytic event tracking *in vivo* and embryonic macrophage dispersal
Figure 2.9: Pioneer Macrophage dispersal and efferocytosis, efferocytic burden across embryonic stages and *Drosophila* wounding model
Figure 2.10: *In silico* modeling of efferocytic burden with consumption limits

Chapter III

Figure 3.1: Development and evaluation of CharOFF for detection of apoptosis and efferocytosis *in vitro*
Figure 3.2: Evaluation of RFP-based apoptosis sensors, CaspRFP detection of apoptosis, CharOFF-ic9 induction of apoptosis and CharOFF fluorescent signature during efferocytosis

Figure 3.3: Macrophage corpse-priming enhances efferocytosis in a time dependent manner
Figure 3.4: Evaluation of miRFP720-SEP engulfment and itBID induction of apoptosis
Figure 3.5: Flow cytometry gating strategy for CharOFF *in vitro* efferocytosis assays

List of Tables

Chapter I:

Table 1.1: *In vitro* and *in vivo* sensors of apoptosis

Table 1.2: *In vitro* and *in vivo* sensors of pH

Table 1.3: Chemical probes used to study efferocytosis

Chapter II:

Table 2.1: Sequences of pHorina, CharON and UAS-CharON

Chapter III:

Table 3.1: Sequences of CharOFF, CharOFF-ic9, CharOFF-itBID

List of Abbreviations

Alzheimer's disease (AD)
Antigen Presenting Cells (APC)
Apolipoprotein E (APOE)
Apoptotic peptidase activating factor 1 (APAF1)
Autism spectrum disorder (ASD)
B-cell lymphoma 2 (BCL2)
B-cell lymphoma extra-large (BCL-xL)
Bcl-2 homologous antagonist killer (BAK)
Bcl-2-associated X Protein (BAX)
Bcl-2-like protein 11 (BIM)
BH3 interacting-domain death agonist (BID)
Bi-molecular Fluorescence Complementation (BiFC)
brain-specific angiogenesis inhibitor 1 (Bai1)
chemokine (C-X3-C motif) ligand 1 (CX3CL1)
cluster of differentiation 14 (CD14)
Cytochrome c (CYCS)
dedicator of cytokines 180 (DOCK180)
Endothelial monocyte-activating polypeptide II (EMAP II)
engulfment adaptor PTB domain (GULP)
Engulfment and cell motility protein 1 (ELMO1)
Fas associated via death domain (FADD)
Fas ligand (FasL)
Fas receptor (CD95)
Flow Cytometry (FACS)
Forster Resonance Energy Transfer (FRET)
Immunoreceptor tyrosine-based activation motif (ITAM)
Immunoreceptor tyrosine-based inhibitory motif (ITIM)
Inhibitor of apoptosis (IAP)
intercellular adhesion molecule 3 (ICAM-3)
lysophosphatidlycholine (LPC)
Mitochondrial outer membrane permeabilization (MOMP)
molecule milk fat globule-EGF factor 8 protein (MFG-E8)

Neural crest cell (NCC)

Neuronal precursor cell (NPC)

Nuclear factor kappa-light-chain-enhancer of activated B cells (NF-κB)

Oligodendrocyte Precursor Cells (OPC)

P53 upregulator modulator of apoptosis (PUMA)

Phosphatidylserine (P.S.)

Proto-oncogene tyrosine-protein kinase MER (MerTK)

Ras-related C3 botulinum toxin substrate 1 (Rac1)

Receptor-interacting serine/threonine-protein kinase 1 (RIPK1)

Retinal pigment epithelium (RPE)

Second mitochondria-derived activator of caspase (Smac)

Second mitochondrial activator of caspases (SMAC)

Stabilin-2 (Stab2)

Suppressor of cytokine signaling 1 (SOCS1)

T-cell membrane protein 4 (TIM4)

TNFRSF associated via death domain (TRADD)

Triggering receptor expressed on myeloid cells 2 (TREM2)

Tumor Necrosis Factor receptor superfamily of genes (TNF)

Tyrosine-protein kinase receptor (Tyro3)

Tyrosine-protein kinase receptor UFO (Axl)

X-linked inhibitor of apoptosis protein (XIAP)

Chapter I

1.1 A Brief History of Cell Clearance

Coined by Carl Clauss and later modified by Elie Metchnikoff, phagocytosis is a composite of the Greek words “phagein” for eating and “kytos” for cell, describing the active process of cellular engulfment [1]. This phenomenon was first observed in the late 19th century; however, it was not until the works of Metchnikoff that the importance of phagocytosis towards maintaining organismal integrity came to fruition. In many of his seminal works, which later earned him a Nobel Prize, Metchnikoff was captivated with the idea and significance of intracellular digestion of particles [2]. Building from his work, the phagocytosis field grew with the likes of Zanvil Cohn and James Hirsch from their work on granulocyte phagocytic activity, followed by a collective effort in uncovering distinct intracellular mechanisms involved in phagocytosis.

Prophetic for his time, Metchnikoff alluded to the possibility of “self-clearance”, noting that the amoeba could have the potential to selectively eliminate unnecessary cells. While the field’s early advances in phagocytic research centered on clearance of intracellular pathogens, clearance of apoptotic bodies, or “efferocytosis” [3], had yet to be fully appreciated for its role in ensuring efficient removal of apoptotic cells and maintaining tissue homeostasis [4]. In the next few sections I will summarize decades of work on cell death and cell clearance which has helped further our understanding of this essential biological process.

1.2 Setting the table: Beginnings of the efferocytic process

Stemming from the Greek term for “leaves falling from a tree” apoptosis is a programmed form of cell death that is characteristic in morphology and down-stream signaling events [5 6]. Divided into two main pathways, the intrinsic and extrinsic pathways, initiation of apoptosis has several modes that ultimately result in similar activation of apoptosis effector molecules.

The intrinsic pathway begins its signaling cascade through recognition of sufficient internal damage or organelle stress within the cell. Many of the insults which can prompt the initiation of the intrinsic pathway are, but not limited to, reactive oxygen species, DNA damage, endoplasmic reticulum stress and growth factor withdrawal [7 8]. The next step in the pathway is

the transfer of damage sensing to activation of BH3 family-member initiators of apoptosis. These members, such as Bcl-2-like protein 11 (BIM), P53 upregulator modulator of apoptosis (PUMA) and BH3 interacting-domain death agonist (BID), serve as a link between cellular stress and activation of the next step of key initiators in the pathway, Bcl-2-associated X Protein (BAX) and Bcl-2 homologous antagonist killer (BAK) [9]. This step in the intrinsic apoptosis pathway is irreversible and commits the cell to death. Two of these family members, BAX and BAK, insert themselves into the outer membrane of the mitochondria to form pores which allow the release of activating molecules from the mitochondrion [10]. While it has been appreciated that this step is irreversible, several other anti-apoptotic members of the BH3 family apply a brake to the process. B-cell lymphoma 2 (BCL2), B-cell lymphoma extra-large (BCL-xL) and other members of this class of BH3 family proteins are inserted into the membrane of the mitochondria and serve to inhibit pore formation via hindrance of pro-apototic members BAX and BAK oligomerization at the outer mitochondrial membrane [11].

Up to this point in the pathway, linkage between upstream initiators and downstream executioner molecules has not been completed. In order to tie the activation of pro-apoptotic BH3 family member proteins to fully-executed intrinsic apoptosis, contents from the permeabilized mitochondria must be released through the pore complexes to complete the transition. Two key molecules in this step are Cytochrome c (CYCS) and second mitochondrial activator of caspases (SMAC) [12]. CYCS, once released from the mitochondria into the cytoplasm, SMAC binds with apoptotic peptidase activating factor 1 (APAF). Upon oligomerization with CYCS, the apoptosome is formed which serves as a supramolecular scaffold for activation of initiator caspase, caspase-9. Packing the second punch in this process, SMAC is critical for sequestration of inhibitor of apoptosis (IAP) proteins via its IAP-binding properties [13]. Together, these two switches license the activation of caspase-9 and subsequent activation of the executioner caspases, caspase-3 and caspase-7, which initiate the canonical morphological and molecular signatures of apoptosis through substrate cleavage [14].

Extrinsic apoptosis is separate from that of intrinsic apoptosis in the initiation of the signaling cascade. Whereas intrinsic apoptosis is dependent upon internal damage signals, extrinsic apoptosis is initiated through the presence of external death receptor activation or absence of pro-survival ligands. A well studied family of receptors which are central to initiation of the extrinsic apoptosis pathway is the Tumor Necrosis Factor receptor superfamily of genes (TNF) and CD95. Both of these pathways exhibit similar mechanics for the initiation of the death process. Upon binding of their ligands, such as Fas ligand (FasL) for CD95, a death-inducing signaling complex is formed which recruits the extrinsic apoptosis initiator caspase, caspase-8.

These signaling complexes are the Fas associated via death domain (FADD) for FAS-mediated signaling or the TNFRSF associated via death domain (TRADD), respectively [15] [16]. Activation through the TNFRSF pathway involves several checkpoints which either promote apoptosis or pro-survival signaling. Acting through the recruitment of Receptor-interacting serine/threonine-protein kinase 1 (RIPK1) to the TRADD complex, several molecules ensure the stability of the signaling hub and activate both pro-survival and pro-inflammatory programs through nuclear factor kappa-light-chain-enhancer of activated B cells (NF-κB) activation [17]. As with many signaling events, it is the strength of the signal which determines whether survival or apoptosis is favored [18]. With sufficient activation and commitment to the apoptotic cascade, these complexes serve as signaling hubs for further downstream signaling events.

Upon transduction of ligand signaling to assembly of the death complexes, caspase-8 undergoes homodimerization and subsequent activation through an autoproteolytic mechanism [19]. While it might seem that upon activation of caspase-8 there is a commitment to apoptosis through subsequent activation of executioner caspases, caspase-3 and caspase-7, however commitment is dependent upon which type of cell is receiving the extrinsic apoptosis signal. Suppressors of apoptosis induction, such as X-linked inhibitor of apoptosis protein (XIAP), regulate the activation of executioner caspases in type 2 cells whereas type 1 cells do not require the activation of pro-apoptotic BH3 family proteins [20]. The intricate nature of the extrinsic apoptosis pathway appears to allow for flexibility through several redundant checkpoints in order to ensure that superfluous cell death does not ensue.

1.3 Intercellular signaling between apoptotic cells and phagocytes

Cells that undergo apoptosis must be cleared by phagocytes or risk undergoing secondary degeneration/necrosis and the resulting aberrant inflammation. The careful balance between cell death and cell clearance is integral to organismal development and tissue health through efficient removal and maintenance of an anti-inflammatory setting [21] [22]. The orchestrated nature of this process has led to seminal discoveries regarding how phagocytes locate apoptotic cells, initiate phagocytosis and maintain tissue homeostasis. Upon a cell undergoing apoptosis, there are several morphological and biochemical changes which occur within the cell. Hallmarks of an apoptotic cell, such as pyknotic nuclei, membrane blebbing and cytoskeletal breakdown are often associated with the programmatic nature of activated caspases cleaving several substrates which maintain cellular homeostasis [23] [24] [25].

Initial work on apoptotic released factors stemmed from the seminal observation that apoptotic cell supernatants exhibited a chemotactic effect on macrophages *in vitro*. Upon exposure to apoptotic stimuli, the authors noted that phospholipase A2 was regulated in a caspase-mediated manner to release the molecule lysophosphatidlycholine (LPC) into the media [26]. The role of LPC in attraction of phagocytes to apoptotic cells has been extensively studied, as well as putative G-protein-coupled receptor G2A, that function on the surface of phagocytes [27]. In addition to the role of G2A as a potential receptor involved in the migration of phagocytes to apoptotic cells, G2A plays a role in macrophage polarization as well as resolution of the apoptotic corpse [28 29].

In addition to morphological changes, activated caspases play a role in releasing factors which are sensed by surrounding phagocytes, alerting them to the presence of a dying cell, termed the “Find Me” stage of efferocytosis [30]. Endothelial monocyte-activating polypeptide II (EMAP II) has been demonstrated to be proteolytically processed and released from apoptotic cells in a caspase dependent manner [31 32]. EMAP II has properties which induce cellular migration, which is in-line with other apoptotic released factors [33]. Whether the precursor of EMAP II, p43, or EMAP II itself is the primary chemoattractant remains to be determined as an additional p43 caspase-mediated product has been identified [34]. It will be interesting to determine the precise role for all of these factors, as well as their role in disease as p43 has been identified as a factor which is upregulated within atherosclerotic lesions [34].

As this field has matured, additional factors have been implicated in the mechanisms by which apoptotic cells influence their environment. The fractalkine chemokine (C-X3-C motif) ligand 1 (CX3CL1) has been demonstrated to serve as an apoptosis-mediated factor which attracts phagocytes. Whereas other released factors function on their own, CX3CL1 was elegantly shown to attach to microparticles generated during apoptotic membrane blebbing and bridge with phagocytes [35].

Beyond the role of CX3CL1, nucleotides have been demonstrated to serve as second messengers to phagocytes during apoptotic cell clearance. The nucleotides adenosine triphosphate (ATP) and uridine triphosphate (UTP) were experimentally determined to be the nucleotides which are released in a Pannexin 1 mediated fashion [36 37]. The assembly and opening of the Pannexin 1 channel is regulated in a caspase-mediated manner, which serves to allow the passage of the nucleotides into the surrounding environment and induce macrophage migration. It is suggested that the primary candidates for nucleotide-mediated migration is through the P2Y and P2X, G-protein-coupled and ionotropic, purinergic receptors [38]. Extending beyond the role of Pannexin 1 in the release of nucleotides, Pannexin 1 has been elegantly

demonstrated to regulate the disassembly of apoptotic cells and release of metabolites which shape the tissue microenvironment [39] [40,41]. As our understanding of Pannexin 1 and nucleotides' role in serving as 'Find Me' signals improves, it will be imperative to further define the role of this channel during development and disease.

1.4 Utensils for Eating: efferocytosis ligands and receptors

1.4.1 Fork, Spoon, Knife, Chopsticks: The variety of tools for eating

Impressive in both quantity and scope, it has been estimated that our bodies turn over around 150 billion cells per day towards maintaining tissue health and homeostasis [42]. This process is highly orchestrated at both the tissue and molecular level, as our laboratory and others have demonstrated, involving numerous cell populations, receptors, and signaling pathways. While complex and distributed across many tissues, the mechanism of cell engagement and internalization has been well studied.

In tandem with the release of "Find Me" signals, the apoptotic cell has an additional role in ensuring its timely removal by exposing Phosphatidylserine (P.S.) on the outer leaflet of its plasma membrane [43]. Phosphatidylserine is exposed in a caspase-dependent manner, distinguishes viable cells from apoptotic cells and serves as a recognition and engagement molecule for a variety of phagocytosis receptors [44] [45].

Upon exposure of P.S., the phagocyte engages the apoptotic cell through a panoply of membrane receptors. The variety of receptors include brain-specific angiogenesis inhibitor 1 (Bai1), T-cell membrane protein 4 (TIM4), Stabilin-2 (Stab2), cluster of differentiation 14 (CD14) and the TAM family which consists of Tyrosine-protein kinase receptor (Tyro3), Tyrosine-protein kinase receptor UFO (Axl) and proto-oncogene tyrosine-protein kinase MER (MerTK) [46] [47] [48] [49] [50]. While diverse in structure and tissue-specific expression, P.S. receptors ultimately elicit a unified response. Upon activation with an apoptotic cell, P.S. receptors signal through downstream adaptor proteins to initiate engulfment.

Bai1, a member of the GPCR family, also known as Brain-specific Angiogenesis Inhibitor 1, was identified through a yeast two-hybrid screen for molecular binders of the critical engulfment regulator engulfment and cell motility protein 1 (ELMO1). This receptor is specific for binding of apoptotic cell membrane phosphatidylserine, and does interact with many other common membrane components. Downstream of activation, Bai1 engages directly with ELMO1, facilitating the engulfment of apoptotic cells [47]. To understand the potential roles for Bai1 in homeostasis and disease, a transgenic mouse overexpressing Bai1 in a colonic-specific manner

exhibited reduced disease in a mouse model of colitis [51]. The role of this receptor in the enteric system was also noted to be important during infection and clearance of apoptotic cells by gastric phagocytes [52]. Beyond the gut, Bai1 has been shown to play a role in the brain, where it is expressed in microglia, and functions to initiate phagosome formation for subsequent degradation of neuronal cell corpses [53]. It will be important to explore whether Bai1 plays an important role in other cell types and tissues during instances of normal cell turnover and disease.

TIM4 is a professional macrophage specific receptor expressed in Antigen Presenting Cells (APC) and Dendritic Cells. TIM4 exhibits specificity for phosphatidylserine and does not bind to other lipid membrane bilayer molecules [54]. Roles for this receptor in maintaining tissue homeostasis has been demonstrated in the peritoneum, where its expression on resident peritoneal macrophages was critical for preventing excess cellular accumulation and aberrant inflammatory responses [55] [48] . In addition, when TIM4 was depleted, along with the P.S. bridging molecule milk fat globule-EGF factor 8 protein (MFG-E8), mice display heighted production of autoantibodies and symptoms associated with autoimmunity [56]. Additional roles for TIM4 as a P.S. receptor will be interesting to watch develop, in addition to how this receptor might be therapeutically targeted for stimulating apoptotic cell clearance.

Stab2, a scavenger receptor expressed in many phagocyte subtypes, binds to many surface membrane molecules such as low-density lipoprotein, glycated products and P.S.. In its initial characterization, Stab2 displayed the ability to bind to both aged Red Blood Cells and Apoptotic Jurkat cells, as well as augment their internalization [57]. Opposed to several P.S. receptors which function downstream through the ELMO1/ dedicator of cytokines 180 (DOCK180) complex, Stabilin-2 has been shown to signal through engulfment adaptor PTB domain (GULP) [58]. A role for this receptor in maintaining homeostasis within the liver has been suggested, as Stab2 knockout mice display heightened accumulation of toxic metabolic products within the liver [50]. In addition to a potential role of Stab2 in liver homeostasis, Stab2 is highly expressed within macrophages and epithelial cells within atherosclerotic plaques [59]. Given the ability of Stab2 to bind to a variety of ligands and signal through an alternative downstream signaling pathway, it will be interesting to dissect the role of Stab2 in other disease states and cell death modalities.

CD14, first noted as a pattern recognition receptor, is a membrane-anchored monomeric receptor for both LPS and P.S., however to an extent it does not bind P.S. preferentially [60] [61]. CD14 has been demonstrated to serve as a phagocytic receptor in macrophages through engulfment of a variety of apoptotic targets, such as lymphocytes and neutrophils. Interestingly,

CD14 was suggested to display a preference for engulfment of lymphocytes over that of neutrophils [62 63]. In addition to having a bonafide role in clearance of apoptotic cells, CD14 has been shown to bind to a plethora of ligands, including intercellular adhesion molecule 3 (ICAM-3) on the surface of apoptotic cells [64]. Demonstrations of CD14's role in clearance of apoptotic cells in a disease or homeostatic state *in vivo* have yet to be formally investigated, however this receptor does appear to be important for the proper clearance of cells.

TAM family proteins, Tyro3, Axl and MERTK, are members of the receptor tyrosine kinase family of proteins. This family of proteins have been extensively investigated for their roles in innate immunity as well as direct roles in efferocytosis [65]. Opposed to many other P.S. receptor which directly engaged with the outer membrane of apoptotic cells, TAM family proteins engaged with bridging molecules Gas6 and ProteinS in a vitamin-K and calcium dependent manner [66 67 68]. These bridging molecules engage directly with P.S. on the outer leaflet of the apoptotic cell membrane and trigger TAM receptor binding and engulfment. Expression of TAM receptors throughout the body is diverse in magnitude and specificity. First evidence of the importance of these receptors was demonstrated through their role in removing aged or dying sperm within the testes as well as suppressing aberrant systemic inflammation [69 70]. In addition to the testes, the TAM receptor MerTK has been demonstrated to play a critical role within the Retinal Pigment Epithelium (RPE) where it serves to engulf rod outer-segments in a diurnal manner, which when abrogated results in a form of retinal degeneration [71 72]. In addition to serving an important role in the RPE, mice deficient in MerTK and Axl within microglia presented with an accumulation of apoptotic cells within the neurogenic niches of the CNS, where apoptotic cells are typically removed in a rapid manner in addition to impaired recovery from a mouse model of Parkinson's Disease [73]. Not just microglia are dependent on TAM receptor signaling, Astrocytes have been shown to be dependent on MerTK signaling for removal of synapses within the CNS [74 75]. Taken together, TAM receptors are prime candidates for evaluating the role of efferocytosis within homeostasis and disease, in addition to serving as potential therapeutic targets to boost clearance in settings of disease.

Another mechanism by which apoptotic cells are recognized through bridging molecules and internalized is through the complement binding to P.S. as well as Milk fat globule-EGF factor 8 (MFG-E8) [76]. Additional molecules such as complement, specifically C1q, has been demonstrated to bind to the P.S. and signal through CD91 on phagocytes [77]. Signaling through the CD91 receptor, which resembles the process of macropinocytosis, is an ancient form of cell and debris clearance which involves actin reorganization and internalization. In addition to the complement and CD91 pathway, the opsonin MFG-E8 is an additional bridging molecule which

serves to decorate the membrane of apoptotic cells and facilitate the engulfment through integrin alphavbeta5 and subsequent ELMO-Dock180-Rac1 signaling cascade [78] [60]. While several of the bridging molecules rely on calcium, MFG-E8 functions in a calcium-independent manner [79]. These molecules add another layer to the complexity and diversity by which apoptotic cells are engaged and disposed of. It will be exciting to determine when and in what context these molecules function, as well as how we could use these mechanisms for therapeutic benefit.

1.4.2 Not one more bite: Negative regulation of efferocytosis

While it may seem that receptor engagement with apoptotic cell ligands is a facile process, there are other factors which can negatively regulate the process of efferocytosis. Several of these factors serve to limit activation of receptors at the nexus between apoptotic cells and phagocytes through suppression of kinase activity or physical sequestration. CD44, a cell surface adhesion receptor, has been demonstrated to reduce receptor motility through formation of a glycosylaminoglycan barrier [80]. Furthermore, phosphatases such as CD45 and CD148 can serve to limit receptor activation. The physical removal of these signals from the interface between apoptotic cells and phagocytes is important for initiation of engulfment [81]. In sum, these phosphatases likely serve as a mechanism to gate the correct activation threshold for initiation of apoptotic cell internalization.

Adding another step of regulation to this process are cell surface inhibitory ligands, which reside on the target cell to effectively stave off engagement and engulfment. One of these 'Don't Eat Me' factors is CD47. CD47 engages with SIRPα on the phagocyte and initiates inhibitory signaling through recruitment of SHP-1 [82]. In addition, it has been suggested that the clustering of this receptor on the surface of the target cell functions to disrupt engagement by the phagocyte [83]. Upon the loss of this clustering, through apoptosis, the inhibitory signal is lost and phagocytosis can proceed. This signaling pathway has been utilized by cancers to avoid detection and removal by phagocytes, offering an attractive therapeutic angle to boost tumor clearance . Furthermore, this pathway has been adopted by neurons to avoid microglial-mediated synapse removal, exemplifying the conserved and important nature of this process in different tissue compartments [84]. It will be important to discover the threshold of CD47, in conjunction with P.S. exposure, which is sufficient to drive engulfment by macrophages .Furthermore, whether additional factors are required to overcome this engulfment blockade.

CD24 is a glycosylated GPI-anchored surface protein which is highly expressed by many tumors [85]. Mechanistically, when a phagocyte encounters this receptor on the target cell, signaling through Siglec-10 elicits a repressive signaling cascade through SHP-1 [86]. Building on these observations, when CD24 or Siglec-10 is inhibited, phagocytic function is restored in a mouse model of breast cancer and tumor burden is reduced [87]. These findings highlight another break on phagocytosis, and one which is expressed by many solid tumors.

B2M or MHC-1 has a well defined function in the adaptive immune system, however the role of B2M in innate immune cells is relatively less well studied. When screening for tumor expressed molecules which act as co-inhbitory signals with CD47, B2M was found to reduce anti-CD47 augmentation of phagocytosis. B2M was found to signal through LILRB1, and when this receptor was inhibited, phagocytosis was boosted and mice displayed reduced tumor volume [88] [89].

CD31 is expressed widely and serves as a tether for homophilic interactions between cells, such as migration of immune cells on the surface of endothelium. CD31 was identified as a 'Don't Eat Me" factor through identification of factors which serve as tethering molecules for viable and apoptotic cells. During apoptosis, CD31 is disabled, supporting engulfment of apoptotic cells by phagocytes [90]. It will be important to determine whether this live versus dead discriminatory feature is shared by different targets.

Whereas many of the "Don't Eat Me" signals described here are cell surface receptors, there are other ways in which a cell prevents engulfment. One of these mechanisms is through surface expression of sialic acid, a molecule which can decorate glycoproteins and glycolipids and increase their net negative charge. To suppress engulfment, these modifications are recognized by sialic acid-binding immunoglobulin type lectins which activate inhibitory signaling through SHP-1 [91]. In contrast, the absence of sialic acid promotes the binding of Galectin-3, which can function through MerTK to stimulate phagocytosis [92]. Interestingly, a lack of sialylation in the brain results in neuronal loss and microglial activation, thought to occur through over pruning of neurons [93]. One potential mechanism is through the increased binding of complement [94]. Furthermore, when the membrane is cleaved of these surface molecules, target cells can readily interact with phagocytes [95]. It will be important to discover how apoptosis modifies these surface residues to promote engulfment. In sum, these diverse mechanisms serve to govern the ability of phagocytes to engage and engulf various targets, likely serving to protect the tissue from unchecked efferocytosis.

Figure 1.1: The wide array of engulfment receptors

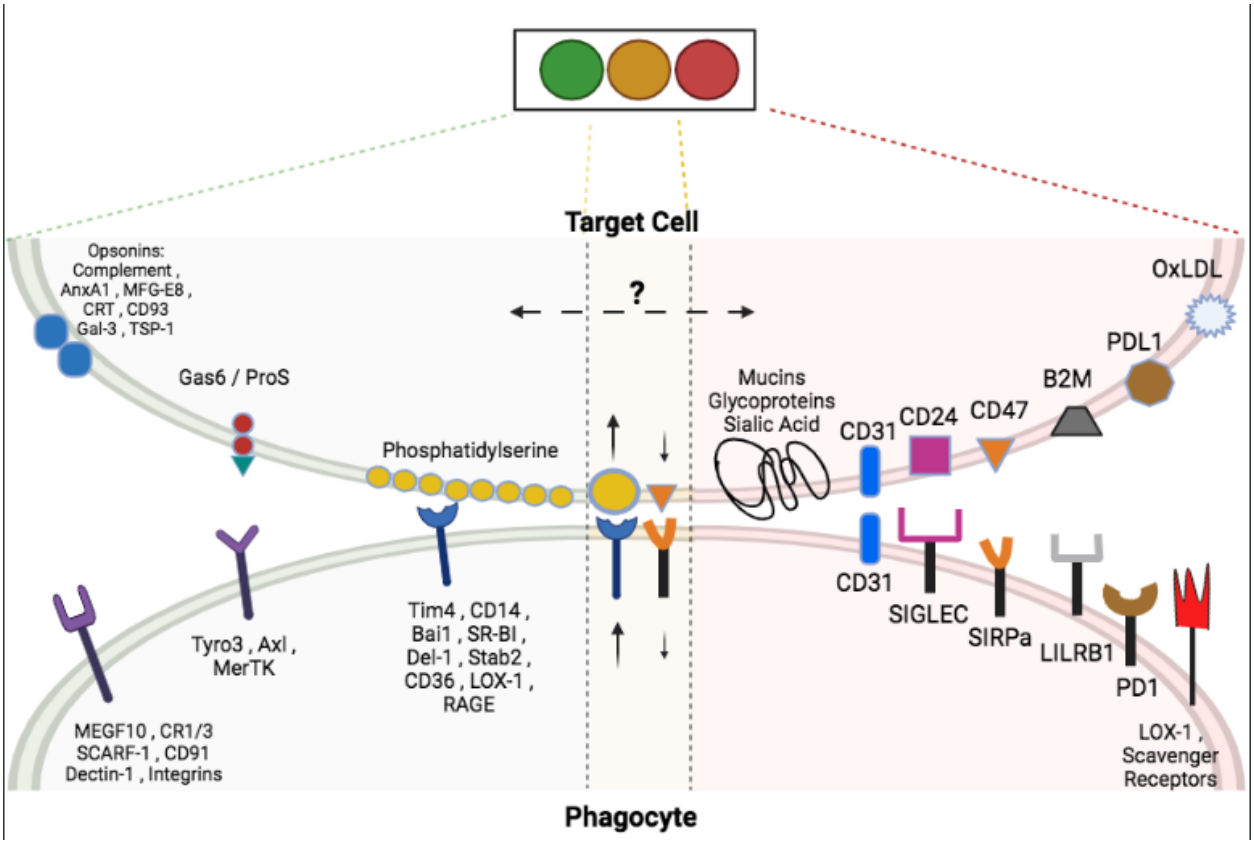

The interface between apoptotic cells and phagocytes includes many activating and inhibitory ligands. For target cells, “Eat Me” signals are displayed on the surface which are recognized by phagocytes. These signals include: Complement [77] [96], Annexins [97], MFG-E8 [98] [99], Calreticulin [100], CD93 [101], Galectin-3 [102], Thrombospondin-1 [103]. On the phagocyte side, there are many receptors which have been demonstrated to facilitate engulfment of apoptotic cells. To categorize these receptors, the mechanism by which they engage with the apoptotic cell have been categorized. Receptors which detect Opsonins on the apoptotic cell include: MEGF10 [74], CR1/CR3 [104], SCARF-1 [105], CD91 [77], Dectin-1 and Integrins [79] [97]. The class of TAM receptors which engage with apoptotic cells through the bridging molecules Gas6 and Protein S include Tyro3, MerTK and Axl [65]. Receptors which directly engage with P.S. include: Tim4 [54], CD14 [61], Bai1 [47], SR-BI [106], Del-1 [107], Stabilin-2 [57], CD36 [108] [109], LOX-1 [110] and RAGE [111].

In contrast, the apoptotic cell may display “Don’t Eat Me” signals which impede a phagocyte’s ability to engulf the target cell. These signals include: Mucins, Glycoproteins [95], Sialic Acid [93 94], CD31 [90], CD24 [87], CD47 [112], B2M [89], PDL1 [113 114] and Oxidized LDL [110 115].

These receptors and ligands are often displayed in concert which, depending on the presence and strength of the signal, mount a phagocytic response or stymie the process. One example by which “Don’t Eat Me” molecules can inhibit “Eat Me” signals is through clustering of CD47. At a critical threshold, during apoptosis, the clustering of CD47 is dispersed and phagocytosis can occur [83]. Furthermore, it appears that the ratio of inhibitory receptor and activation domains via CD47-SIRPα dictate the ability for engulfment to occur [116].

1.4.3 Rest and Digest: Post-engagement signaling during efferocytosis

In the final step towards apoptotic cell internalization, the phagocyte and the apoptotic cell physically engage at an immunological synapse (Figure 1.2). Focusing on the Bai1 pathway, upon engagement with the apoptotic cell, the phagocyte undergoes dynamic cytoskeletal rearrangement via downstream activation of Ras-related C3 botulinum toxin substrate 1 (Rac1) to facilitate ingestion of the apoptotic body. Of the known adaptor proteins that signal downstream of P.S. receptors, the ELMO1/Dock180 complex have been identified as key players [117]. On their own, DOCK180 and ELMO1 are unable to stabilize the nucleotide-free transition state of Rac1, however, as a protein complex they function as a bi-partite guanine nucleotide exchange factor to promote activation of Rac1 and subsequent cytoskeletal rearrangement. Highlighting the importance of these receptors and downstream signaling modules, numerous elegant studies have demonstrated the lack of these pathways results in worsened injury resolution, aberrant tissue development, and faulty cell clearance [51 53].

Figure 1.2: Intracellular signaling during efferocytosis

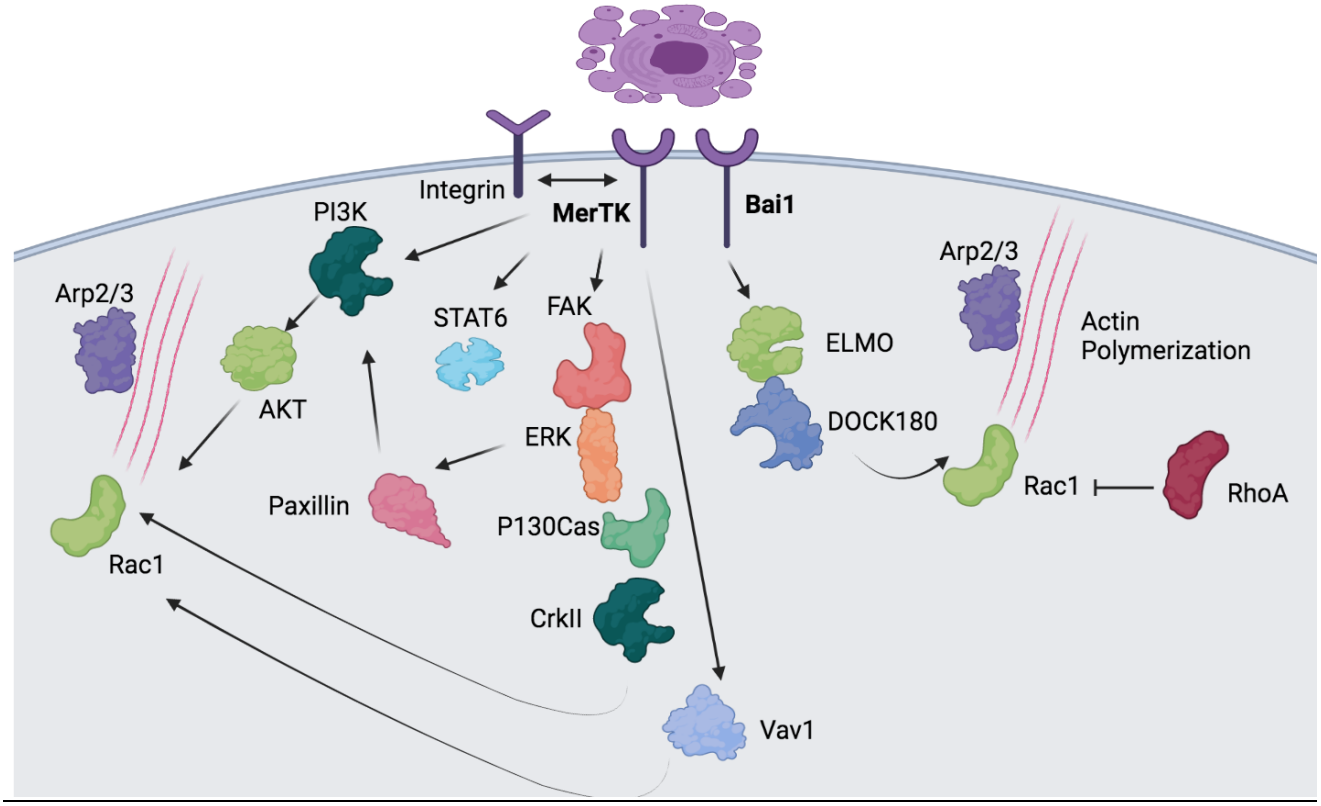

Upon receptor engagement, several pathways are engaged in order to facilitate engulfment of the target cell. Beginning with the receptor Bai1, upon engagement with P.S. through the thrombospondin domain of Bai1, ELMO is recruited and subsequently engages with DOCK180 through an SH3 domain [47]. Through the activation of Rac1, F-actin is formed at the cell edge in order to facilitate target engagement and internalization [118]. There are negative feedback loops which must be inactivated in order for the process to occur, such as removal of RhoA from the emerging phagocytic cup [119]. Signaling through MerTK shares many similar features, yet is distinct in many ways. Upon engagement with the apoptotic cell through bridging molecules such as Protein S and Gas6, MerTK is activated and signals through Integrin alphavbeta5 [120]. FAK, ERK, and P130Cas/CrkII to activate Rac1 and regulate actin polymerization [121]. Additional signaling nodes which may contribute to MerTK mediated engulfment include activation of an ERK-Paxillin-PI3K pathway [122] and Vav1 phosphorylation [123].

Figure 1.3: Down the hatch: Digesting the meal

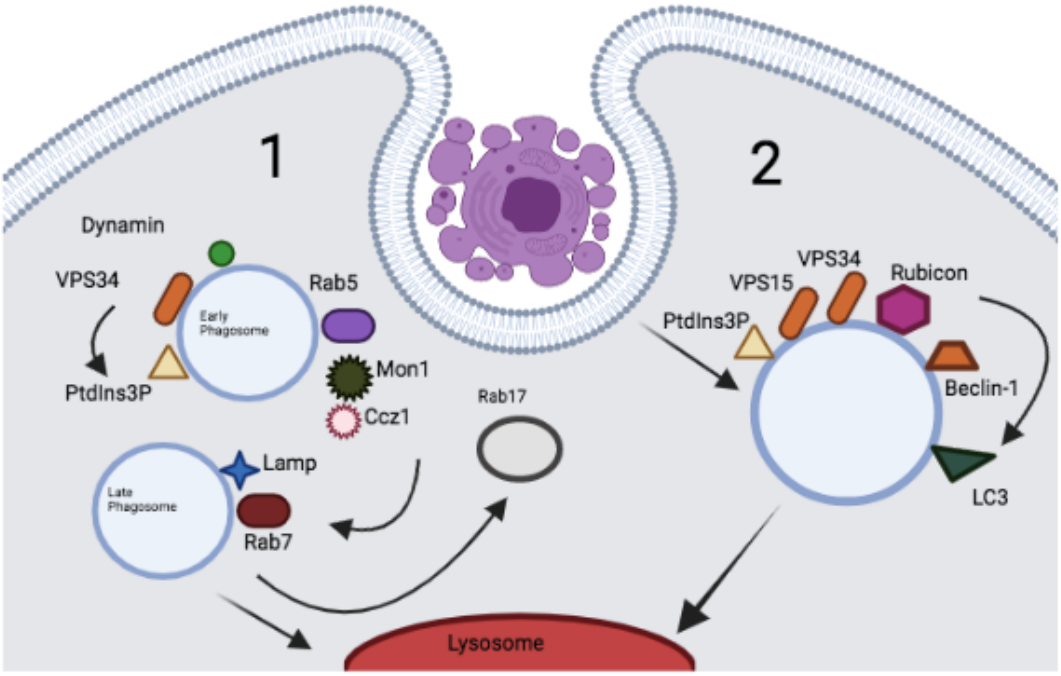

Upon engagement with the apoptotic cell, phagocytes must internalize and process the cargo. One of the pathways which has been well characterized is through the sequential RAB-mediated processing of the phagosome and fusion of the phagosome with the lysosome (Figure 1.3, (1)). Features of pathway include the initiation of PIP3 to the phagosome through VPS34, association of the phagosome with RAB5, recruitment and activation of RAB7 through Mon1-Ccz1, and finally lysosomal fusion [124] [125]. Alternative routes for cargo processing include the RAB17 recycling endosome, which limits the presentation of apoptotic-derived antigens from reaching MHC II processing and presentation [126].

A second route for apoptotic corpse processing is through LC3-associated phagocytosis (LAP) (Figure 1.3, (2)). To begin, PIP3 is localized to the phagosome through VPS34, VPS15, Beclin-1 and Rubicon. After deposition of PIP3, NOX2 is able to bind, generate reactive oxygen species, recruit LC3 associated components and ultimately fuse the LC3-containing phagosome with the lysosome. Defects within this pathway can contribute to lupus-like disease in mice [127] [128]. The LAP pathway is essential for establishing an anti-inflammatory milieu, as defects in this pathway result in increased type I interferon signaling and pro-inflammatory signaling in

macrophages [129]. Taken together, these two well-defined pathways permit the rapid and controlled disposal of internalized cargo, which when perturbed can result in a variety of disease states [130] [131]. It will be interesting to parse the differences in these two pathways, whether they are uniquely employed by specific phagocytes, and whether target identity or size can influence the routes of disposal [132].

Figure 1.4: Maintaining homeostatic balance during efferocytosis

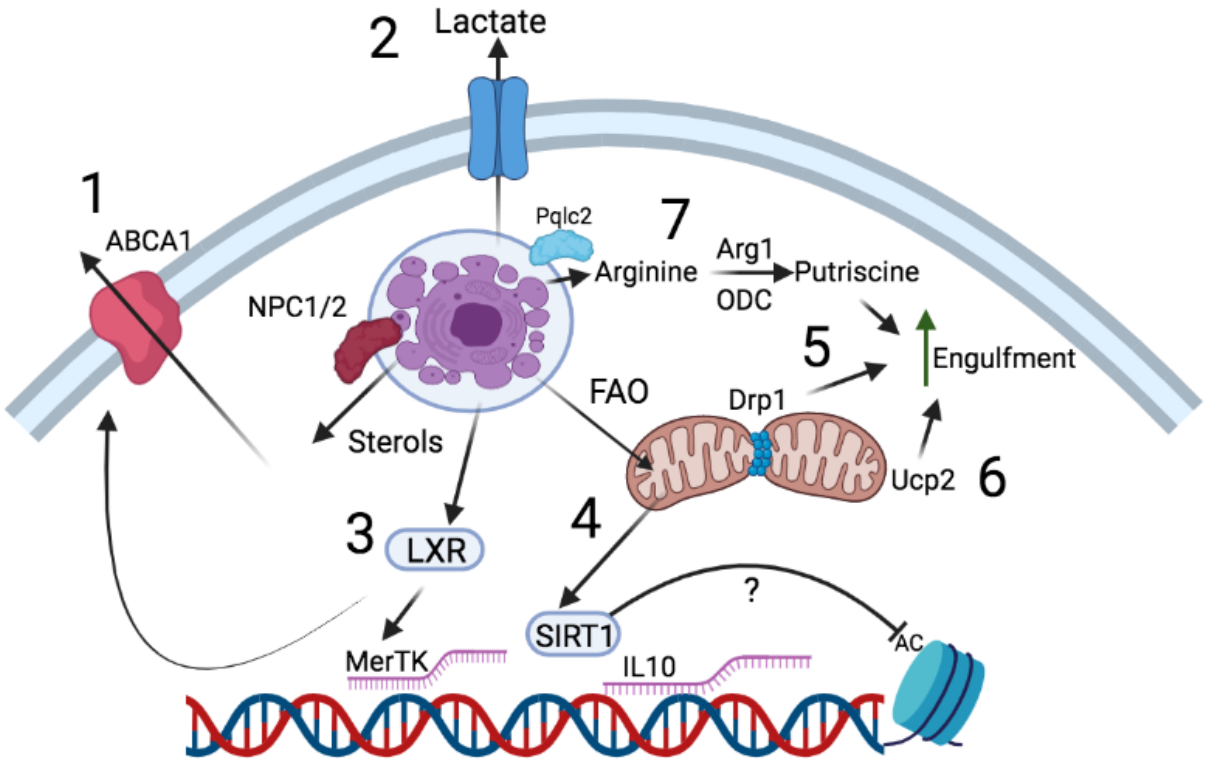

Phagocytes are often challenged with large quantities of apoptotic cells, which they must efficiently clear to prevent aberrant inflammation and maintain high levels of clearance. Phagocytes utilize several circuits which ensure that they are able to maintain their homeostasis during efferocytosis, such as efflux of cholesterol from the apoptotic cell through ABCA1 (**1**) [133] [134], acute activation of Glycolysis and efflux of Lactate (**2**) [135], sterol activation of LXR and upregulation of P.S. receptor MerTK (**3**) [136], utilization of Fatty Acid Oxidation for NAD+ mediated SIRT1 activation and IL-10 release (**4**) [137], Drp1 mediated mitochondrial fission for continued clearance (**5**) [138], Ucp2 mediated mitochondrial membrane potential uncoupling to promote continued clearance (**6**) [139], and catabolism of apoptotic cell derived Arginine to Putriscine for promoting second corpse uptake (**7**) [140]. All of these intricate circuits point to the myriad of ways in which phagocytes adapt to the increased metabolic load of ingesting an apoptotic cell. Several questions remain, such as: what is the limit of phagocytes during efferocytosis, how do phagocytes balance both Glycolysis and FAO to promote continued

clearance, does the activation of SIRT1 affect histone deacetylation [141], and do other transporters utilize additional substrates for maintaining efferocytic energetics?

1.5 Phagocyte anti-inflammatory signaling during efferocytosis

Once a cell undergoes programmed cell death, it must be cleared efficiently in order to avoid the execution of a secondary necrotic program which is pro-inflammatory (Figure 1.3, Figure 1.4) [142]. This process is impressive in scope, as it is estimated that billions of cells undergo programmed death and removal each day, and any perturbations to this mechanism could result in aberrant inflammation. Initial studies on macrophage mediated clearance of apoptotic cells identified several factors which are actively secreted into the surrounding environment to promote an anti-inflammatory milieu. In order to better characterize the ways in which macrophages shape their environment upon encountering an apoptotic cell, several studies have focused on the earliest steps within this process when apoptotic cells release their 'Find Me' signals.

Two common 'Find Me' signals have been characterized for their anti-inflammatory and pro-resolving nature when released from dying cells. Beginning with the 'Find Me' factor CX3CL1, several groups have found that exposure of cells to CX3CL1 mediates an anti-inflammatory environment. Specifically, CX3CL1 was found to suppress neuronal cell death as well as augment the ability of microglia to phagocytose debris [143]. The story is not always so straight-forward, as the excessive promotion of pro-resolving inflammatory programs can lead to negative consequences, such as those observed in the kidney where the receptor for CX3CL1 promoted fibrosis [144].

In addition to the well-defined 'Find Me' signal CX3CL1, the inflammatory nature of nucleotides which are released from apoptotic cells have also been characterized extensively. Upon release, nucleotides are sensed via purinergic receptors in phagocytes, as well as adenosine receptors A2A and A2B. Engulfing macrophages have been shown to upregulate A2A upon encountering apoptotic cells, and the loss of this receptor promoted pro-inflammatory skewing of macrophages in a peritonitis model as well as a zymosan model [145] [146]. The precise nature of how adenosine is generated through membrane ectonucleotidase enzymes, CD39 and CD73, during the process of efferocytosis will be important to uncover [147] . In addition, identification of the tissue specificity of this process, as the variety of tissue-resident macrophages are unique with respect to their apoptotic targets and tissue milieu, is an important question to address. Interestingly, the presence of apoptotic cells served to skew the macrophages into an anti-inflammatory phenotype in the presence of pro-inflammatory stimuli such as LPS, and only when anti-TGF-B antibodies were used did these macrophages revert to a pro-inflammatory state [21] [22].

The anti-inflammatory nature extends beyond the signals which are emitted by the dying cell. Upon engaging with an apoptotic cell, phagocytes modulate a variety of intracellular signaling programs to ensure that the apoptotic cell is disposed of and resolved in an efficient manner. In addition, macrophages actively remodel the environment to promote an anti-inflammatory environment through secreted factors [55]. Several studies have begun to dissect the importance of engulfment receptors for initiating this program and influencing the surrounding environment. Key observations were made through the loss of P.S. receptor TIM-4, where loss of this receptor led to the increased cellularity in the peritoneum, increased levels of TNFa, increased production of autoantibodies and increased apoptotic bodies [48] [127]. In addition, mice which lack TIM-4 downstream signaling components lead to the production of autoantibodies and increased production of pro-inflammatory molecules [57].

Beyond the very well characterized role of TIM-4 in resolving apoptotic corpses and initiating an anti-inflammatory environment, other P.S. receptors and their downstream processes influence the surrounding environment as evidenced by deficiencies in the Stabilin family, TAM family, CD300 family and Bai1 in mouse models. Upon direct engagement of Stabilin 2 with surface displayed P.S., macrophages upregulate TGF-B, as well as through the downstream signaling partner GULP [148] [149]. The well characterized TAM family of receptors has diverse roles in maintaining tissue homeostasis. Importantly, when phagocytes engage with an apoptotic cell through MerTK, downstream NF-κB signaling is repressed, in addition to suppression of STAT signaling and upregulation of suppressor of cytokine signaling 1 (SOCS1) [150] [151]. Serving as bonafide P.S. receptors, the CD300 family has been shown to be important for efficient clearance of apoptotic cells. For instance, CD300b engages with DNA-X Activation protein 12 (DAP12) and this signaling pathway has been shown to be important for inflammatory skewing of macrophages [152] [153]. In addition to CD300b, CD300a has been demonstrated to signal through its immunoreceptor tyrosine-based inhibitory motif (ITIM) during efferocytosis which is important for suppression of inflammatory signaling [51]. Following in line with P.S. receptor engagement and induction of downstream anti-inflammatory signaling modules, Bai1 was shown to be important *in vivo* for suppression of aberrant inflammation in the gut, as loss of this receptor led to the upregulation of an inflammatory phenotype within the gut and worsened gastritis in a DSS mouse model [154]. Receptor engagement, downstream activation and actin rearrangement are important for clearance, but also might influence macrophage polarization and tissue resolution through modulation of cell morphology [155].

Common to many of these signaling pathways is the upregulation of LXR-α/β which is triggered through the accumulation of cholesterol in macrophages during engulfment [136].

Interestingly, the accumulation of cholesterol from engulfed cells leads to an upregulation of engulfment receptors, thus providing a positive feedback loop to ensure that apoptotic cells are cleared [156]. A potential autocrine mechanism may exist through IL-10, as IL-10 macrophages preferentially clear apoptotic cells [137]. Furthermore, this circuit involves accumulation of sterols, increase in Th2 associated cytokines and promotion of proresolving mediators, along with use of apoptotic cargo triggered fatty acid oxidation [157] [136]. When this circuitry is disrupted, autoantibodies increase and symptoms associated with glomerulonephritis manifest within the kidney, in addition to a marked decrease in upregulation of canonical anti-inflammatory mediators such as TGF-β and IL-10 [158]. Furthermore, macrophages which frequently encounter apoptotic cells downregulate several nucleic acid sensing molecules, such as TLR9, dampening their ability to respond to potential non-self signals [159].

Additional evidence for the importance of efferocytosis triggered signaling is the upregulation of transcriptional programs through nuclear receptors upon corpse internalization. In addition to efferocytosis mediated LXR-α/β signaling, PPAR-δ is another nuclear receptor which has similar importance in establishing an anti-inflammatory phenotype following apoptotic cell engulfment. Cells which lack PPAR-δ fail to promote tolerance and skew towards an anti-inflammatory state [160] [140]. In addition to nuclear receptors, Arg1 is controlled by apoptotic cell derived signals such as L-arginine. Arg1 activation has been demonstrated to be important for continual clearance of apoptotic cells and anti-inflammatory signaling, as depletion of Arg1 reduced multiple corpse uptake and reduced digestive capacity through Rag-Ragulator activation [161] [162] [137]. In light of this evidence, it is tempting to speculate that apoptosis and efferocytosis are a critical circuit that is routinely executed in order to maintain tissue homeostasis within tissues, or even promote critical processes such as neurogenesis [163] [164]. Several lines of *in vitro* and *in vivo* evidence suggest that deficiencies in either the cell death or cell clearance process lead to exacerbated disease or initiation of disease. While much has been described, improvements in the ability to track apoptosis and efferocytosis *in vivo* will help in further defining this critical biophysical process as it occurs during homeostasis and disease.

1.6 Cell death and cell clearance in the CNS

The CNS is an active site of cell death and cell clearance, both in development and disease. In this section, phagocytes of the CNS and pathologies that arise from defects in clearance will be discussed. Neurodegenerative and neurodevelopmental disorders exhibit a wide variety of symptoms, and it is becoming increasingly aware that many of them share a common feature of neuronal dysfunction and cell death. Specifically, Alzheimer's Disease, Fragile X Syndrome and Parkinson's Disease are different in etiology, yet mounting evidence suggests that apoptosis and cell clearance mechanisms may play a critical role in disease progression.

1.6.1 Identity of CNS Phagocytes

Microglia

Arising from yolk sac progenitors and colonizing the CNS beginning at E9.5-10.5, microglia are the tissue-resident phagocytes who sense, respond and influence neural development [165] [166] [167] . These professional phagocytes arrive within the developing CNS before the onset of rapid neurogenesis within the cortex and display high heterogeneity [168] [169] [170]. Central to their function as professional phagocytes, microglia are critical for clearance of neuronal cells during development as well as postnatal neurogenesis [171] [172] [173] [53].This critical role has been well characterized in a variety of organisms, where colonization in the Zebrafish CNS coincides with waves of neural precursor apoptosis [174] [175]. As is commonly used to define a role for a cellular population, the removal of microglia from the CNS results in aberrant neuronal connectivity and increased abundance of neuronal cells during development and postnatal neurogenesis [176] [177] [178]. Emerging roles for microglia in clearance, and maintenance of neuronal integrity and connectivity, implicates microglia as both sentinels and sculptors within the CNS.

To begin, microglia express and employ a variety of receptors and downstream signaling cascades for engagement, internalization and clearance of neurons. Detailed transcriptional analysis of the cerebellum and developing white matter identified subsets of microglia which exist in a primed state to respond to high-levels of cell turnover [179] [73]. The transcriptional state and phagocytic receptor repertoire dictates how microglia respond to apoptotic cells. Elegant work has implicated the TAM (Tyro3, Axl, MerTK) family in microglia mediated clearance of apoptotic cells within the Sub-Ventricular Zone [53]. In addition, it appears that microglia use P.S.

receptors in a concerted effort to promote the steps of tethering and internalization of apoptotic cells [180]. Furthermore, microglia have been shown to promote cell death and subsequent clearance within the CNS, acting as both the initiator and resolver in the Efferocytic process [181] [182]. It will be exciting to uncover additional mechanisms by which microglia use single or combinations of P.S. receptors to remove dying cells, as a variety of forms of cell clearance are beginning to emerge. One of which is through microglia trogocytosis (partial engulfment) of synaptic boutons within the hippocampus [183].

We are beginning to appreciate the role of phagocytic microglia in shaping neuronal development beyond the physical removal of cells. Interestingly, secreted factors from phagocytic microglia have been shown to modulate the rate of neurogenesis and neuron survival [184] [185] [186] [187]. These works suggest that microglial processing of corpses serves as an important relay between the removal and maintenance of neurons. When this process is disturbed, such as through elimination of the gene SLC37A2, microglia displayed enlarged phagosomes and reduced corpse resolution [188]. Furthermore, microglia lacking IFNAR1 resulted in microglia with a similar phenotype, highlighting the importance and scope of the corpse disposal process [189]. Taken together, these multiple lines of evidence implicate microglia as primary phagocytes within the CNS and highlight the importance of microglial phagocytosis in shaping proper neuronal development.

Monocytes

Separate in location and origin, the function and ontogeny of non-parenchymal macrophages within the CNS is an area of intense investigation. CNS macrophages consist of meningeal macrophages, choroid plexus macrophages, perivascular macrophages and border associated macrophages [190] [191] [192]. Presence of monocytes within the different niches of the CNS is an area of active investigation, furthering our understanding of the ontogeny and characteristics of CNS monocytes [191] [190] [193]. In certain instances, reservoirs of monocyte-derived precursors can supply the CNS during experimental conditions and certain periods of development, which might give rise to additional layers of spatial and functional heterogeneity of the CNS macrophage compartment [194] [195] [196] [197] [198]. Interestingly, beyond the classical sources of monocytes, the meninges have recently been implicated as an active site of monocyte development with well defined roles in disease [199]. To date, the phagocytic role of monocytes within the CNS has been restricted to instances of injury or disease.

In many disease settings, monocytes are able to gain access to the CNS parenchyma in response to inflammatory cues [200]. Infiltrating monocytes have been shown to adopt an efferocytic transcriptomic signature and were confirmed to contain apoptotic material [201]. Not

restricted to response in ischemic stroke, monocyte derived macrophages play a beneficial role in a mouse model of intracerebral hemorrhage and mouse models of stroke. Monocytes were found to be critical for hematoma and erythrocyte clearance through P.S. receptors AXL and MerTK, when these receptors were absent the mouse had worsened recovery and impaired neurological function [202]. In addition, monocytes display the highest level of phagocytosis and participate in the recovery phase of a mouse model of stroke, with delayed recovery and larger infarct area when their STAT6-mediated efferocytic function is impaired [203] [204].

Future studies on relative phagocytic contribution between resident microglia and monocyte derived macrophages during development would be of great benefit to better understand to what extent and how these two professional phagocyte populations align and differ in their efferocytic roles.

Astrocytes

Well known for their supporting roles, Astrocytes are increasingly becoming a focus for neuroimmunology research as their functions within the CNS are better defined. The close apposition of Astrocytes to neuronal dendrites and spines, in addition to their expression of several phagocytosis-associated genes, prompted a closer look at their potential for neuron pruning and clearance.

Pioneering *in vivo* work from Tsai et. al brought forth the idea that regional disruption of Astrocytes altered the number of excitatory synapses, suggesting that beyond the other roles Astrocytes play, they are important for maintenance of circuitry [74]. Further evidence for Astrocyte involvement in synaptic regulation was evaluated within the developing dorsal Lateral Geniculate Nucleus (dLGN), where Astrocytes were found to have cleared presynaptic material. When phagocytic receptors MEGF10 and MerTK were ablated, there was a deficit in the phagocytic capacity of these Astrocytes. Interestingly, when Astrocytes were compared to Microglia in terms of their phagocytic potential, Astrocytes surpassed Microglia during later stages of dLGN developmental clearance [205]. This is an intriguing finding given the reduced corpse processing and acidification potential of Astrocytes and ability of Astrocytes to modulate microglial phagocytic activity [206] [75]. Beyond the dLGN, extensive analysis of Astrocytes within the Hippocampus later revealed that Astrocytes shape Hippocampal circuitry, with MEGF10 deficiency resulting in altered Hippocampal memory formation [207].

In addition to the role of Astrocyte-MEGF10 signaling in mediating synaptic clearance, MEGF10 has been shown to be important for clearance of apoptotic neurons within the developing cerebellum [208]. The extent to which Astrocytes are able to survey and sculpt both

neuronal circuitry and apoptotic cells implicates them as a primary phagocyte and candidate for future research in developmental cell clearance.

Oligodendrocyte Precursor Cells

Oligodendrocyte Precursor Cells are a specialized glia which arise from the neuroepithelium and populate the developing mouse brain from E12.5 to E15 [209]. Recent work using serial electron microscope evaluation within the visual cortex identified OPCs containing neuronal material, strengthening their case as a phagocyte *in vivo* [210]. Furthermore, OPCs have been shown to be capable of efferocytosis in a rat model of EAE [211] (Nguyen, 1997). More recently, using a sophisticated imaging and focal-ablation technique in mice, OPCs were observed to be capable of polarizing towards the site of neuronal apoptosis and extended processes into the spatial void [212]. These lines of evidence suggest that OPCs are capable of sensing and responding to cell death, however the extent to which they participate in homeostatic clearance is yet to be fully evaluated.

Neural Precursor Cells

Neural Precursor Cells (NPC) give rise to both mature neurons and glia during development. In addition, they were found to execute efferocytosis during mouse development within neurogenic niches. Their phagocytic potential was found to be dependent upon ELMO1, as ELMO1 deficient NPCs exhibited reduced efferocytosis [213]. Interestingly, as this population of cells resides within neurogenic niches, their proximity to developmentally generated apoptotic positions them well to respond and clear dying cells. Furthermore, it will be interesting to explore whether NPCs which are capable of efferocytosis form a unique population from their neighbors.

Neural Crest Cells

Neural Crest Cells (NCCs) play a central role during development, giving rise to many diverse and functionally distinct cell types. Roles of NCCs during development are wide ranging, highlighting their inherent plasticity and importance during this critical period. Remarkably, NCCs were identified as a primary phagocyte during Zebrafish development, exhibiting high levels of clearance and surveillance within the peripheral nervous system [214]. It will be important to further define the targets, response of NCCs to efferocytosis and whether the collective population or subsets of NCCs are capable of clearance.

Retinal Pigment Epithelium

Lining the rear of the retina is a specialized phagocyte, the retinal pigment epithelium (RPE), serves many roles one of which is responsible for engulfing photoreceptor rod outer segments (R.O.S) on a daily basis [72]. This clearance rhythm is necessary for retinal health, as defects in the P.S. receptor MerTK in RPE results in a progressive form of blindness [215]. Mechanisms by which a RPE engages with the R.O.S. is akin to phagocyte and apoptotic cell interactions [216] [217]. In particular, the RPE employs several distinct receptors including MerTK, Integrins and scavenger receptors [218] [219] [217]. Furthermore, R.O.S. display P.S. in a diurnal pattern, signaling the RPE to phagocytose them in an orderly and routine fashion. It will be important to uncover the totality of receptors which are important for R.O.S. clearance, as evidence suggests, simple substitution is not sufficient for proper function [220]. In addition, mechanisms by which RPE handle the significant metabolic burden from R.O.S. clearance will be important to tease apart for potential therapeutic intervention.

1.6.2 Cell Clearance in CNS Pathologies

Alzheimer's Disease

At the cellular level, Alzheimer's disease (AD) is characterized by extracellular b-amyloid (AB) plaques and intracellular neurofibrillary tangles [221]. The mechanisms by which these macromolecules contribute to neurotoxicity remains an open question, however evidence in both animal models and post-mortem human tissue suggests that apoptosis may contribute to the progressive neuronal loss during disease course [222] [223].

Using the 5XFAD mouse model of AD, early neuronal AB accumulation correlated with Caspase-3 staining within the pyramidal neurons [224]. Evidence for apoptotic neuronal loss in AD

is not restricted to mouse models. Through post-mortem analysis of human AD brains, Caspase-3 staining and morphological signs of apoptosis were detected in the hippocampus, frontal and entorhinal cortices [225] [226]. However, apoptosis is not the only form of neuronal cell death during AD progression, as other forms of cell death such as necroptosis have been suggested to contribute to cellular loss [227]. Taken together, mouse models and human subjects of AD suggest a role for apoptosis in AD, however the mechanisms and extent to which AD-associated pathology induces apoptosis have yet to be fully elucidated.

Serving as the resident macrophages in the brain, much work related to phagocytes in AD disease progression centers around the role of microglia [228] [229]. Numerous studies have demonstrated the impact of AD pathology on microglial activity, as well as microglial-associated mutations which increase Alzheimer's risk [230]. In addition, pathological hallmarks of AD, such as AB deposition, have been shown to increase the prevalence of aberrant neuronal synapse pruning by microglia through the complement system, further impairing neuronal function [231]. Not limited to synapse pruning, amyloid deposition was suggested to decrease the phagocytic capacity of microglia in brain slices from 5XFAD mice [232]. While there have been many significant advances in understanding underlying microglia in AD pathology, questions regarding alterations or impairment of other CNS phagocytes during AD progression remain unanswered.

Many genetic mutations or linkages to late-onset AD are within genes that are expressed in Microglia, underscoring the potentially important role these glial cells play in the pathology of AD and prompting elucidation of the identified genes and pathways in AD [233] [234]. In addition, rare mutations such as a loss of function mutation within the receptor TREM2 greatly contribute to AD progression in humans [235]. Several of these genes have roles in the process of phagocytosis, highlighting the potential link between cell clearance and AD progression such as triggering receptor expressed on myeloid cells 2 (TREM2), CD33 and APOE.

Beginning with TREM2, this receptor is highly expressed in microglia and has been demonstrated to bind to both AB, P.S. and Apolipoprotein E (APOE) which are ligands and targets present within the AD brain [236] [237]. Loss of this receptor results in clearance defects within microglia, and over-expression of this receptor in a mouse model reduced AB deposition [238] [239]. In addition, AD risk associated mutations within the receptor result in similar defects with regards to containment of AB plaques and removal of dead cells [240] [241]. Furthermore, presence of TREM2 in microglia shapes their response and results in microglia adopting a Damage Associated Microglia signature, which is present in many neurodegenerative diseases and has been shown to modulate AB deposition and clearance [242] [243]. It will be important to determine the beneficial or detrimental role of TREM2 in AD progression, as mouse models hint at

opposing phenotypes and disease progression when TREM2 is eliminated early or later during disease course [244] [245].

Recent evidence has implicated a role of CD33 in AD disease progression, with certain mutations linking to increased or decreased disease susceptibility [246] [247]. CD33, a member of the Sialic acid-binding immunomodulatory receptor family, and its risk variants have been shown to modulate the efficiency of AB engulfment as well as binding to C1q which interacts with AB [248] [249]. CD33 has been demonstrated to signal through both DAP12 and act upstream of TREM2, and loss of function of this receptor improved deposition of AB mouse models of AD. However, these loss of function of CD33 and TREM2 resulted in divergent skewing microglia, with absence of CD33 shifting microglia towards a more proinflammatory state which has been shown to be deleterious for AB clearance [250] [251]. Interestingly, CD33 expression and phagocytic function differ between human and mice, as loss of human CD33 increased engulfment, however loss of mouse CD33 did not [252]. It will be important to uncover the full extent of molecular interactions of CD33, as targeting this receptor could provide an avenue for therapeutic benefit.

Fragile X Syndrome

Fragile X Syndrome is a heritable cause of autism spectrum disorder (ASD), presenting as deficits in social proficiency, intellectual ability and numerous behavioral and neurological impairments arising from mutations within the FMR1 gene [253]. Cellular deficiencies in Fragile X patients and FMR1 mutant model organisms have been previously attributed to neuronal deficits. Specifically, immature synaptic outgrowths, aberrant synaptic plasticity and decreased neuronal apoptosis have been described [254]. In addition, decreases in the rate and location of apoptosis within the developing brain of FMR1 knockout mice were observed, potentially contributing to neuronal dysfunction [255]. Altogether, there is evidence to suggest a role for FMR1 in central nervous system development with regards to cell death and cell elimination.

As many of Fragile X studies focus on neuronal milieu, recent work suggests that FMR1 deficiency affects immune response and clearance [256]. Unexpectedly, when FMR1 was reduced in *Drosophila* glia and subjected to axotomy there was an increase in uncleared corpses and reduced glial uptake. In addition, there was a decrease in the rate of neuronal pruning during development, suggesting a role of defective clearance in a model of Fragile X, potentially through the regulation of Rac1 [257]. As FMR1 is known to regulate the mRNA translation, it will be interesting to define which mRNAs are regulated in a FMR1 dependent manner, and how these might function during the process of phagocytosis.

Beyond studies in *Drosophila*, there is evidence for the expression of FMR1 in several cell types in the mouse brain such as microglia and astrocytes which have been shown to possess clearance capability [258] [259]. Furthermore, altered neuronal structure with an increase in spine densities and reduced numbers of microglia are observed in FMR1 knockout mice. As these studies have demonstrated the important role of FMR1 in phagocytosis, it will be important to determine the cell-type specific role of FMR1 in development and uncover how FMR1 modulates phagocytosis in mammalian systems.

Parkinson's Disease

Parkinson's Disease (PD) is a progressive neurodegenerative disease which presents clinically as a loss of motor function with tremor, rigidity and instability. Pathologically, this disease is thought to progress through abnormal deposition of proteins such as alpha synuclein, resulting in the gradual death of dopaminergic neurons within the substantia nigra, the loss of which contributes to the motor deficits [260] [261]. While much has been discovered with regards to alpha synuclein and genetic contributions to PD, processes such as phagocytosis are emerging as a potential contributing factor and avenue for therapeutic intervention.

Microglia have been implicated in the progression of PD, largely thought to occur through their activation and subsequent damage or removal of neurons, such as those in the substantia nigra [262]. In addition to their putative role in promoting neuronal loss through aberrant inflammation, microglia are implicated in the phagocytosis of alpha synuclein which can either lead to improved or worsened outcomes [263] [264]. Furthermore, accumulation of alpha synuclein in microglia impairs their phagocytic activity which could enhance pathology, such as through transfer via exosomes [265] [73] . Linking PD pathology to P.S. receptors, it has been demonstrated that removal of P.S. receptors AXL and MERTK enhanced the lifespan in a mouse model of PD [266]. Taken together, it will be important to discern the pathways which regulate microglia removal of alpha synuclein, how toxic accumulation of alpha synuclein impairs microglial function, and contributions of other cells such as Astrocytes to disease progression [267] [268].

An emerging idea in PD research is phagocyte removal and killing of neurons. It has been previously shown that stressed or damaged neurons are removed by microglia [269] [270]. In a mouse model of PD, inhibiting the ability of microglia to phagocytose neurons reduced dopamine neuron loss [271] [272]. Furthermore, serum and monocytes from PD patients displayed enhanced phagocytic properties, underscoring the potential role of excessive phagocytosis in PD [273]. The potential role of phagocytes in potentiating PD, and what mechanisms govern the

tipping point which leads to phagocytosis, will be an interesting area of research to watch with therapeutic potential.

1.7 Cell Death and Cell Clearance In Drosophila

Drosophila have provided a foundational understanding of cell death and cell clearance pathways. Many of the same pathways used by *Drosophila melanogaster* macrophages are utilized by mammalian macrophages during cell clearance. In addition to the plethora of genetic studies and genetic tools that are available, *Drosophila* are visually transparent during early stages of development, offering a window into early developmental cell death and cell clearance. Many of these reasons prompted us to use *Drosophila* for testing CharON in an *in vivo* setting. In this section, I will review background, signaling, macrophage and glial mediated efferocytosis during *Drosophila* embryonic development.

1.7.1 Background and Signaling

Much of the foundational understanding of developmental cell death and cell clearance was discovered through the use of *Drosophila* as a model organism. Commonly referred to as the 'Fruit Fly', *Drosophila* emerged as a tractable and viable candidate for elucidation of development through the advocacy and foundational research of Thomas Morgan who quickly realized their potential as a model organism [274]. With quick gestational periods and relatively low-maintenance, *Drosophila* empowered developmental, molecular and genetic biologists to make great strides towards understanding fundamental phenomena. Key to our understanding of cell clearance pathways in *Drosophila* was extensions from the early work on mutants of the cell death abnormality (CED) family of proteins in *C. elegans.* This work demonstrated the importance of evolutionarily conserved apoptotic cell receptors and downstream actuators during development [274]. Similar to *C. elegans*, *Drosophila* are genetically tractable and amenable to live-imaging in order to understand biological processes such as efferocytosis signaling at the organismal level. During development, several tissues undergo extensive remodeling with a high rate of apoptosis which is subsequently cleared by the compartment-specific macrophages [275] [276]. In particular, three major phagocyte populations have been extensively studied in regards to their specialization, cells that they phagocytose and roles in development. These phagocytes are the central nervous system Glia, Hemocoel Hemocytes (Macrophages) and the Follicular Cells of the ovary [277] [278] [279].

Similar to other studies in different model organisms, the three stages ("Find Me", "Engage Me", "Digest Me") have been characterized in the *Drosophila*. Beginning with the

attraction of phagocytes to sites of apoptosis, “find-me” signals have not been fully elucidated in the *Drosophila* as extensively as they have in the mammalian system. However, evidence exists to implicate the production or release of H2O2 at sites of damage within the *Drosophila* as a chemoattractant for macrophages [280] [281]. Engagement of the macrophage with the apoptotic cell has been demonstrated to be critical for establishing proper wounding response . In addition, finely detailed analysis of macrophage engagement with apoptotic cells has unveiled distinct modes of process extension for proper clearance [282]. Phagocyte interactions with apoptotic cells have implicated three main apoptotic cell receptors which have been well characterized with respect to their cell-specific function and downstream signaling - Croquemort, integrin *βv* and Draper.

Starting with Croquemort, the mammalian CD36 homolog, which was first characterized in macrophages, has been demonstrated to be critical for clearance of apoptotic cells during embryogenesis [283] [284]. Furthermore, Croquemort appears to be specific to macrophages as loss of receptors within epithelial tissues did not have an overt phenotype, however defects within phagosome fusion were noted. In addition, lack of this receptor resulted in susceptibility to infection, suggesting that this receptor is important for engagement and clearance of bacteria [285]. In addition to the importance of Croquemort for hemocyte engagement with apoptotic cells, members of the integrin, specifically integrin *βv*, family have been implicated in macrophage-mediated clearance during development [286]. The Integrin *βv* receptor appears to have diverging downstream signaling to that of the receptor Draper, another key receptor which is critical for glial and macrophage efferocytic function. To start, Draper was identified to have a critical role within the CNS where it is primarily expressed on CNS Glia. The first noted cellular phenotype was its role in glial mediated clearance within the CNS, as a lack of this receptor resulted in the abundance of uncleared apoptotic corpses [287] [288]. Building on this work, it was later discovered that there is more than meets the eye with regards to Drapers role in apoptotic neuron clearance. A detailed study of Draper’s role in the developing CNS noted that the presence of uncleared apoptotic neurons was not a deficit in physical removal of the cells, but was attributed to a lack of digestion and processing of the ingested cargo. In addition, another molecule, Simu was implicated as an additional tethering receptor which acts in concert with Draper during development to remove apoptotic neurons [289]. Draper does not seem to have a preference for a certain target cell type, as a loss of Draper resulted in deficits within developmental pruning of the mushroom body, a process which involves similar mechanisms of apoptosis [290] [291]. Interestingly, Draper has a splice-variant which is not expressed in glia during the initial waves of neuronal apoptosis within the CNS. Draper-II differs structurally from that of Draper,

containing an ITIM instead of Draper's ITAM (immunoreceptor tyrosine-based activation motif), which serves to suppress the ability of Draper to activate downstream signaling and subsequent apoptotic cell removal [292] .

Downstream efferocytosis signaling pathways within *Drosophila* phagocytes are similar to those found in their mammalian counterparts, many of the same conserved proteins play a vital role in initiation of cell clearance. The three *Drosophila* genes crk, mbc and CED-12 are homologs to the mammalian counterparts crkII, DOCK180 and ELMO, respectively. Upon receptor recruitment through ITAM activation via src-mediated phosphorylation, these three proteins form a Rho-GEF complex which in turn activates Rac1 to facilitate actin rearrangement [293]. In addition to the crk, DOCK180 and ELMO pathway, new insights into alternative downstream signaling during efferocytosis has been elucidated through the role of Eato (CED-6) in its role in mammary gland remodeling by follicle cell phagocytes [294]. Taken together, *Drosophila* has furthered our understanding of both efferocytosis signaling and function during development, all of which is owed to the power of *Drosophila* as a model organism.

1.7.2 Macrophage Mediated Cell Clearance within the Ventral Nerve Cord

During *Drosophila* development, there is an abundance of apoptotic cell death in several regions as the organism shapes its tissues. One area which receives much attention with regards to cell death and cell clearance is the *Drosophila* Ventral Nerve Cord (VNC). The VNC is the ventral most region of the *Drosophila* embryo, composed of neural tissue that undergoes extensive remodeling as the organism takes shape [295]. Early work has identified much about the extensive cell death in this area, noting the high-rate of cell turnover around stages 12 to 16 [296]. It is thought that the majority of these cells belong to the classification of neuroblasts or ganglion mother cells. In order to define the extent of cell death, comparative studies between wildtype and apoptosis-mutant H99 flies, revealed that there was a wave of cell death constant through the early stages and peaked around stage 15-17 [297]. As with any tissue that exhibits a high level of cell turnover, it is the role of phagocytes to remove the corpses in order to ensure proper development and avoid aberrant inflammation [298] [299]. Within the ventral niche of the developing nerve cord, the major phagocytes are the mesoderm derived hemocytes, commonly referred to as macrophages.

Beginning in the anterior of the developing *Drosophila* embryo, the hemocytes or macrophages migrate through the tissue in a stereotypic manner. First, they travel a linear path from anterior to posterior, and upon tiling the mid-section of the embryo they begin their lateral movement towards the sides of the embryo. This orchestrated movement, and the factors which

are essential for proper migration such as VEGF, has been well characterized and coincides with the emergence of apoptotic cells [300]. In addition to the march of macrophages along their determined developmental routes, efferocytosis plays a critical role in establishing the identity and fitness of these cells to respond to damage. A seminal study which put forth this idea employed a variety of genetic methods to inhibit efferocytosis in order to determine the role of efferocytosis in macrophage priming for tissue injury response [288]. Intracellular signaling through JNK and upregulation of the P.S. receptor Draper was critical for establishing this priming phenomenon.

Within physiological systems, a balance is required for maintaining homeostasis, and shifts can induce profound consequences. In particular, one such study furthered the understanding of this priming phase through induction of apoptosis during VNC development, implicating the role of P.S. receptor Simu as a key player in regulating apoptotic cell clearance and subsequent response to tissue damage [301]. Extending the findings of cell clearance during *Drosophila* embryonic development will be critical to furthering our understanding of the intricate dance between apoptosis and efferocytosis. In particular, the *Drosophila* VNC can serve as an *in vivo* platform for genetic and chemical perturbations in order to determine cell intrinsic and extrinsic roles. While much has been uncovered, more fine-grained approaches and use of genetically encoded efferocytosis reporters such as CharON will be necessary to establish a deep understanding of macrophage and apoptotic cell interactions during this developmental period.

1.7.3 Glial Mediated Cell Clearance within the Drosophila CNS

Within the developing CNS, the high levels of neuronal turnover must be properly attended to by phagocytic glia in order to prevent neurodegenerative conditions [171 302 277]. Much like the mammalian CNS which has several different variants of glia which have unique structure, function and roles, *Drosophila* glia are specialized in their own right. Within the developing CNS there are six subtypes of glia, classified based on their location and functionality, they are named cortical glia, wrapping glia, astrocyte-like glia, perineural and subperineural. Out of these six different types of glia within the CNS, three of them have been shown to possess phagocytic ability, the ensheathing, cortical and astrocyte-like glia [303].

During *Drosophila* embryogenesis it is estimated that 30-40% of all newborn neurons die via apoptosis. Beginning early during development within the CNS, the majority of apoptotic cell clearance is done through cortical glia [302]. These cells are able to adapt to the high burden of apoptotic cells, and when these cells fail to clear the corpses in an efficient manner signs of

neurodegeneration have been reported [287]. While cortical glia are critical in shaping the early periods of development within the CNS, ensheathing glia and astrocyte-like glia are critical for the larval and metamorphosis stages [304]. Taken together, these phagocytic glia are functionally distinct yet have unique phagocytic attributes which are crucial for proper development of the organism.

1.8 Current tools for studying phagocytosis, apoptosis, and future design

1.8.1 Current Tools available for Apoptosis Detection

There has been much development in the space of genetically encoded fluorescent apoptosis reporters, bringing the possibility of dissecting dynamics of apoptosis *in vivo* one step closer to a reality. Many of these reporters rely on dynamic changes in fluorescence via Forster Resonance Energy Transfer (FRET), Bi-molecular Fluorescence Complementation (BiFC) or Subcellular localization of fluorescence.

To start, FRET relies on the energy transfer from a donor fluorescent molecule to an acceptor fluorophore. The difference in excitation and emission between these two molecules can be determined via FRET efficiency [305]. This process has been exploited to monitor caspase activity via placement of a caspase cleavage motif between donor and acceptor fluorescent proteins [306]. Upon caspase activation and motif cleavage, the FRET efficiency is reduced, a process which can be monitored via fluorescent microscopy or Flow Cytometry [307]. While the response of the reporter to caspase activity is rapid, on the order of minutes, evaluation of FRET signal *in vivo* can be difficult due to small fluorescent changes and cellular expression heterogeneity.

Rather than using a tandem pair of fluorescent proteins to monitor caspase activity, several probes have begun using BiFC to monitor apoptosis *in vitro* as well as *in vivo* [308] [309] [310]. Of note, recent developments in rationally designed de-novo protein cages have permitted the use of a single, split-GFP molecule to be used for caspase-3/7 detection. Both ZipGFP and FlipGFP rely upon caspase-3/7 cleavage and separation of a coiled-coil cage which sterically hinders GFP from associating and fluorescing in absence of apoptosis. Upon caspase activation, the cages are split and GFP is able to fold and mature, providing single-fluorophore detection of apoptosis *in vitro* as well as transient *in vivo* expression [311] [312].

Finally, rather than using whole-cell fluorescence as a read-out for caspase activity, three reporters have used extracellular and subcellular localization of fluorescent proteins to determine apoptosis. First, a group fused YFP to a secreted form of Annexin-V, labeling cells

which have exposed Phosphatidylserine upon apoptosis. This method has been demonstrated in both Zebrafish and Mice, however there is a high background signal [313] [314]. In addition, another group used the process of mitochondrial outer membrane permeabilization (MOMP) as a dynamic readout. Upon MOMP, second mitochondria-derived activator of caspase (Smac) is released from the inner mitochondrial space into the cytoplasm to sequester anti-apoptotic Xiap signaling. Using this step as a potential fluorescent reporter, Smac was fused to GFP to determine when this release occurs and monitor apoptosis [315]. Taking another approach, Bardet et al. tethered nuclear-localized GFP to the membrane via a caspase-3/7 motif containing linker [316]. When cut by caspase-3 or caspase-7, the nuclear-GFP translocates to the nucleus. Overall, these reporters are dynamic and rapid in their detection of executioner caspase activity, however *in vivo* analysis of apoptosis via localized fluorescence poses challenges due to inherent differences in cellular size, transparency and analysis of subcellular events [317].

An exhaustive list of these apoptosis reporters is described in the Table below, detailing the sensor type, fluorescence molecules used and whether the tool has been used in an *in vitro* or *in vivo* setting.

Table 1.1: *In vitro* and *in vivo* sensors of apoptosis

Name	Sensor Type	Spectra	*In Vitro*	*In Vivo*
SCAT	FRET (CFP/YFP)	CFP donor / YFP acceptor	+	+
INDIA	FRET	GFP, RFP	+	+
ZipGFP	BiFC	GFP	+	+
FlipGFP	BiFC	GFP	+	+
xC3ai	BiFC	CFP, GFP, RFP	+	+
iCasper	BiFC	FR	+	+
CA-GFP	BiFC	GFP	+	-
CaspaseTracker	Gal4-ON	GFP	+	+
SMAC-GFP	Subcellular	GFP	+	+
Apoliner	Subcellular	GFP	+	+
SECA5	Ex-cellular	GFP	+	+

1.9 Current Tools available for Acidic Environment Detection

Fluorescent proteins have been tailored in a wide variety of ways to sense biological processes, one of which is for sensing of cellular pH and acidic subcellular compartments. Many native fluorescent proteins have remarkable sensitivity or insensitivity to acidic environments, allowing the fluorescent signature of these proteins to serve as markers for relative pH within a compartment [318].

To harness this inherent quality, groups have fused eGFP (acidic sensitive) and RFPs (acidic insensitive) to autophagy markers in order to image this process *in vitro* as well as *in vivo* [319]. Furthermore, many groups have mutated RFPs in order to generate a single-fluorophore probe that is sensitive to acidic environments, increasing in brightness with a decrease in pH [320] [321]. By using a single fluorophore to determine relative pH, these probes can be used in conjunction with additional fluorescent proteins, expanding the possibilities for monitoring more than one biological process at a time. While these single fluorophore probes offer a significant advantage for monitoring acidification events, their changes in fluorescence upon protonation in an acidic environment could benefit from protein engineering efforts.

Table 1.2: *In vitro* and *in vivo* sensors of pH

Name	Fluorophore	pKa	Acidic Dynamics	In Vitro?	In Vivo?
eGFP, mCherry Tandem Fluorophore	GFP	6.0	Fluorescence Decrease	+	+
SEP	GFP	7.6	Fluorescence Decrease	+	-
Phluorin	GFP	Und.	Fluorescence Decrease	+	-
Phuji	RFP	7.7	Fluorescence Decrease	+	-
mCherryEA	RFP	Und.	Fluorescence Increase	+	-
mKeima	RFP	6.5	Fluorescence Increase	+	+
pHRed	RFP	6.6	Fluorescence Increase	+	+
Phlorina	RFP	6.9	Fluorescence Increase	+	+

1.9.1 Chemical labeling for phagocytosis assays

Of the methods to detect phagocytic events, chemical labeling of apoptotic cells is the most widely used technique. Commonly used reagents to label targets for phagocytosis are TAMRA, CyPher5e, PSVue, PSiva, Annexin V, pHRodo, PKH dyes and Acridine Orange. These chemical dyes are bright and photostable, permitting the ability to determine events of phagocytosis via microscopic or flow cytometry analysis. The main difference between these dyes is their ability to respond to acidic environments, labeling substrates and fluorescent spectrums. Detailed below is a chart which specifies these properties as well their potential use *in vitro* as well as *in vivo*.

Table 1.3: Chemical probes used to study efferocytosis

Name	Spectrum (Ex./Em.)	Acidic Sensitivity (Y/N)	*In Vitro* Use (Y/N)	*In Vivo* Use (Y/N)	References
TAMRA	546nm / 579nm	N	Y	N	322 139
Cypher5e	644nm / 663nm	Y	Y	Y	323 324 325
PSVue	794nm / 810nm	N	Y	Y	326
PSiva	488nm / 530nm	N	Y	Y	327 328
Annexin V	Conjugation Dependent	N	Y	Y	329 330
pHRodo	509nm / 533nm 560nm / 585nm	Y	Y	N	331 170
PKH-26 / 67	551nm / 567nm 490nm / 502nm	N	Y	N	53
Acridine Orange	500nm / 526nm	N	Y	Y	332 333

These probes all have limitations in that they are limited in their ability to work *in vivo*, as well as target specific cells. In addition, many of these probes suffer from significant non-specific binding, which inhibits their ability to precisely target populations of cells or tissues of interest. Finally, for these probes to work *in vivo*, the dye must be introduced to the organism in an invasive manner which could compromise tissue integrity and affect the output. Given these concerns and potential for confounding results, it is best to use these chemical dyes in a limited manner or avoid them, if possible, for *in vivo* use.

1.11 Publications I have been apart of during my PhD dissertation work

1. Kristen K Penberthy, Claudia Rival, Laura S. Shankman, Michael H. Raymond, Jianye Zhang, Justin S. A. Perry, Claudia Z. Han, Tal Burstyn-Cohen, Krzysztof Palczewski, Jeffrey J. Lysiak, and Kodi S. Ravichandran. “PtdSer receptors MerTK and BAI1 are not interchangeable in the retinal pigment epithelium.” *Scientific Reports.* (2017).
2. Sho Morioka*, Justin S. A. Perry*, Michael H. Raymond, Christopher B. Medina, Yunlu Zhu, Liyang Zhao, Vlad Serbulea, Suna Onengut-Gumuscu, Norbert Leitinger, Sarah Kucenas, Jeffrey C. Rathmell, Liza Makowski, Kodi S. Ravichandran. “Efferocytosis induces a novel SLC program to promote glucose uptake and lactate release.” *Nature.* (2018).
3. Justin S. A. Perry, Sho Morioka, Christopher B. Medina, J. Iker Etchegaray, Brady Barron, Michael H. Raymond, Christopher Lucas, Suna Onengut-Gumuscu, Eric Delpire and Kodi S. Ravichandran. “Interpreting an apoptotic corpse as anti-inflammatory involves a chloride sensing pathway.” *Nature Cell Biology.* (2019).
4. Jeremy J. P. Shaw, Timothy L. Boyer, Emily Venner, Patrick J. Beck, Tristen Slamowitz, Tara Caste, Alexandra Hickman, Michael H. Raymond, Pedro Costa-Pinheiro, Mark J. Jameson, Todd E. Fox, and Mark Kester. “Inhibition of Lysosomal Function Mitigates Protective Mitophagy and Augments Ceramide Nanoliposome-Induced Cell Death in Head and Neck Squamous Cell Carcinoma.” *Molecular Cancer Therapeutics.* (2020).
5. Pedro Costa-Pinheiro, Abigail Heher, Michael H. Raymond, Kasey Jividen, Jeremy J. P. Shaw, Bryce Paschal, Susan J. Walker, Todd E. Fox, and Mark Kester. “Role of of SPTSSB-regulated *de novo* Sphingolipid Synthesis in Prostate Cancer Depends on Androgen Receptor Signaling.” *iScience.* (2020).
6. Christopher D. Lucas, Christopher B. Medina, David A. Dorward, Michael H. Raymond, Brady Barron, Turan Tufan, Finnius A. Bruton, Magdalena E.M. Oremek, J. Iker Etchegaray, Sanja Arandjelovic, Emily Farber, Suna Onngut-Gumuscu, Eugene Ke, Moira KB Whyte, Adriano G. Rossi, Kodi S. Ravichandran. “Pannexin 1 initiated bidirectional epithelial - macrophage crosstalk promotes tissue repair.” *Science Immunology.* Under Review (2021).
7. J. Iker Etchegaray, Kristen Penberthy, Sofia Gasperino, Yosuke Nagasaka, Soumen Paul, Vikram Seshadri, Michael H. Raymond, Ana Royo Marco, Jonathan Pinney, Marta

Stremska, Brady Barron, Christopher D. Lucas, Nishikant Wase, Ira Tabas, Yong Fan, Emil Unanue, Bijoy Kundu, Bradley Gelfand, Tal Burstyn-Cohen, Justin S. A. Perry, Kodi S. Ravichandran. “A local source of insulin in the eye governed by phagocytosis and starvation.” *Nature.* Under Review (2021).

8. Kendra E. Liu, Michael H. Raymond, Kodi S. Ravichandran, Sarah Kucenas. “Clearing your mind: mechanisms of debris clearance after cell death during neural development.” *Annual Review of Neuroscience*. Under Review (2021).
9. Michael H. Raymond, Andrew J. Davidson, Yi Shen, Daniel R. Tudor, Christopher D. Lucas, Sho Morioka, Justin S. A. Perry, Julia Krapivkina, David Perrais, Linus J. Schumacher, Robert E. Campbell, Will Wood, and Kodi S. Ravichandran. “Coordination, challenges, and compromise in macrophage efferocytosis *in vivo.*” *Science.* In Revision (2021).

Chapter II

Coordination, challenges, and compromises in macrophage efferocytosis *in vivo*

2.1 Abstract

Apoptosis of cells and their subsequent removal by the process of 'efferocytosis' occurs in nearly all tissues during development, homeostasis, and disease. While significant mechanistic progress has been made, the ability to track cell death and subsequent corpse removal *in vivo* has remained a challenge due to technical limitations. Here, we develop a genetically encoded fluorescent reporter, denoted CharON, that can concurrently track both emerging apoptotic cells and their efferocytic clearance by phagocytes. Using CharON and the *Drosophila* embryo as a model system, we could visualise and validate the key steps of efferocytosis *in vivo,* and for the first time directly measure coordinated clearance of apoptotic corpses in a living organism. This analysis also uncovered novel challenges macrophages face during efferocytosis *in vivo*. When confronted with a dense field of apoptotic corpses *in vivo*, macrophages adopt an 'eat-first, digest-later' strategy, prioritising debris uptake over corpse acidification and degradation. In trying to achieve rapid clearance, individual macrophages display huge variation in corpse burden, with additional consequences. When challenged with a necrotic wound, macrophages with high apoptotic corpse burden are impaired in necrotic debris uptake, despite migrating to the wound site. Enforcing phagocyte 'eating limits' via modeling suggest that macrophages benefit from 'unrestrained' uptake and variable corpse burden, as the alternative of 'equal distribution' drastically increases clearance time. This represents a 'gamble' or functional compromise, wherein macrophages maximise clearance of developmental/ homeostatic apoptosis, while jeopardizing resolution after tissue damage. This efferocytic strategy introduces an inherent vulnerability, with ramifications for diseases where macrophages encounter overwhelming cell death. Collectively, these live tracking studies advance new concepts in macrophage efferocytosis *in vivo*.

2.2 Introduction

Efferocytosis is an essential process during tissue development, homeostasis and resolution of inflammation during various diseases. Interactions between apoptotic cells and phagocytes involve intercellular signaling programs which ensure proper corpse engagement and disposal. While significant progress has been made in defining the specific molecules on apoptotic cells and the receptors on phagocytes and the relevance of these molecules to human disease (e.g. via knockout animals and disease models), due to the longstanding difficulty in clearly tracking cell clearance *in vivo,* much of our understanding has been focusing on end points of the process, and in turn, inference. Here, we develop a genetically encoded fluorescent reporter of apoptosis and efferocytosis ('CharON') to track and quantify cell clearance during *Drosophila* embryogenesis at the tissue and single-cell resolution.

2.3 Material and Methods

2.3.1 *In vitro* cell death assays

Jurkat cells (ATCC) were treated with 150mJ of UV-C in a StrataLinker 1800 or 10 μM of ABT-737 (Abcam ab141336) in RPMI 1640 supplemented with 10% FBS and 1% Pen Strep with Glutamine. Cells were collected at indicated time points, stained 1:50 with Pacific Blue Annexin V (Biolegend #640917) and collected on an Attune Flow Cytometer (ThermoFisher). For each sample, 10,000 gated events were recorded, and data was processed in FlowJo V10. For each sample, singlet gates were used to distinguish single cells from doublets, followed by sub-gating on constitutively expressed RFP for analysis of GFP+ and Annexin V+ events. All RFP+, GFP+ and Annexin V+ event gates were set against the respective negative controls.

2.3.2 In vitro live cell imaging engulfment assays

UV-induced apoptotic CharON expressing Jurkat cells were co-cultured with mouse J774 macrophages (ATCC TIB-67) at 1:2 apoptotic cell:phagocyte ratios in 24 well plates and spun at 500rpm for 1 minute. Images were collected every 10 minutes for 24 hours on a Nikon Eclipse Ti2 scope using 40x magnification and kept under 37C and 4% CO2 for the duration of the experiment. Raw Tiff images were exported for analysis using Fiji software.

Engulfment events were manually curated through identification of apoptotic pH-GC3ai (GFP+) cell internalization by J774 macrophages using co-localization between the apoptotic cell and the macrophage through brightfield. Upon identification of engulfment events, manually drawn circular regions of interest (ROI) were placed over identified events and tracked throughout the duration of the experiment. Intensity of phagocytic events were calculated using background subtracted GFP and RFP values.

2.3.3 Plasmid construction

In brief, all CharON constructs were inserted into a lentivirus backbone for expression in Jurkat cells. Gibson assembly PCR reactions using oligonucleotides (Integrated DNA Technologies) with 15bp overhangs were used to amplify and insert transgenes into restriction sites downstream of a SFFV promoter with an upstream CBX3 UCOE (UCOE-SFFV). In addition, P2A or T2A elements were used downstream of pH-GC3ai for bi-cistronic expression of mCherry or pHlorina. Sanger sequencing was used to verify sequences of inserted transgenes.

For construction of pH-CaspGFP, GC3ai was amplified from plasmid pCDH-puro-CMV-GC3AI (Addgene #78910). Mutation of GC3ai Q204H was performed via overlapping PCR and inserted into lentivirus UCOE-SFFV. CharON was constructed using pH-CaspGFP and pHlorina separated by a P2A site for bi-cistronic expression.

2.3.4 CharON expressing transgenic *Drosophila* generation

CharON construct was cloned downstream of UAS sequence in pUASt-ATTB, which in turn was used to generate transgenic CharON flies. This was recombined with daughterless GAL4 (da-gal4) to drive ubiquitous expression throughout embryo[320] (*;; da-gal4, uas-charon*) . Srp-GMA was used to label macrophages (*; srp-GMA; da-gal4, uas-charon*).

2.3.5 Imaging of *Drosophila* embryos

Embryos laid on apple juice agar plates overnight were collected in cell strainers (Falcon), dechorionated with bleach (Jangro), and washed with purified water. Embryos at developmental stages 12-16 were mounted on double-sided tape on a glass slide in droplets of VOLTALEF oil (VWR), beneath a bridging coverslip (No. 1.0, SLS Ltd) sealed on top of two supporting coverslips (No. 1.5, SLS Ltd)[333]. Z-stacks of the ventral side of embryo were captured using a Zeiss LSM 880 (with Airyscan fast) confocal microscope using a plan-apochromat 40x objective with a NA of 1.3. Epithelial wounds were generated using laser ablation (nitrogen-pumped Micropoint ablation laser tuned to 435 nm, Andor Technologies) as previously described[334]. The acquisition software used was Zen Black (Zeiss). Alternatively, a spinning disc confocal microscope (Perkin Elmer Ultraview) using a plan-apochromat 63x objective with a NA of 1.4 and a Hamamatsu C9100-14 camera, was used for long-term, live-imaging of macrophage dispersal. The acquisition software used was Volocity (Perkin Elmer).

2.3.6 Image analysis

ImageJ (NIH) was used for all image analysis. For quantification of efferocytosis across embryogenesis, individual 20 µm z-stacks of 5 embryos per developmental stage (25 total) were imaged using scanning confocal microscopy and quantified for each genotype. CharON labelled corpses that were superficial to the VNC were isolated by cropping in on a 5 µm z-stack that minimally contained a cluster of apoptotic bodies. These were then flattened (average intensity projection) and each apoptotic body was outlined manually using pH-CaspGFP signal. Apoptotic

bodies deeper within the VNC were isolated by z-projecting (average intensity) the slices from the top 5 μm of the z-stack into the embryo. Apoptotic corpses were again outlined manually using pH-CaspGFP signal. For identification of apoptotic bodies specifically within ventral macrophages, 5 μm z-stacks that minimally contained the macrophages (guided by srp-GMA label) were isolated and z-projected (average intensity). CharON-labelled apoptotic corpse bodies were outlined manually using pHlorina signal (due to pH-CaspGFP overlap with srp-GMA). Area and mean intensities within these outlines were measured and their numbers counted.

For time-lapse imaging of macrophage efferocytosis, dispersing macrophages (embryonic stages 12-13) were imaged using spinning disc microscopy (1 z-stack/minute). Engulfed apoptotic bodies with strong pH-CaspGFP signal (detectable above srp-GMA) were identified and a 2 μm z-stack that minimally contained the corpse was isolated (position of this z-stack adjusted in x, y, and z for every frame to ensure apoptotic body was contained centrally within z-stack as it moved around embryo within a macrophage). These z-stacks were flattened (maximum intensity projections) and the apoptotic body was outlined manually in each frame (starting from moment of uptake). Mean intensities within these outlines were then calculated for each frame. Following background subtraction, fold-change in intensity from initial value were calculated and plotted.

Macrophage speeds, chemotaxis (FMI) and distances travelled were calculated by manually tracking cell centroids using the ImageJ Manual tracking and chemotaxis tool plugins. For analysis of ventral macrophage basal migration and inflammatory chemotaxis in response to wounding, stage 15 embryos (5 unwounded and 5 wounded embryos respectively) were imaged using scanning confocal microscopy (1 z-stack/minute). The number of CharON-labelled apoptotic bodies within each macrophage was determined in the initial z-stack (as described above) and macrophages were then tracked, again using ImageJ Manual tracking and chemotaxis tool plugins. Responders to wounds were defined as macrophages that moved to the wound edge, wherein tracking was stopped. Non-responders represent cells that were never recruited to the wound edge and were tracked throughout the entire time-lapse. Necrotic debris uptake at wounds was observed as fluorescent-negative ‘vacuoles’/voids within the GFP-labelled macrophages. The uptake of such debris was scored for each macrophage for the entire time it was at the wound edge. Although we could not anticipate this previously, the wounding laser did not hinder the pHlorina signal from becoming visible once acidified (e.g., when fused with apoptotic cell-containing phagosomes).

All the images present in the figures and movies of this manuscript are z-projections and are adjusted only for contrast and brightness, with occasional use of the ‘despeckle’ tool in imageJ to adjust for noise (never used during quantification).

2.3.7 Lentivirus production, purification, and transduction

All lentivirus production was performed using Lenti-X HEK293T (Takara) grown in DMEM supplemented with 10% FBS and 1% Pen Strep with Glutamine. Cells were transfected at 80% confluency in 6-well plates with 2 ug total of psPAX2 packaging (Addgene #12260), pMD2.G envelope (Addgene #12259) and transfer plasmids at a 4:1:4 ratio. Supernatants were collected 48h after transfection and concentrated following the Lenti-X Concentrator (Takara) protocol.

Jurkat cells were plated in 24-well plates at 200k/well in RPMI 1640 supplemented with 10% FBS, 1% Penn Strep with Glutamine and 8µg/mL Polybrene. Purified viral supernatants were added to the wells and spun at 800g for 45min at 32 °C. After 24h, the cells were pelleted, washed in PBS and cultured in RPMI 1640 supplemented with 10% FBS and 1% Penn Strep with Glutamine. Transgene expression was assessed 72 hrs after transduction.

2.3.8 *Drosophila* heatmap generation

Processed GFP and RFP image z-stacks from each developmental stage were substacked into VNC (1-30) and sub-VNC (31-99) regions using Fiji software. Images were corrected for alignment using the Rotate feature before importing into Ilastik for object identification. Using Ilastik, a model was trained on GFP and RFP channel images in order to segment apoptotic and acidification events, respectively. Segmented images were used for object identification, followed by object masking for quantification of events. A total of five embryos per stage were used to evaluate the total number of events within the VNC.

2.3.9 General pHlorina genetic construction methods and materials

All synthetic DNA oligonucleotides for cloning and library construction were purchased from Integrated DNA Technologies (IDT). Taq DNA polymerase (New England Biolabs) was used for error-prone PCR (EP-PCR). PCR products and products of restriction digests were purified using gel extraction kit (BioBasic) according to the manufacturer's protocols. Restriction enzymes and ligases were purchased from New England Biolabs or Thermo Scientific. The DNA sequences were analyzed at the University of Alberta Molecular Biology Service Unit (MBSU).

2.3.10 pHlorina protein engineering

Engineering of pHlorina was carried out by site directed mutagenesis and multiple rounds of Error-prone PCR (EP-PCR) using plasmids encoding mApple as a template. All synthetic DNA oligonucleotides for cloning and library construction were purchased from Integrated DNA Technologies (IDT). Taq DNA polymerase (New England Biolabs) was used for EP-PCR. PCR products and products of restriction digests were purified using gel extraction kit (BioBasic) according to the manufacturer's protocols. Restriction enzymes and ligases were purchased from New England Biolabs or Thermo Scientific. The DNA sequences were analyzed at the University of Alberta Molecular Biology Service Unit (MBSU). All site-directed mutagenesis was performed using the Quikchange lightning mutagenesis kit (Agilent) and primers designed according to the manufacturer's guidelines. EP-PCR products were digested with XhoI and HindIII and ligated into pBAD/His B vector digested with the same two enzymes and used to transform electrocompetent *Escherichia coli* strain DH10B (Thermo Fisher Scientific), which were then plated on agar plates containing LB medium supplemented with 0.4 mg/ml ampicillin and 0.02% w/v L-arabinose. Single colonies were picked and inoculated into 4 ml of LB medium with 0.1 mg/ml ampicillin and 0.02% w/v L-arabinose and then cultured overnight. Protein was extracted using B-PER bacterial extraction reagent (Thermo Fisher Scientific) as per manufacturer guidelines. Screening for pH sensitivity of extracted proteins was performed with a Safire2 fluorescence plate reader (Tecan) by measuring protein fluorescence excitation and emission spectra in buffers of pH 5.0 and 7.5. Plasmids were purified with the DNA miniprep kit (Thermo Fisher Scientific) and then sequenced using the BigDye Terminator Cycle Sequencing kit (Applied Biosystems). We combined approaches of rational site-directed mutagenesis and random mutagenesis to improve the pH-induced fluorescence change. Based on pHluorina0.1 (mApple Ile161Cys/Lys163Glu), we first randomized position Ala217, the corresponding residue of a crucial mutation in pHRed, which rendered a larger ratio change compared to its template mKeima. The Ala217X (X = all 20 common amino acids) mutant library was expressed and screened by measuring the excitation spectra at pH 5.5 and 7.5. One variant with the largest excitation ratio change was selected and designated as pHlorina0.2. Sequencing revealed pHlorina0.2 had a mutation of A217T, Which is similar to the A217S mutation in pHRed[335]. To increase the brightness of the pHlorina0.2, another saturation mutagenesis was performed at the position 143, The brightest variant in this 143X library, pHlorina0.3, possessed a W143Y mutation. Multiple rounds of random mutagenesis and screening for maximum red fluorescence increase at acidic pH were performed based on pHlorina0.3, eventually led to pHlorina.

2.3.11 Imaging of pHlorina in cell culture for calibration of pH dependency

HeLa cells were grown in DMEM supplemented with 10% fetal calf serum, 1% sodium pyruvate, and 1% Glutamax with 1% penicillin/streptomycin and maintained at 37°C in 5% CO_2. pDisplay-pHlorina was made by subcloning pHlorina into the pDisplay vector (Life Technologies), between the BglII and SalI restriction sites. The pDisplay vector is translated into a protein consisting of the N-terminal signal peptide, pHlorina, and a C-terminal transmembrane domain of platelet-derived growth factor receptor (PDGFR) which enables anchoring of the fused protein to the cell surface, hence its sensitivity to changes in extracellular pH. Twenty-four hours before imaging, cells were transfected with 2 µg of plasmid DNA and 6 µl of X-TREMEGene-HP (Roche), mixed in PBS for 10 min and added directly in the culture medium. 4 h later, 30000 cells were plated on 18-mm glass coverslips. Live cell imaging was done at 37°C. Cells were perfused with solution containing 135 mM NaCl, 5 mM KCl, 0.4 mM $MgCl_2$, 1.8 mM $CaCl_2$, 20 mM HEPES, and 1 mM D-glucose, adjusted to pH 7.4 and 315 mOsmol/L. For pH titration, solutions were prepared as the HBS solution described above using as pH buffers HEPES for solutions at pH 7-10, PIPES for solutions at pH 6 and 6.5 and MES for solutions at pH 5 and 5.5. TIRF imaging was performed on an inverted microscope (IX71; Olympus) equipped with an Apochromat N oil 60× objective (NA 1.49), a 1.6× magnifying lens, and an electron multiplying charge coupled device camera (QuantEM:512SC; Roper Scientific). Samples were illuminated by a 473-nm laser and a coaligned 561-nm laser. Emitted fluorescence was filtered using a 620/60 nm filter (Chroma Technology Corp.) for pHlorina imaging. In situ pH titration revealed pDisplay-pHlorina has a pK_a of 6.2 and n_H of 1.6, with a maximum $\Delta F/F_0$ of 2.6 (**Supplemental Data 2c**). During imaging, we noted the presence of brightly fluorescent clusters which are not sensitive to change in extracellular pH, which is likely to be acidic intracellular organelles such as the lysosome. To verify this, we applied ammonium chloride (NH_4Cl, 50 mM) to neutralize the luminal pH of intracellular organelles. This treatment cancelled the fluorescence of bright clusters, suggesting the fluorescence is from pHlorina signal in intracellular organelles (**Supplemental Data 2c**). Taking advantage of the ratiometric dual excitation, we also imaged the cells under 473 and 561 nm laser excitation, the bright fluorescent clusters were only visible with 561 nm excitation but not with 473 nm excitation (**Supplemental Data 2e**), further confirming that bright fluorescent clusters are from pHlorina in an acidic environment.

2.3.12 pHlorina *in vitro* characterization

To purify the proteins, electrocompetent *E. coli* strain DH10B (Invitrogen) was transformed with the plasmid of interest using a Micropulser electroporator (Bio-Rad). Transformed bacteria were cultured overnight on agar plates containing LB and ampicillin. Single colonies were picked and grown overnight in 4 mL LB supplemented with ampicillin at 37 °C. For each colony, the 4 mL culture was then used to inoculate 250 mL of LB medium with ampicillin and grown to an optical density of 0.6. Protein expression was induced with the addition of 0.02% L-arabinose and the culture was grown overnight at 37 °C. Bacteria were harvested at 10,000 rpm, 4 °C for 10 min, lysed using a cell disruptor (Constant Systems) and then clarified at 14,000 rpm for 30 min. The protein was purified from the supernatant by Ni-NTA affinity chromatography (ABT) according to the manufacturer's instructions. The buffer of the purified protein was exchanged with 10 mM Tris-Cl, 150 mM NaCl, pH 7.3 with Amicon ultra centrifugal filter (MWCO 10,000) for a final protein concentration of approximately 10 µM. Fluorescence intensity as a function of pH was determined by dispensing 2 µL of protein solution into 50 µL of the desired pH buffer in triplicate into a 384-well clear-bottom plate (Nunc) and measured in a Safire2 plate reader. pH Buffer solutions from pH = 3 to pH = 11 were prepared according to the Carmody buffer system.

2.3.13 *In Silico* macrophage efferocytosis

The effect of varying macrophage consumption limit was explored *in silico* via agent-based modelling (NetLogo agent based modelling suite[336]). A fixed number of macrophages (300) and corpses (1,800) were randomly distributed within a domain. Macrophages moved at rate of 1 pixel/iteration in any direction, but preferentially moved in the direction of a corpse (biased walk). If adjacent to more than one corpse, then the choice of corpse was random, and multiple macrophages were prohibited from co-inhabiting the same pixel. Once a consumption limit was reached, macrophages no longer engulfed corpses and switched to moving without bias (random walk). The simulation was run until all corpses were cleared or for a maximum of 1,000 iterations. Each simulation was repeated 100 times under the varying consumption limits to yield standard deviations.

2.4 Results

2.4.1 Generation of 'CharON' to concurrently track both apoptosis and efferocytosis

To take a genetic approach to track both apoptosis and efferocytosis *in vivo*, we engineered two probes that could be expressed in tandem. For the apoptosis reporter, we focused on designs where the cleavage by executioner caspases 3 and 7 could induce a fluorogenic 'turn-on' response of an engineered green fluorescent protein (GFP) (*Fig. 1A*) [308]. Previous attempts to generate such caspase-inducible GFP reporters have had mixed success. Of these, we tested GC3ai, FlipGFP and ZipGFP in Jurkat cells and, in our hands, found GC3ai to be the best reporter of apoptosis [310 311 332]. Further, the appearance of the caspase-induced green fluorescence signal of GC3ai strongly aligned with phosphatidylserine exposure on the apoptotic cells, as measured by Annexin-V (*Supplemental Data 1A, 1B, 1C*). We modified GC3ai further to develop a new caspase-inducible GFP that we named pH-CaspGFP. As a major limitation of GC3ai is photo-quenching in the acidic environment of the endosomes/lysosomes, we engineered pH-CaspGFP to be partly acid-resistant by incorporating a Q204H mutation into the parent GC3ai molecule (*Fig. 1A*) [337]. This mutation in pH-CaspGFP preserved the GFP intensity during early stages of efferocytosis (compared to parent GC3ai, *Fig. 1D* and *Supplemental Data 1D, 1F*).

When pH-CaspGFP was stably expressed in Jurkat cells, apoptosis could be faithfully detected after different apoptotic stimuli, including ultraviolet-C irradiation and after treatment with ABT-737 (a BCL-2 inhibitor) or Staurosporine (*Fig. 1A and 1B*). Two other controls are worth noting: first, the GFP+ apoptotic events scored via pH-CaspGFP fully matched the Annexin V^+ events, and this was corroborated at different time points after death induction (*Supplemental Data 1E, 1G*); second, when pH-CaspGFP expressing cells were treated with the pan-caspase inhibitor Q-VD, the apoptosis/caspase-dependent GFP+ signal was essentially eliminated (*Fig. 1B*), confirming caspase dependency. pH-CaspGFP was also compatible with detection of apoptosis induction in multiple cell types, including T cells (Jurkat cells), fibroblasts (LR73 cells) (*Fig. 1C*) and monocytes (THP-1 cells) (*Supplemental Data 2A, 2B*).

To detect engulfed apoptotic cells specifically undergoing corpse acidification and digestion in phagocytes, we engineered a new ratiometric red fluorescent pH sensor. Using mApple as a template, we created a library in which residues 161 and 163, both in close proximity of the chromophore, were randomized[338] (*Fig. 1E,* see Methods). Screening of this library led to the identification of mApple *Ile161Cys*/*Lys163Glu* with a large ratiometric pH response and high brightness. Further engineering via site-directed and random mutagenesis ultimately yielded a high-performance ratiometric pH sensor, which we designated pHlorina (**pH**-sensitive f**lu**o**r**escent

ratiometric **in**dicator derived from m**A**pple, and pronounced '*florina*') (*Fig. 1E,* see Methods). When going from pH 7.5 to pH 5, pHlorina exhibits >20-fold excitation ratiometric change, and >6-fold red fluorescence intensity increase (excitation 560 nm, emission 620 nm), with an apparent pK_a of 6.1 and Hill coefficient (n_H) of 1.1 (*Fig. 1F, Supplemental Data 2C, 2E*). To assess the utility of pHlorina in tracking efferocytosis, we stably transduced Jurkat cells, rendered them apoptotic, and incubated with mouse J774 macrophages for time-lapse imaging (*Fig 1G, left, Supplemental Data 3A*). Upon corpse internalization, we could detect 3.4 fold increase in pHlorina fluorescence (*Fig. 1G*), and this was inhibited by the acidification inhibitor Bafilomycin (*Fig. 1G, Supplemental Data 2D, 2F*). Thus, the novel RFP sensor pHlorina can track internalized apoptotic corpses during acidification/digestion in phagocytes.

Figure 2.1: Evaluation and engineering of a pH-Stable apoptosis reporter and RFP pH sensor

A) **Apoptosis sensor design**. (top) Schematic of pH-CaspGFP design. Upon apoptosis induction, a Caspase-3/7 linker is cleaved resulting in GFP fluorescence. (bottom) pH-CaspGFP expressing Jurkat cells were induced to undergo apoptosis via a pulse of UV-C irradiation, and after incubation for additional 4 hours, the fraction of GFP+ and Annexin V+ cells were determined.

B) **pH-CaspGFP detects multiple apoptotic stimuli**. pH-CaspGFP expressing Jurkat cells were killed with UV-C, 20nM ABT-737 and 1μM staurosporine and measured for GFP+ events over four hours. To block apoptosis (and to test GFP signal arising), Jurkat cells were pre-treated with 50μM Q-VD.

C) **pH-CaspGFP detects apoptosis in multiple cell types.** Stably pH-CaspGFP expressing Jurkat cells and LR73 cells were rendered apoptotic via UV and 1μM staurosporine, respectively. GFP+ cells were assessed via time-lapse imaging.

D) **pH-CaspGFP improves phagosomal stability**. (top left) Schematic of *in* vitro engulfment assay: GC3ai and pH-GC3ai apoptotic Jurkat cells were co-cultured with J774 macrophages in order to capture efferocytic events. Upon internalization, GFP fluorescence intensity was tracked over 2 hours. (right) Time-Lapse images of GC3ai (Top) or pH-CaspGFP Apoptotic Jurkat cells engulfed by J774 Macrophages. Arrows indicate phagosomes containing apoptotic Jurkat cells. (Two-Way ANOVA, ** = p<.0021, * = p<.0332)

E) **Development of pHlorina, an RFP Sensor for detection of efferocytosis**. (left) Modeled structural representation of pHlorina and mutations relative to the parental RFP mApple (based on mCherry structure, PDB 2H5Q). (middle) Excitation spectra of purified pHlorina protein from 400 nm to 600 nm at pH 5.0 (red) and pH 7.5 (blue). (right) Emission spectra of purified pHlorina with 560 nm excitation at pH 5.0 (red) and pH 7.5 (blue).

F) **pH titration of pHlorina *in vitro***. (left) pH titration of purified pHlorina from pH 10.0 to pH 4.0 with 560 nm excitation and 620 nm emission. (right) Cell surface expression of pHlorina in mammalian cells and fluorophore pH response to pH 7.0, pH 5.0 and pH 9.0 buffers.

G) **pHlorina detects phagosomal acidification during efferocytosis.** (left) Schematic of *in vitro* engulfment assay to determine pHlorina fluorescence during efferocytosis. Bafilomycin is used to determine the dependence of pHlorina response to phagosomal acidification. (right) *In vitro*

engulfment response of pHlorina fluorescence during internalization is dependent upon acidification of the phagosome. Apoptotic pHlorina-expressing Jurkat cells were co-cultured with J774 macrophages to detect efferocytic events. (Unpaired T-Test, **** = p<.0001).

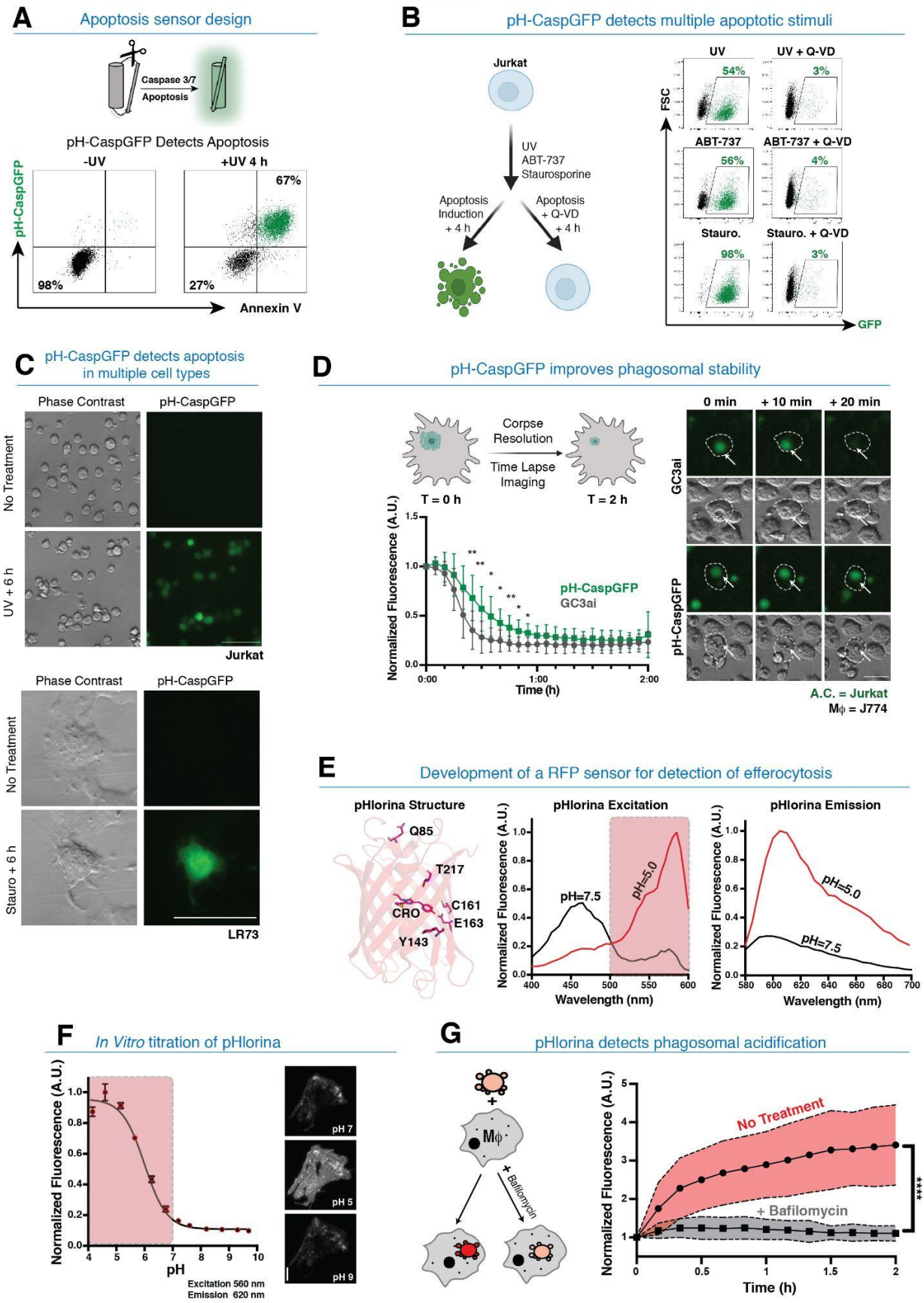
A
Apoptosis sensor design
Caspase 3/7
Apoptosis
pH-CaspGFP Detects Apoptosis
-UV
+UV 4 h
pH-CaspGFP
67%
98%
27%
Annexin V
B
pH-CaspGFP detects multiple apoptotic stimuli
Jurkat
UV
ABT-737
Staurosporine
Apoptosis Induction + 4 h
Apoptosis + Q-VD + 4 h
UV
UV + Q-VD
54%
3%
FSC
ABT-737
ABT-737 + Q-VD
56%
4%
Stauro.
Stauro. + Q-VD
98%
3%
GFP
C
pH-CaspGFP detects apoptosis in multiple cell types
Phase Contrast
pH-CaspGFP
No Treatment
UV + 6 h
Jurkat
Phase Contrast
pH-CaspGFP
No Treatment
Stauro + 6 h
LR73
D
pH-CaspGFP improves phagosomal stability
Corpse Resolution
Time Lapse Imaging
T = 0 h
T = 2 h
Normalized Fluorescence (A.U.)
pH-CaspGFP
GC3ai
Time (h)
0 min
+ 10 min
+ 20 min
GC3ai
pH-CaspGFP
A.C. = Jurkat
Mϕ = J774
E
Development of a RFP sensor for detection of efferocytosis
pHlorina Structure
Q85
T217
C161
CRO
E163
Y143
pHlorina Excitation
pHlorina Emission
Normalized Fluorescence (A.U.)
pH=7.5
pH=5.0
Wavelength (nm)
F
In Vitro titration of pHlorina
Normalized Fluorescence (A.U.)
pH
Excitation 560 nm
Emission 620 nm
pH 7
pH 5
pH 9
G
pHlorina detects phagosomal acidification
Mϕ
+ Bafilomycin
No Treatment
+ Bafilomycin
Normalized Fluorescence (A.U.)
Time (h)
****

Next, we combined the above two probes to generate a single promoter driven cassette to genetically express both pH-CaspGFP and pHlorina reporters in tandem, split by a P2A self-cleaving site for equimolar expression [339]. We denote this construct 'CharON' ('Caspase and pH Activated Reporter, Fluorescence ON) referring to *Charon*, who in Greek mythology ferries the recently deceased across the river separating the living from the dead (*Fig. 2A*). Our expectation was that CharON expressing cells undergoing apoptosis would become GFP+ (with low RFP); and after being engulfed by phagocytes and passing through the acidic phagolysosome, the GFP fluorescence would be gradually quenched while the red pHlorina signal would gradually increase (*Fig. 2A*). When apoptotic CharON expressing Jurkat cells were mixed with BFP^+ mouse J774 macrophages, the signals from pH-CaspGFP and pHlorina allowed all the stages of efferocytosis to be visualised through live-cell imaging (*Fig. 2B, Video 1*). Both fluorescent components of CharON exhibited a wide dynamic range (*Fig. 2C*), with a 17-fold increase in average pHlorina/pH-CaspGFP ratio in the first 2 hours after corpse internalization (*Fig. 2C*). In addition, we noticed that CharON could detect multiple efferocytic events, with some macrophages proficiently engulfing multiple corpses (*Fig. 2D, Video 2*). These data established CharON as a powerful new tool for tracking apoptosis and early stages of efferocytosis.

2.4.2 CharON visualises in vivo efferocytosis

The development of the genetically-encoded CharON offered a unique opportunity to explore efferocytosis *in vivo,* within transgenic animals. Programmed cell death is critical for tissue remodeling and patterning during *Drosophila* development and apoptosis during embryogenesis has been well-characterized [294 339]. Furthermore, the powerful genetics of *Drosophila* and the excellent live-cell imaging possible in the translucent embryo offered an ideal model to visualise and interrogate efferocytosis *in vivo* through CharON.

We generated CharON transgenic flies, wherein the GAL4/UAS system was used to drive the ubiquitous expression of CharON throughout the embryo (*Fig. 2E*). We focused on the ventral side of the embryo where there is a wave of apoptosis in the developing Central Nervous System (CNS) during mid-late embryogenesis [294 278] . Live-cell imaging of developing CharON embryos (stages 12-16) captured the induction of developmental apoptosis at the whole organism level (i.e., via pH-CaspGFP fluorescence) (*Fig. 2E, Supplemental Data 4A, 4B*). Furthermore, at the embryo-wide level, this coincided with an increasing pHlorina signal, indicative of developmental efferocytosis.

The apoptotic burden from the embryonic *Drosophila* CNS is shared by two distinct phagocytes: the phagocytic glia and the dispersing ventral hemocytes (macrophages) (*Fig. 2F*)[295]. The highly motile macrophages on the ventral side of the embryo, disperse through the hemocoel ('blood-cavity') immediately below the developing CNS[171]. The macrophages cannot access the apoptotic corpses within the CNS but have a critical role in clearing the superficial corpses occurring at the interface between the blood-cavity and the CNS[340].

To visualise efferocytosis within these two distinct regions during embryogenesis, we simultaneously imaged CharON superficial to the CNS and deep within the CNS (*Fig. 2F, Video 3*). Within both these locations, CharON activity revealed coordinated efferocytosis. However, interestingly, CharON also highlighted distinct differences in the efferocytic dynamics. For example, efferocytosis within the CNS was highly sporadic across the embryonic stages imaged (12-16), representing constant, autonomous engulfment by individual phagocytic glia. This manifested itself as only a weak trend for increasing CharON activity with increasing embryonic time (*Fig. 2G*). However, superficial to the CNS, the macrophage-mediated clearance of apoptotic corpses was far more synchronized in the hemocoel, appearing as a choreographed wave of apoptosis and efferocytosis, yielding a strong increase in pHlorina activity with increasing embryonic time (*Fig. 2H, Video 3*). CharON also highlighted differences in corpse size between phagocytic glia and macrophages, underscoring nuances of efferocytosis and variability in

burdens placed on the distinct phagocytes that populate different regions (*Supplemental Data 3E, 3F)*.

Figure 2.2: Caspase and pH Activated Reporter, Fluorescence ON (CharON) detects apoptosis and efferocytosis *In Vitro* and *In Vivo*.

A) **Design of CharON transgene and fluorescent signature**. (top) CharON transgene design. Arrow indicates the promoter driving expression of pH-CaspGFP and pHlorina in one transcribed product. The P2A site between pH-CaspGFP and pHlorina ensures equivalent expression of both reporters. (bottom) Fluorescent signature of an apoptotic CharON expressing cell (green) as it is engulfed by a Macrophage (blue), and the resulting change in fluorescence.

B) **CharON detects efferocytic events *in vitro***. J774 macrophages were incubated with apoptotic CharON expressing Jurkat cells to detect efferocytic events. CharON GFP and RFP signal was evaluated via Time-Lapse imaging during the efferocytic process. A.C. = Apoptotic Cell, Mϕ = Macrophage.

C) **CharON fluorescence during efferocytosis**. (left) Individual CharON GFP and RFP spectrum during engulfment. (right) Ratiometric CharON (RFP/GFP) response during engulfment. (Two-Way ANOVA, Sidak's multiple comparison test, **** =p<.0001)

D) **CharON detects multiple engulfment events *in vitro***. (left) Schematic of *in vitro* engulfment of multiple CharON corpses by a macrophage over 2 hours. (right) Images of successive engulfment events by a single macrophage; arrows indicate internalized and acidified corpses revealed by the pHlorina signal.

E) **Generation of CharON expressing *Drosophila***. The CharON construct was inserted downstream of the UAS promoter region, allowing tissue-specific expression in *Drosophila* using the GAL4 system. CharON *Drosophila* embryos were imaged during developmental stages 12-16 to detect Apoptotic (GFP+) and Efferocytic (GFP+/- , RFP+) events.

F) **Evaluation of CharON *Drosophila* during embryonic development**. Embryo outlines highlight gross anatomical changes during embryonic stages 12-16 (orientated Dorsal side *up*, Ventral side *down*). At embryonic stage 14, efferocytosis peaks within the central nervous system (CNS) on the ventral side of the embryo (dashed box). Within this region (expanded dashed boxes), apoptotic corpses within the CNS are engulfed by phagocytic glia (pink dashed box), whereas the ventral-most corpses at the interface between the CNS and the 'blood-cavity' (hemocoel) are engulfed by the macrophages (blue dashed box). In both these regions, CharON visualises the key steps of *in vivo* efferocytosis (pink and blue boxes respectively). Schematic adapted from[341] . Scale bars =10 µm.

G and H) **Efferocytosis increases during embryogenesis on ventral side of the embryo**. CharON ratio (pHlorina signal/pHCaspGFP signal) of individual corpses in CNS (g), and blood-cavity (hemocoel) (h), across the embryonic stages 12-16 (5 embryos/stage). CharON ratio increased during embryogenesis (One-Way ANOVA, **** =p<.0001).

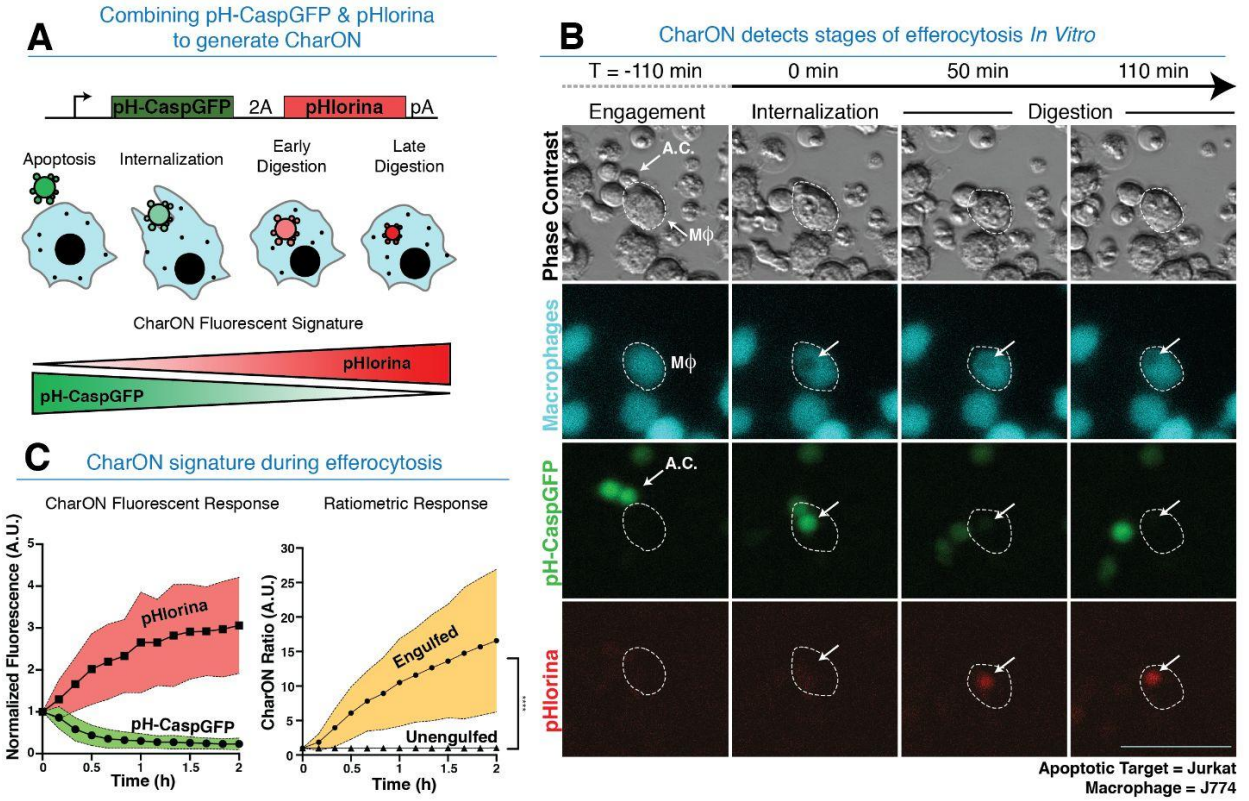
A
Combining pH-CaspGFP & pHlorina to generate CharON
pH-CaspGFP
2A
pHlorina
pA
Apoptosis
Internalization
Early Digestion
Late Digestion
CharON Fluorescent Signature
pHlorina
pH-CaspGFP
B
CharON detects stages of efferocytosis In Vitro
T = -110 min
0 min
50 min
110 min
Engagement
Internalization
Digestion
Phase Contrast
Macrophages
pH-CaspGFP
pHlorina
A.C.
Mϕ
Apoptotic Target = Jurkat
Macrophage = J774
C
CharON signature during efferocytosis
CharON Fluorescent Response
Ratiometric Response
Normalized Fluorescence (A.U.)
CharON Ratio (A.U.)
Time (h)
pHlorina
pH-CaspGFP
Engulfed
Unengulfed

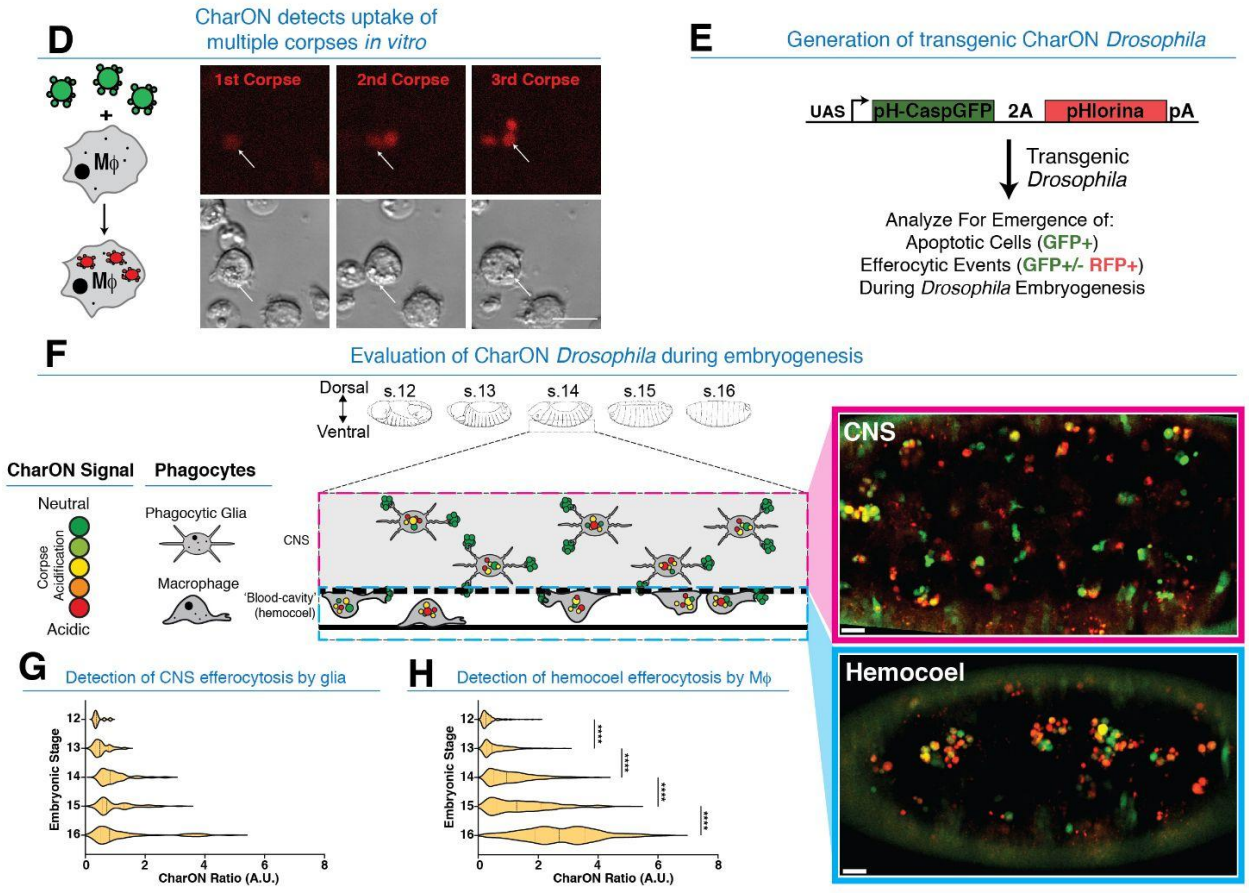
D
CharON detects uptake of multiple corpses in vitro
1st Corpse
2nd Corpse
3rd Corpse
Mϕ
E
Generation of transgenic CharON Drosophila
UAS
pH-CaspGFP
2A
pHlorina
pA
Transgenic Drosophila
Analyze For Emergence of:
Apoptotic Cells (GFP+)
Efferocytic Events (GFP+/- RFP+)
During Drosophila Embryogenesis
F
Evaluation of CharON Drosophila during embryogenesis
Dorsal
Ventral
s.12
s.13
s.14
s.15
s.16
CharON Signal
Phagocytes
Neutral
Corpse Acidification
Acidic
Phagocytic Glia
Macrophage
CNS
Blood-cavity (hemocoel)
CNS
Hemocoel
G
Detection of CNS efferocytosis by glia
H
Detection of hemocoel efferocytosis by Mϕ
Embryonic Stage
CharON Ratio (A.U.)

2.4.3 Macrophages prioritize corpse uptake over degradation

We chose to focus on macrophage efferocytosis due to its synchronised pattern of CharON activity and because of the important role macrophages have in clearing cellular debris during human development and disease. Macrophage-specific expression of moesin-GFP (GAL4 independent) was combined with the ubiquitous expression of CharON (GAL4 driven) to allow *in vivo* macrophage efferocytosis to be visualised through live-cell imaging (*Video 4*). For the first time, this allowed the full efferocytic program to be observed *in vivo*, including apoptosis, macrophage recruitment and target binding ("Find Me"), internalization ("Eat Me") and corpse acidification and degradation ("Digest Me") (*Fig. 3A, Video 5*).

Drosophila macrophages populate the ventral side of the embryo through a highly stereotyped developmental migration, occurring between embryonic stages 12-15 (*Fig. 3B*) [281]. During this journey, they engulf apoptotic corpses arising from the underlying CNS, the total clearance of which coincides with their full dispersal (stage 15)[342]. Quantification of pHlorina positive corpses specifically within macrophages allowed quantification of this process, with corpse burden peaking as expected at embryonic stage 15 (*Fig. 3C*). After an initial lag, the pHlorina intensity also increased with increasing developmental time, particularly between stages 15-16 (post-clearance), again consistent with macrophages prioritizing corpse uptake over degradation (*Fig. 3D*). This was mirrored by the decrease in internalized corpse size, which represents further evidence of degradation (*Fig. 3E*). Thus, macrophages prioritize quick clearance/'corpse clean-up' of the tissue during early developmental dispersal (e.g. stages 12-13), and largely suspend the 'corpse digestion' until later in embryogenesis (stages 14-16).

Tracking macrophages during efferocytosis allowed quantification of their *in vivo* chemotaxis towards CharON-labelled corpses, revealing that macrophages could sense and migrate as far as 8% of the embryo length to fulfill this role (*Fig 3F-3H*) [73]. Of note, the recruitment of multiple macrophages was sometimes required to clear a single, fragmenting apoptotic corpse (*Video 6*). Interestingly, the recruitment of macrophages to corpses and the subsequent uptake of apoptotic bodies took considerably less time (~5-7 min) compared to the time taken to maximally acidify the engulfed debris (~25 min), suggesting that the digestion steps of efferocytosis are likely the more rate limiting steps in clearing high corpse numbers within a tissue. Strikingly, macrophages maintained their high motility throughout the entire efferocytic process and readily moved towards and engulfed further corpses before acidification of their existing corpse burden (*Video 7*). Based on previous *in vitro* studies using cultured and primary phagocytes, it has been thought that the stages of cell clearance from corpse sensing to engulfment to digestion occur as a continuum [343]; however, these *in vivo* data collectively imply

that macrophages prioritize corpse uptake over degradation, when confronted with a large number of developing apoptotic corpses, and adopt a strategy of ‘eat-first, digest-later’. This may in part explain why it is often difficult to detect apoptotic cells even in tissues with high turnover (now revealed through CharON), and such rapid removal of emerging apoptotic cells may help avoid secondary necrosis of the apoptotic cells.

Figure 2.3: A macrophage efferocytic program is orchestrated during development to ensure removal and degradation of CNS corpses.

A) **CharON visualises the different stages of efferocytosis during *in vivo* imaging**. Time-lapse imaging of a GFP-labelled macrophage (MΦ, blue dashed outline) performing efferocytosis of a CharON-labelled apoptotic corpse (A.C., white dashed outline) within the *Drosophila* embryo (stage 12). Apoptosis induces pH-CaspGFP (green) activation in the dying cells and attracts the macrophage (green), leading to target binding and uptake. Following internalisation, acidification and degradation of the corpse is detected through increasing pHlorina signal (red) Scale bar =(10 μm). Please note that the corpse binding internalization only took ~5 minutes, while the subsequent digestion took 5x longer.

B) **Increasing CharON signal detected during macrophage dispersal and efferocytosis**. Diagrams and representative images highlighting the dispersal of *Drosophila* GFP-labelled macrophages (green) and their efferocytosis of CharON-labelled corpses (pH-CaspGFP (green) and pHlorina (red) on the ventral side of the embryo (outlined) during stages 12-16. Scale bar =10 μm.

C to E) **Mean corpse acidification, size, and corpses per macrophage**.

c, Mean macrophage corpse burden (corpses/macrophage, embryo averages, 5/stage) increases across embryonic stages 12-16 (One-Way ANOVA,*= p<=.0002, **** =p<.0001).

d, Mean corpse size (μm^2, embryo averages, 5/stage) decreases in macrophages across embryonic stages 12-16 (One-Way ANOVA, ** = p<=.0021).

e, Mean pHlorina corpse signal reflecting corpse acidification (embryo averages, 5/stage) increases in macrophages across embryonic stages 12-16 (One-Way ANOVA, ** = p<=.0021, *** = p<=.0002, **** =p<.0001).

F to H) **Quantification of macrophage migration to apoptotic cells**.

f, Centroid measurement is the macrophage distance from uncleared apoptotic cells. Travelled distance is the total travel distance during macrophage migration towards uncleared apoptotic cells. Euclidean distance is the shortest distance from macrophage initial location to point of engulfment.

g, Measurement of macrophage Forward Migration Index (FMI) during macrophage recruitment. Forward Migration Index (FMI) demonstrates strong directed migration during efferocytosis. FMI +1.0 = perfect migration towards corpse, FMI -1.0 = perfect chemotaxis away from corpse, FMI 0

= random migration. FMI (x) = migration of cells on the same axis as the corpse (strong, positive chemotaxis), FMI (y) = movement of the same macrophages on the perpendicular axis to corpses (random).

h, Measurement of macrophage speed during migration towards an apoptotic cell.

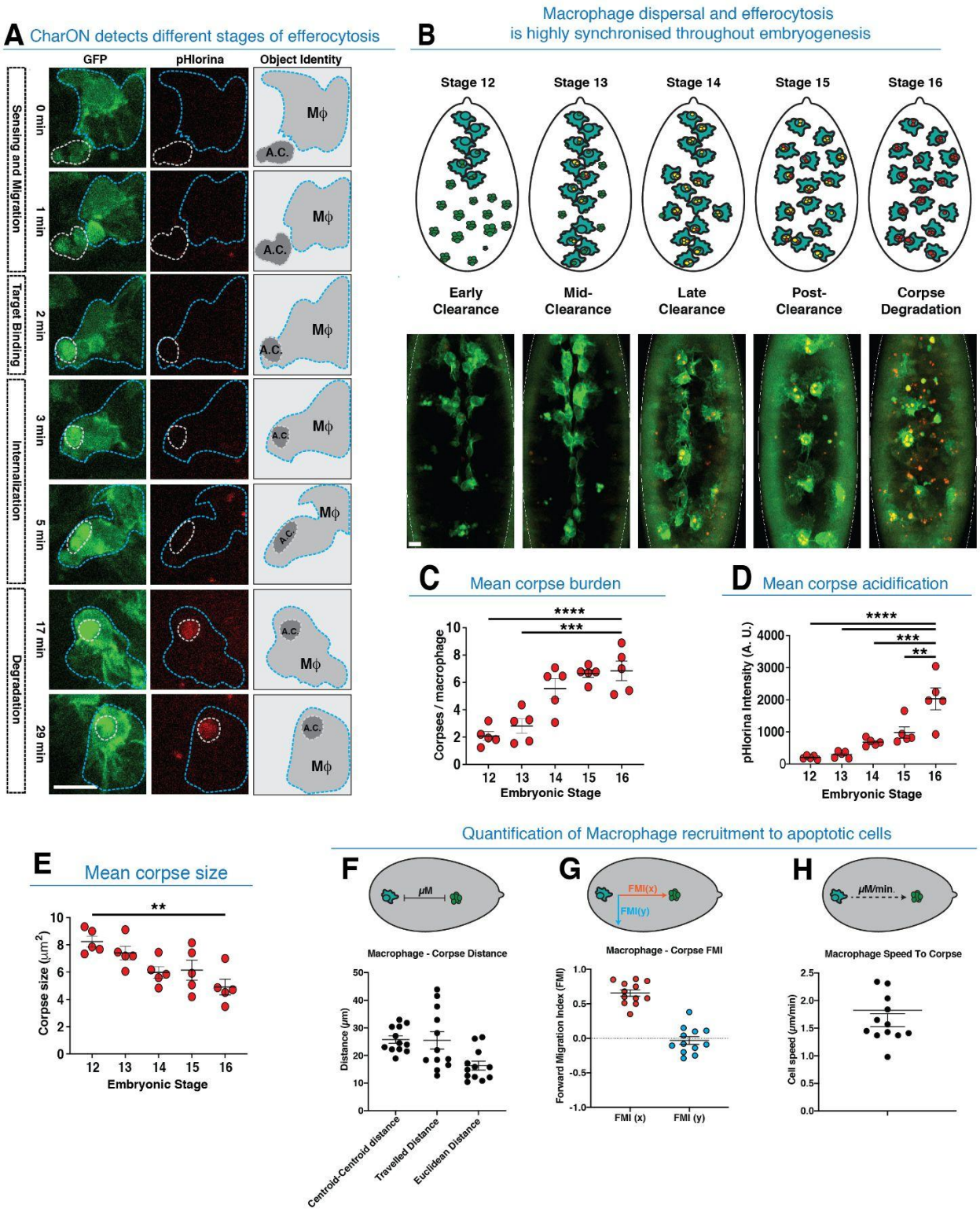
A CharON detects different stages of efferocytosis
GFP
pHlorina
Object Identity
Sensing and Migration
Target Binding
Internalization
Degradation
0 min
1 min
2 min
3 min
5 min
17 min
29 min
Mϕ
A.C.
B
Macrophage dispersal and efferocytosis
is highly synchronised throughout embryogenesis
Stage 12
Stage 13
Stage 14
Stage 15
Stage 16
Early Clearance
Mid-Clearance
Late Clearance
Post-Clearance
Corpse Degradation
C
Mean corpse burden
Corpses / macrophage
Embryonic Stage
D
Mean corpse acidification
pHlorina Intensity (A. U.)
Embryonic Stage
E
Mean corpse size
Corpse size (μm²)
Embryonic Stage
Quantification of Macrophage recruitment to apoptotic cells
F
Macrophage - Corpse Distance
Distance (μm)
Centroid-Centroid distance
Travelled Distance
Euclidean Distance
G
Macrophage - Corpse FMI
Forward Migration Index (FMI)
FMI (x)
FMI (y)
H
Macrophage Speed To Corpse
Cell speed (μm/min)

2.4.4 Macrophage prioritization of uptake results in corpse burden heterogeneity

Live-cell imaging of dispersing macrophages revealed that the first, 'pioneer' macrophages to emerge on the ventral side of the embryo (stages 11/12) are confronted with a dense field of CharON-labelled (pH-CaspGFP positive) apoptotic corpses (*Video 7, Supplemental Data 5A*). We found that the rapid uptake of these corpses by the dispersing macrophages resulted in dramatic disparities in macrophage corpse burden. For example, by embryonic stage 15 (post-clearance), macrophages which had engulfed an excessive number of apoptotic bodies (as many as 20) were found in immediate proximity to macrophages that had taken up very little debris (*Fig. 4A*). When we quantified macrophage corpse burden during their dispersal, apoptotic bodies were distributed unequally during this efferocytic clearance (*Supplemental Data 5B*). Variation in macrophage corpse burden was observed from the very start of dispersal (stage 12), with a subset of macrophages exhibiting corpse numbers that were at least 2 standard deviations above the others at every developmental stage (*Fig 4B*). We then classified these macrophages as having either no corpse burden, low corpse burden (≤3 corpses), medium corpse burden (4-6 corpses) or high corpse burden (≥7 corpses) (*Fig 4C*). Within the macrophages classified as having high corpse burden, remarkable examples of macrophages with extreme corpse burden (≥10 corpses) were also observed. Interestingly, during embryogenesis (stages 12-16), a population of macrophages with extreme corpse load emerge before clearance has completed (stage 15). In contrast, while the number of macrophages with low corpse burden steadily decreased during embryogenesis, there was still a significant population of macrophages with low corpse burden even post-clearance (stages 15-16) (*Fig 4C*). These data suggest that when a high concentration of apoptotic cells emerge, the corpse burden is not shared equally among resident macrophages and that a subset of macrophages demonstrate unrestrained uptake to ensure rapid clearance, resulting in unequal corpse burdens.

We tested this concept using agent-based modelling of macrophage efferocytosis, where each macrophage is considered an 'agent' with specific function to seek and consume corpses. This modeling demonstrated that when equal corpse distribution is 'enforced' through restrictive consumption limits, simulated clearance time drastically increased (*Fig. 4D*). Conversely, releasing the macrophages from such consumption limit led to rapid corpse clearance *in silico*

and yielded the unequal corpse burden (*Fig. 4E, Video 8*).

While macrophages can robustly internalize even an extreme number of corpses, we explored whether high corpse load induced any subsequent adaptation. We quantified mean pHlorina intensity levels in macrophages with low, medium, and high corpse burdens over the course of their dispersal (*Fig. 4F*). During stages 12-15, mean pHlorina intensity increased equally over the three groups. However, at stage 16 (post-clearance/peak degradation) there was a dramatic increase in mean pHlorina intensity in macrophages with high corpse burden, implying macrophages with greater corpse load are not limited in their digestive capacity, and may even increase their ability to acidify their cargo (perhaps a version of positive feed-back). Taken together, macrophages can adapt and compensate for high corpse burden by enhancing corpse degradation.

2.4.5 Macrophages compromise between apoptotic and necrotic corpse uptake *in vivo*

We next explored whether there were any consequences of varying corpse burden for *in vivo* macrophage behavior. Tracking of dispersed macrophages (stage 15) demonstrated that corpse burden had no effect on basal motility, despite low and high corpse burdens representing very different physical loads (*Video 9*). To study the inflammatory chemotaxis of these macrophages, we used laser-ablation to generate epithelial wounds in stage 15 embryos and tracked the responding cells (*Supplemental Data 5C*). Addressing how macrophages confront the presence of mixed corpses is particularly relevant for diseases such as atherosclerosis where both apoptotic and necrotic corpses arise in the same tissue neighborhood. In our *Drosophila* embryo model, macrophages with high corpse burdens were found to readily migrate towards laser-induced wounds and there was no significant difference in corpse burden between responding and non-responding macrophages (*Fig. 4G, Fig. 4H, Video 10*).

Laser-induced wounding of *Drosophila* embryos is not associated with apoptosis. Instead, the wound is entirely necrotic, as demonstrated by the lack of pH-CaspGFP fluorescence (*Fig. 4G, Video 10*). One role of the recruited inflammatory macrophages is to clear necrotic debris, which we could readily observe as fluorescence-negative particles taken up by the GFP positive macrophages. Although macrophages with high corpse burden were recruited to the wound comparably, once at the wound, macrophages with high corpse burden were significantly less likely to engulf necrotic debris (*Fig. 4I*). This suggested that macrophage efferocytic capacity is not limitless *in vivo*, rather can reach a certain type of 'satiety' (*Fig. 4I*). Therefore, the rapid clearance of developmental apoptosis and the unequal corpse burden that arises because of this 'eat-first, digest-later' strategy, has consequences for the ability of macrophages to subsequently clear necrotic debris in response to tissue damage. Thus, despite their extraordinary robustness and plasticity, macrophages face an efferocytic compromise within the complex environment found *in vivo.*

The above approach also allowed us to ask whether the apoptotic and necrotic cargo within the same macrophage may fuse. Remarkably, rapid acidification of necrotic corpses sometimes occurred through fusion with phagosomes containing a pre-acidified apoptotic corpse (*Fig. 4J, Video 11*). In contrast to acidification of apoptotic corpses cleared as part of development, which took approximately 30 minutes, swift acidification of engulfed necrotic debris was observed following contact with a pHlorina positive, internalized apoptotic corpse. This perhaps hints at modalities by which macrophages may promote rapid degradation of necrotic debris, potentially during inflammation.

Figure 2.4: Macrophage efferocytic heterogeneity during development

A) **Macrophages take up different corpse loads.** (left) Ventral view of embryo (stage 15, post-clearance) with GFP-labelled macrophages (green) and CharON-labelled apoptotic corpses (pH-CaspGFP (green) and pHlorina (red). Two adjacent macrophages with very different corpses burdens are highlighted (dashed-boxes) and magnified in subsequent images (middle and right). Macrophage cell bodies are outlined in white. Scale bar =10 μm.

B and C) **Quantification of heterogeneity in macrophage corpse burden.** b, The range in corpse number/macrophage is non-uniform (****) during late stage embryogenesis (stage 16). Macrophages with corpse burden 1 and 2 standard deviations from the mean are highlighted (blue and orange boxes respectively) for each embryonic stage (D'Agostino & Pearson Normality test, p<=.0001). c, Macrophages with no corpse burden (0 corpses), low (1-3 corpses), medium (4-6 corpses) or high corpse burden (7+) are indicated. Some within the high group display extreme corpse burden (10+). Although corpse burden increases with developmental time (stages 12-16), macrophages exhibit most variation during stages 15-16.

D and E) ***In silico* modeling of macrophage corpse burden.** d, *In silico*, equal corpse burden can be enforced with strict macrophage consumption limits (top). Increasing consumption limit (middle and bottom) introduces unequal corpse burden, recapitulating the *in vivo* distribution. Histograms are representative, endpoint distributions from final iteration of simulations. See other corpse limits and distributions in Supplemental Data 5d. e, *In silico* clearance time is drastically reduced when per macrophage consumption is greater. Simulation was run until clearance was completed or the time to achieve 1,000 iterations. Simulations were repeated 50x to yield standard deviations.

F) **High corpse burden promotes macrophage adaptation.** Mean corpse acidification/macrophage increases uniformly during clearance (up to embryonic stage 15), regardless of corpse burden. However, by stage 16, macrophages with high corpse burdens (7+) have significantly (*) elevated mean corpse acidification/macrophage, implying adaptation to their increased burdens (One-Way ANOVA, * = p<=.0332).

G and H) **Macrophage inflammatory chemotaxis to wounds.** g, After laser-induced wounding at stage 15 (post-clearance), GFP-labelled macrophages (green) were recruited to the wound edge (dashed oval), and their apoptotic corpse burdens measured through CharON (green/red). Three macrophages with Medium-High corpse burdens that start equidistant from the wound edge (0 min), were tracked (white dots/lines) over 20 min. While one macrophage

did not respond to the wound, high corpse burden does not appear to impede the chemotaxis of the other two macrophages. Scale bar =10 μm. h, (left) Schematic of response/non-response of macrophages (green) to wounds (gray). (right) Apoptotic corpse burden of macrophages does not impair responding to wounds (1 hr post-wounding).

I) **Corpse burden impairs necrotic clearance.** (left) Diagram highlighting uptake of necrotic debris by macrophages (green) after recruitment to the wound (gray). (right) Inflammatory macrophages with high developmental corpse burdens are significantly (*) less likely to engulf necrotic debris at the wound (Unpaired t-test, , * = p<=.0332).

J) **Macrophage clearance of necrotic debris.** Time-lapse imaging of a GFP-labelled macrophage (green) containing CharON-labelled apoptotic corpses (pH-CaspGFP (green) and pHlorina (red)), engulfing necrotic debris at the wound ('fluorescent-negative' vacuole). In the absence of caspase cleavage during necrosis, the activation of pH-CaspGFP in CharON helped distinguish the developmental apoptotic corpses from the wound-induced necrosis. However, acidification of necrotic debris is detectable via pHlorina, occurring rapidly after interaction (phagosomal fusion) with an acidified apoptotic corpse. Scale bar =10 μm.

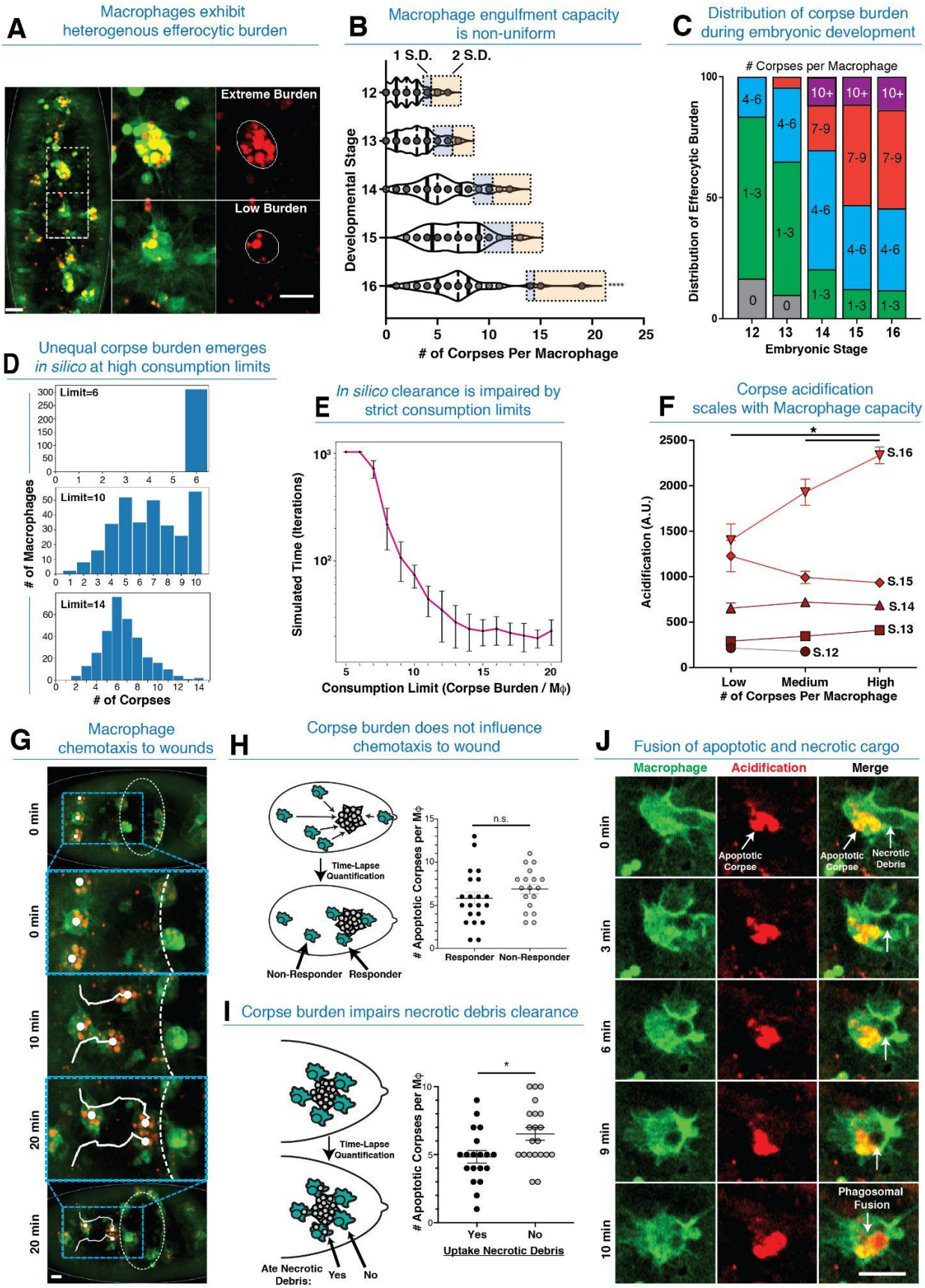
A
Macrophages exhibit heterogenous efferocytic burden
Extreme Burden
Low Burden
B
Macrophage engulfment capacity is non-uniform
1 S.D.
2 S.D.
Developmental Stage
# of Corpses Per Macrophage
****
C
Distribution of corpse burden during embryonic development
Corpses per Macrophage
Distribution of Efferocytic Burden
Embryonic Stage
4-6
1-3
0
10+
7-9
D
Unequal corpse burden emerges in silico at high consumption limits
Limit=6
Limit=10
Limit=14
# of Macrophages
# of Corpses
E
In silico clearance is impaired by strict consumption limits
Simulated Time (Iterations)
Consumption Limit (Corpse Burden / Mϕ)
F
Corpse acidification scales with Macrophage capacity
Acidification (A.U.)
S.16
S.15
S.14
S.13
S.12
Low
Medium
High
# of Corpses Per Macrophage
G
Macrophage chemotaxis to wounds
0 min
0 min
10 min
20 min
20 min
H
Corpse burden does not influence chemotaxis to wound
Time-Lapse Quantification
Non-Responder
Responder
Apoptotic Corpses per Mϕ
n.s.
Responder
Non-Responder
I
Corpse burden impairs necrotic debris clearance
Time-Lapse Quantification
Ate Necrotic Debris:
Yes
No
Apoptotic Corpses per Mϕ
*
Yes
No
Uptake Necrotic Debris
J
Fusion of apoptotic and necrotic cargo
Macrophage
Acidification
Merge
0 min
3 min
6 min
9 min
10 min
Apoptotic Corpse
Necrotic Debris
Phagosomal Fusion

Figure 2.5: Evaluation of Apoptosis Probes, pH-CaspGFP

A) Jurkat cells stably expressing GC3ai, ZipGFP and FlipGFP were subjected to 150mJ UV-C and monitored over 1-hour intervals for the appearance of GFP+ events via flow cytometry. N=3 independent experiments. (Two-Way ANOVA, **** =p<.0001)

B) (left) Fold changes in fluorescence of GC3ai, ZipGFP, and FlipGFP expressing Jurkat cells were compared after 4 hours of UV-C exposure. GFP Fold Change was calculated compared to T=0 hr. (One-Way ANOVA, **** =p<.0001) (right) Fidelity of apoptosis detection of GC3ai, ZipGFP and FlipGFP stably expressing Jurkat cells were determined through proportion of double-positive (Annexin V+ / GFP+) events (One-Way ANOVA, **** =p<.0001).

C) Phosphatidylserine on apoptotic cells (measured via Annexin V) on GC3ai (green triangle), ZipGFP (grey square) and FlipGFP (blue square) expressing Jurkat cells upon UV-C exposure over a time course.

D) pH-CaspGFP (orange) and GC3ai (green) GFP+ and Annexin V+ signals were determined over a time course upon UV-C exposure. (One-Way ANOVA, n.s. = not significant)

E) pH-CaspGFP stably expressing Jurkat cells were subjected to either UV-C (black circle), ABT-737 (blue square) or Staurosporine (magenta triangle) and monitored over 4 hours for double-positive (Annexin-V+ / GFP+) events.

F) GFP+ Fold Change in pH-CaspGFP stably expressing Jurkat cells after 2 and 4 hours post-exposure to UV-C, ABT-737 or Staurosporine, compared to T=0 hr.

G) Time-course of Annexin V+ (grey square) and GFP+ (green circle) events upon exposure of pH-CaspGFP stably expressing Jurkat cells to UV-C, ABT-737 or Staurosporine. In addition, cells pretreated with caspase inhibitor Q-VD was used as a control (triangle).

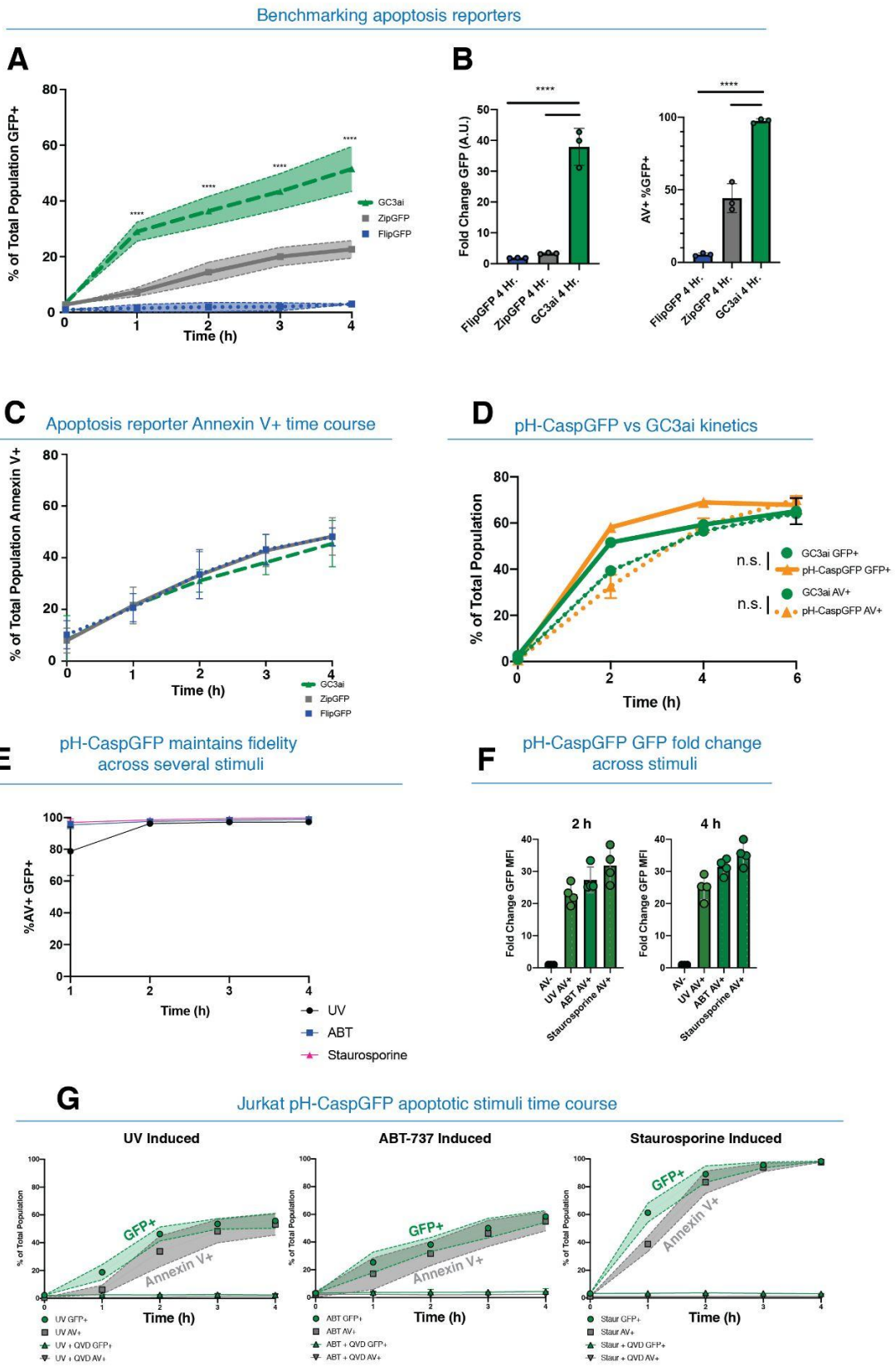
Benchmarking apoptosis reporters
A
% of Total Population GFP+
Time (h)
GC3ai
ZipGFP
FlipGFP
B
Fold Change GFP (A.U.)
AV+ %GFP+
FlipGFP 4 Hr.
ZipGFP 4 Hr.
GC3ai 4 Hr.
C
Apoptosis reporter Annexin V+ time course
% of Total Population Annexin V+
D
pH-CaspGFP vs GC3ai kinetics
% of Total Population
n.s.
GC3ai GFP+
pH-CaspGFP GFP+
GC3ai AV+
pH-CaspGFP AV+
E
pH-CaspGFP maintains fidelity across several stimuli
%AV+ GFP+
UV
ABT
Staurosporine
F
pH-CaspGFP GFP fold change across stimuli
2 h
4 h
Fold Change GFP MFI
AV-
UV AV+
ABT AV+
Staurosporine AV+
G
Jurkat pH-CaspGFP apoptotic stimuli time course
UV Induced
ABT-737 Induced
Staurosporine Induced
GFP+
Annexin V+
% of Total Population
Time (h)

Figure 2.6: Evaluation of pH-CaspGFP in THP-1 and pHlorina expression in mammalian cells

A) THP-1 cells stably expressing pH-CaspGFP were treated with UV-C (top row), ABT-737 (middle row), or Staurosporine (bottom row) and analyzed after 4 hours for presence of GFP+ events. Cells pretreated with caspase inhibitor Q-VD were used as a control.

B) Time-course of THP-1 cells stably expressing pH-CaspGFP after treatment with UV-C (top), ABT-737 (middle) or Staurosporine (bottom) and collection of GFP+ (green circle) and Annexin V+ events (grey square, indicative of phosphatidylserine flipping during apoptosis). Cells pretreated with caspase inhibitor Q-VD was used as a control (triangle).

C) Left: Quantification of cell fluorescence intensity at pH values ranging from pH 5 to 9.8 (n=5 cells), with pH 7 values normalised to 100. Right: Representative image of HeLa cells transfected with pDisplay-pHlorina before and after the application of a solution at pH 7, containing 50 mM NH_4Cl.

D) Apoptotic cell-derived fluorescence change of pHlorina over a time Course (fold change) after internalization by macrophages binned into 30 minute intervals. Fluorescence intensity fold change was compared to T= 0 min. (Two-Way ANOVA, **** = p<.0001).

E) Representative images of HeLa cells transfected with pDisplay-pHlorina, with fluorescence excited with 561 nm or 473 nm Laser , at extracellular pH of 5, 7, and 9.

F) Unengulfed and Engulfed pHlorina expressing Jurkat cells were compared during *in vitro* efferocytosis assays to determine fluorescence response. (Unpaired T-Test, **** = p<.0001).

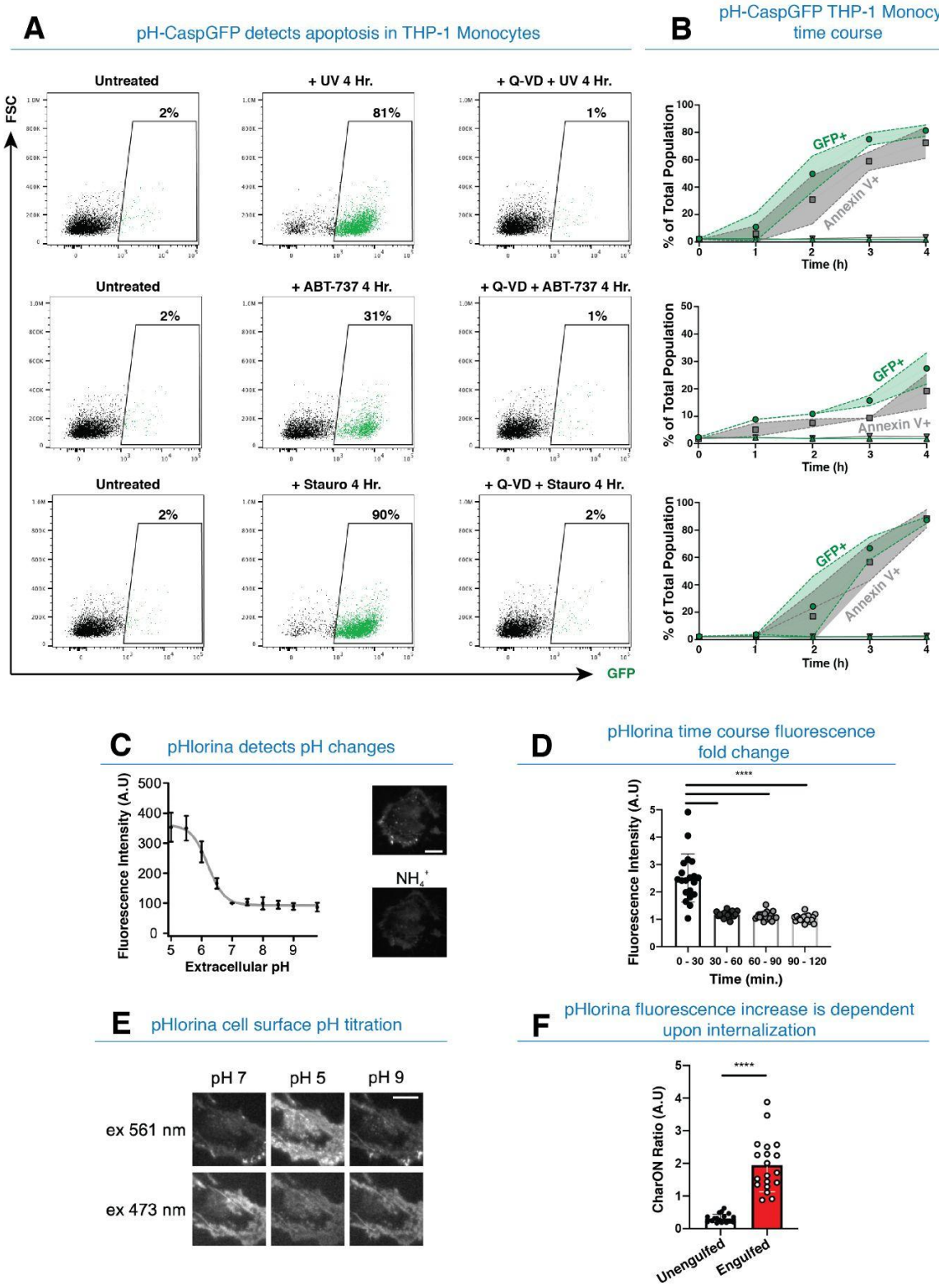
A
pH-CaspGFP detects apoptosis in THP-1 Monocytes
Untreated
+ UV 4 Hr.
+ Q-VD + UV 4 Hr.
2%
81%
1%
Untreated
+ ABT-737 4 Hr.
+ Q-VD + ABT-737 4 Hr.
2%
31%
1%
Untreated
+ Stauro 4 Hr.
+ Q-VD + Stauro 4 Hr.
2%
90%
2%
FSC
GFP
B
pH-CaspGFP THP-1 Monocyte time course
% of Total Population
Time (h)
GFP+
Annexin V+
C
pHlorina detects pH changes
Fluorescence Intensity (A.U)
Extracellular pH
NH4+
D
pHlorina time course fluorescence fold change
Fluorescence Intensity (A.U)
Time (min.)
0 - 30
30 - 60
60 - 90
90 - 120
****
E
pHlorina cell surface pH titration
pH 7
pH 5
pH 9
ex 561 nm
ex 473 nm
F
pHlorina fluorescence increase is dependent upon internalization
CharON Ratio (A.U)
Unengulfed
Engulfed
****

Figure 2.7: In vitro evaluation of pHlorina during efferocytosis and CharON Drosophila expression during embryonic development

A) Mouse J774 Macrophages (cyan) were co-cultured with apoptotic pHlorina expressing Jurkat cells (red) during *in vitro* engulfment assays. Arrows indicate engulfment of pHlorina expressing Jurkat cells by Mouse J774 Macrophages starting at T = 0 min.

B) Embryo-wide CharON expressing *Drosophila* GFP (pH-CaspGFP) signal during stages 12 through 16 of embryogenesis. N = 4 embryos.

C) Embryo-wide CharON expressing *Drosophila* RFP (pHlorina) signal during stages 12 through 16 of embryogenesis. N = 4 embryos.

D) Embryo-wide CharON expressing *Drosophila* CharON Ratio (pHlorina / pH-CaspGFP) signal during stages 12 to 16 of embryogenesis. N = 5 embryos.

E) Average size of corpses within the CNS region of the embryo from stages 12 to 16.

F) Average size of corpses within the hemocoel (blood cavity) region of the embryo from stages 12 to 16 (One-Way ANOVA, ** = $p<.0021$).

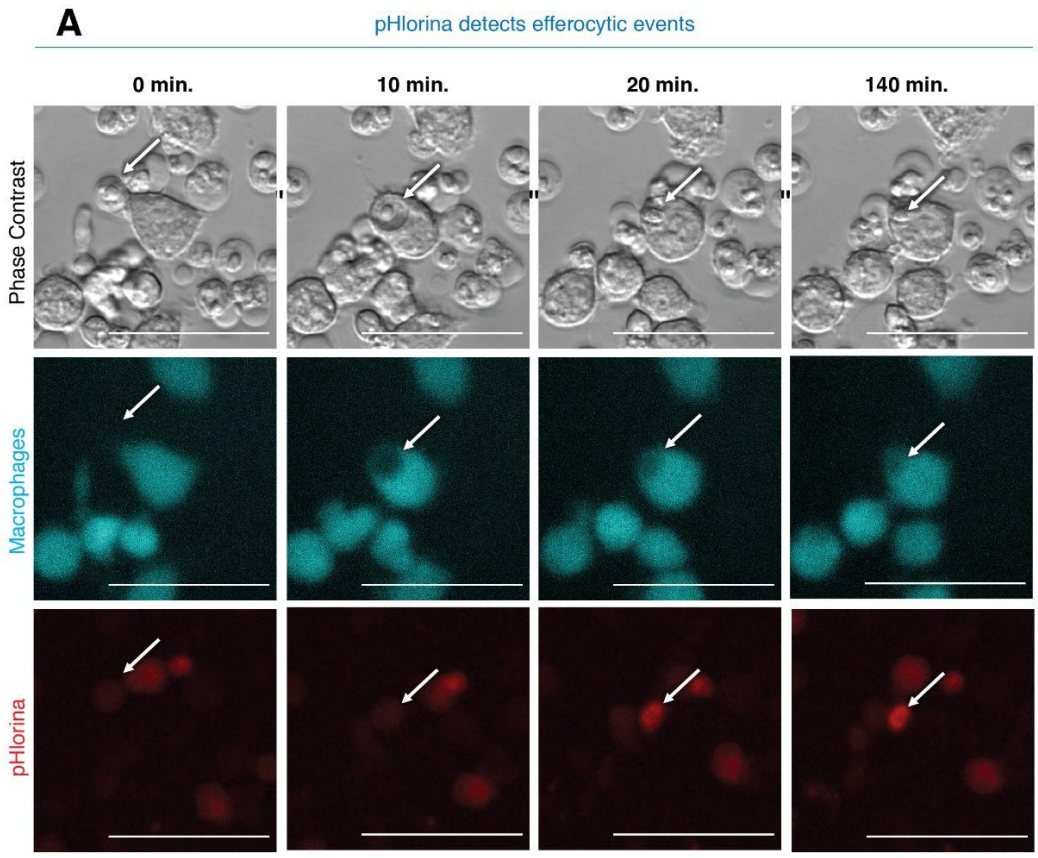
A
pHlorina detects efferocytic events
0 min.
10 min.
20 min.
140 min.
Phase Contrast
Macrophages
pHlorina

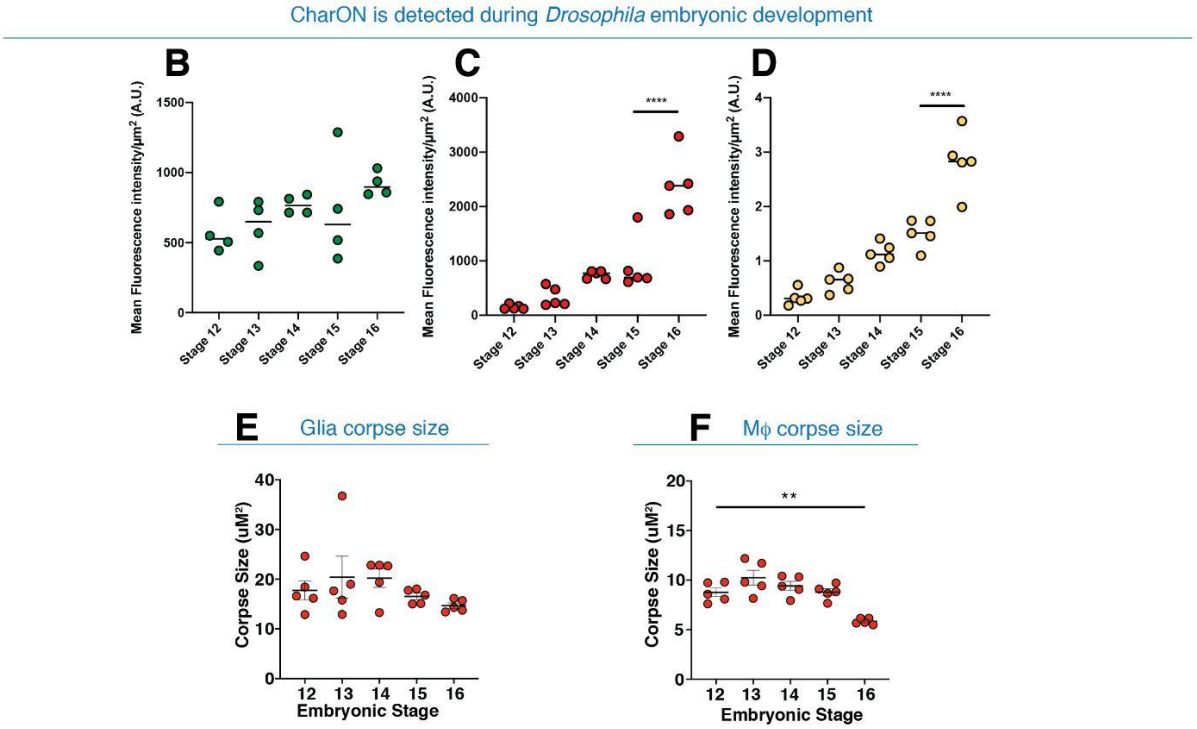
CharON is detected during Drosophila embryonic development
B
C
D
Mean Fluorescence intensity/µm² (A.U.)
Stage 12
Stage 13
Stage 14
Stage 15
Stage 16
****
E
Glia corpse size
F
Mϕ corpse size
Corpse Size (uM²)
Embryonic Stage
**

Figure 2.8: CharON fluorescent signature during development, efferocytic event tracking *in vivo* and embryonic macrophage dispersal

A) Apoptosis (pH-CaspGFP) and Acidification (pHlorina) of CharON expressing *Drosophila* was evaluated within the ventral notochord across stages 12 to 16. Events were thresholded and segmented using Ilastik.

B) (left) Quantification of Apoptosis (pH-CaspGFP); (right) Acidification (pHlorina) within CharON expressing *Drosophila* across stages 12 to 16 of embryogenesis. (One-Way ANOVA, ** = $p<.0021$, * = $p<.0332$)

C) (left) *Drosophila* Macrophages (mCherry, white) dispersing around Dorsal side of embryo during embryonic stages 12: (Early Arrival), 14 (Dorsal Migration), and 16 (Lateral Migration). (right) Corpse size and pHlorina intensity, as determined via CharON, was evaluated at stages 12, 14 and 16. Least Square Regression fit was employed.

D) (left) Tracking of CharON fluorescence (pH-CaspGFP and pHlorina) during macrophage mediated efferocytosis. Upon internalization (T=0 min), an event was tracked over 1 minute intervals. Fluorescence was normalised to T=0 min. (right) Fold change in normalised CharON fluorescence response during macrophage-mediated efferocytosis.

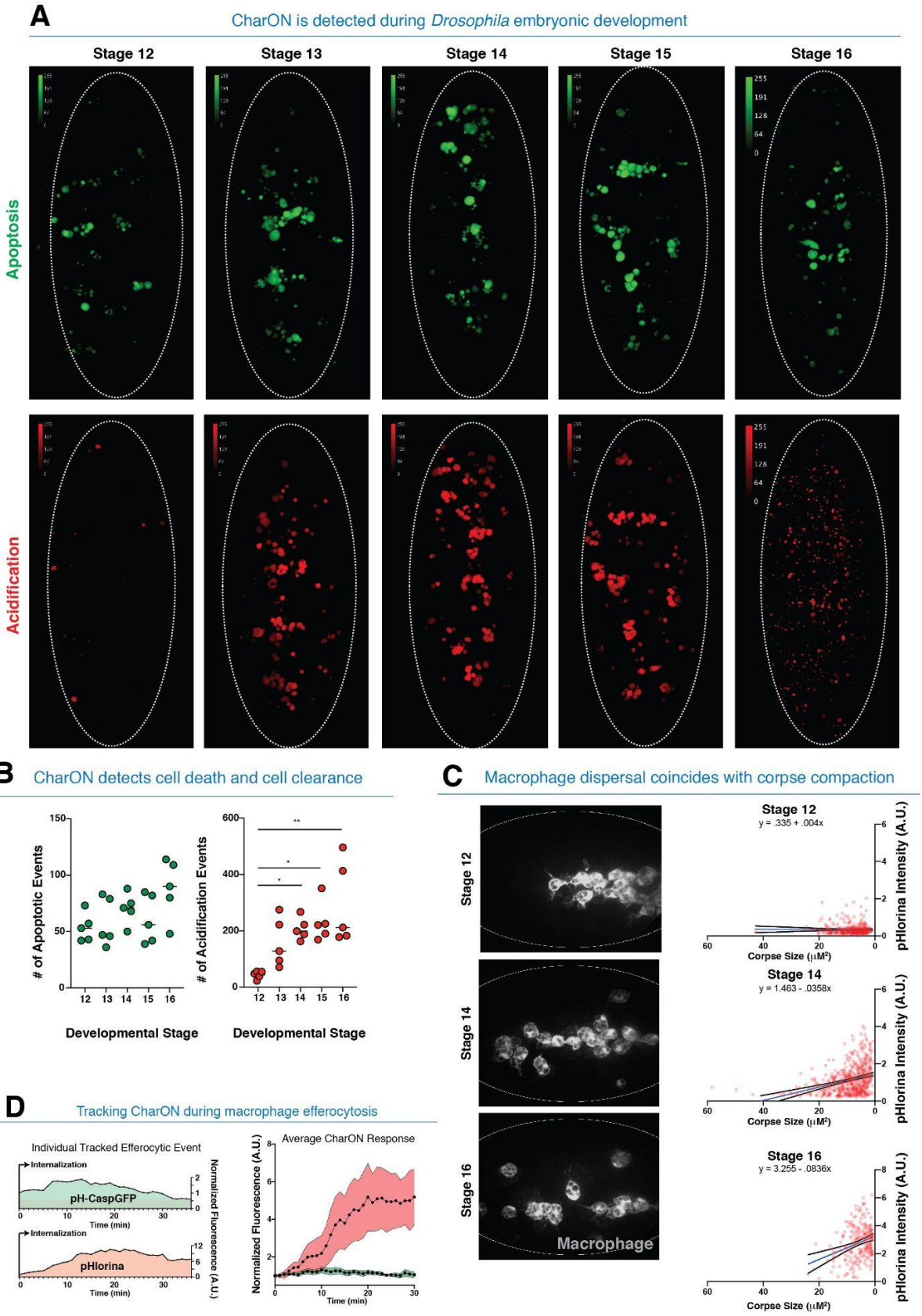
A
CharON is detected during Drosophila embryonic development
Stage 12
Stage 13
Stage 14
Stage 15
Stage 16
Apoptosis
Acidification
B
CharON detects cell death and cell clearance
# of Apoptotic Events
# of Acidification Events
Developmental Stage
Developmental Stage
C
Macrophage dispersal coincides with corpse compaction
Stage 12
Stage 14
Stage 16
Macrophage
Stage 12
y = .335 + .004x
Stage 14
y = 1.463 - .0358x
Stage 16
y = 3.255 - .0836x
pHlorina Intensity (A.U.)
Corpse Size (μM²)
D
Tracking CharON during macrophage efferocytosis
Individual Tracked Efferocytic Event
Internalization
pH-CaspGFP
pHlorina
Time (min)
Normalized Fluorescence (A.U.)
Average CharON Response
Normalized Fluorescence (A.U.)
Time (min)

Figure 2.9: Pioneer Macrophage dispersal and efferocytosis, efferocytic burden across embryonic stages and Drosophila wounding model

A) Diagrams and representative images highlighting how the first ('pioneer') GFP-labelled macrophages (MΦ, white dashed outlines) that arrive on the ventral side of embryo (early-stage 12) are confronted by a high concentration of CharON-labelled apoptotic corpses (pH-CaspGFP, blue dashed outlines). Embryo outlined in white, embryonic stages 12-13. Scale bar = (10 μm).

B) Absolute number of corpses /macrophages increases with increasing developmental time (embryonic stages 12-16).

C) Diagram highlighting laser-ablation (blue) of embryo (stage 15), resulting in epithelial wound (gray). GFP-labelled macrophage (green), carrying their developmental load of CharON-labelled corpse (yellow/red) are recruited to the wound as part of inflammation to clear necrotic debris at the wound.

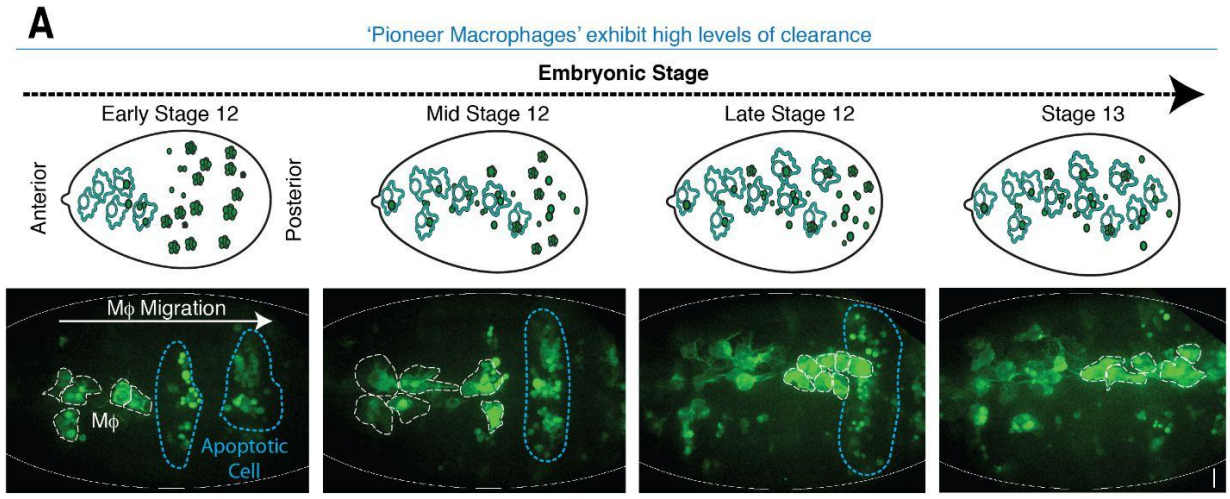
A
'Pioneer Macrophages' exhibit high levels of clearance
Embryonic Stage
Early Stage 12
Mid Stage 12
Late Stage 12
Stage 13
Anterior
Posterior
Mϕ Migration
Mϕ
Apoptotic Cell

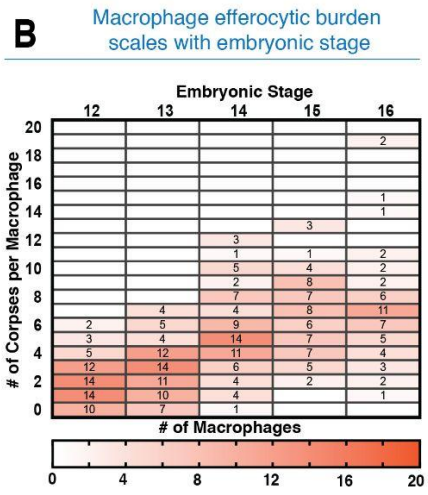
B
Macrophage efferocytic burden scales with embryonic stage
Embryonic Stage
12 13 14 15 16
# of Corpses per Macrophage
0 2 4 6 8 10 12 14 16 18 20
# of Macrophages
0 4 8 12 16 20

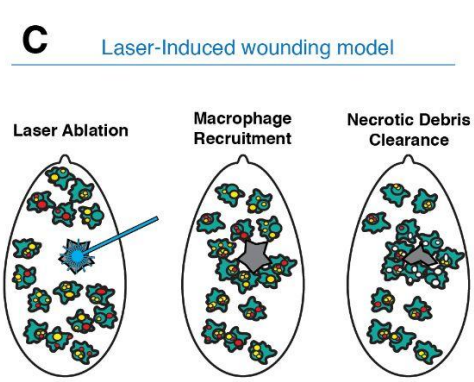
C
Laser-Induced wounding model
Laser Ablation
Macrophage Recruitment
Necrotic Debris Clearance

Figure 2.10: In silico modeling of efferocytic burden with consumption limits

A) Agent-based modeling iterations of consumption limit ranging from 6 to 14 corpses/macrophage shows distribution of corpse numbers/macrophage. Histograms are representative, endpoint distributions from final iteration of simulations.

A

Strict consumption limits shape Macrophage corpse distribution

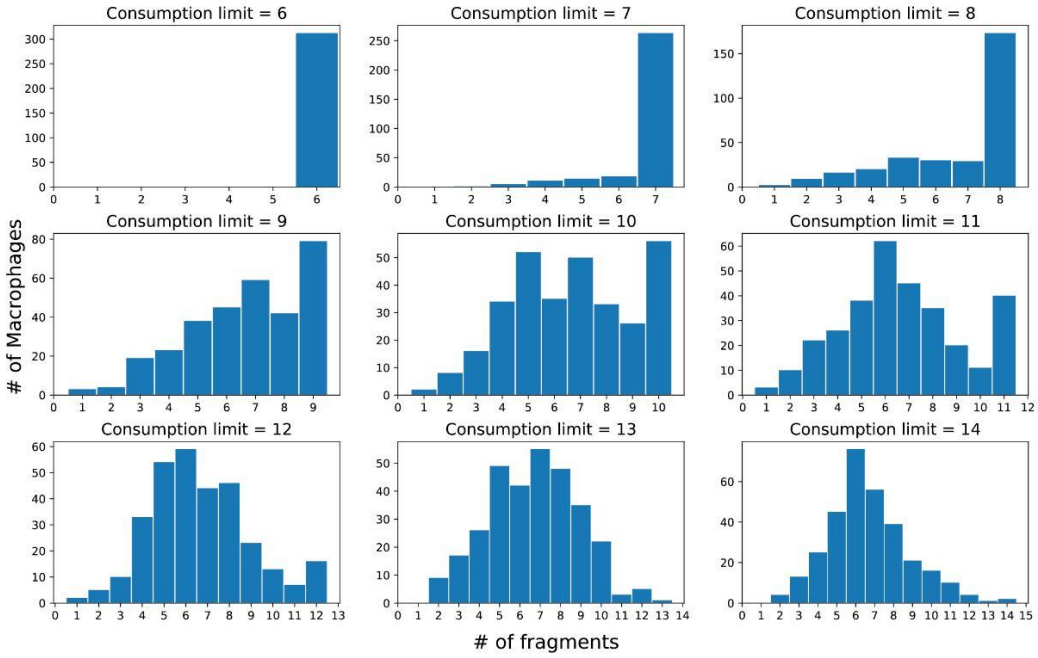

Table 2.1: Sequences of pHlorina, CharON and UAS-CharON

pHlorina:

Gccaccatggtgagcaagggcgaggagaataacatggccatcatcaaggagttcatgcgcttcaaggtgcacatggagggctccg
tgaacggccacgagttcgagatcgagggcgagggcgagggccgcccctacgaggcctttcagaccgctaagctgaaggtgacca
agggtggccccctgcccttcgcctgggacatcctgtcccctcagttcatgtacggctccaaggtttacattaagcacccagccgacatc
cccgactacttcaagcagtccttccccgagggcttcaggtgggagcgcgtgatgaacttcgaggacggcggcattattcacgttaacc
aggactcctccctgcaggacggcgtgttcatctacaaggtgaagctgcgcggcaccaacttcccctccgacggccccgtaatgcaga
agaagaccatgggctatgaggcctccgaggagcggatgtaccccgaggacggcgccctgaagagcgagtgtaaggagaggctg
aagctgaaggacggcggccactacgccgccgaggtcaagaccacctacaaggccaagaagcccgtgcagctgcccggcgcctа
catcgtcgacatcaagttggacatcgtgtcccacaacgaggactacaccatcgtggaacagtacgaacgcactgagggccgccact
ccaccggcggcatggacgagctgtacaagtaa

Kozak

CharON:

Gccaccatgatcaagatcgccaccaggaagtacctgggcaagcagaacgtgtacgacatcggcgtggagagggaccacaacttc
gccctgaagaacggcttcatcgccagcaactgcttcaacgaattcatggacaagcagaagaacggcatcaaggcgaacttcaaga
tccgccacaacgtcgaggacggcagcgtgcagctcgccgaccactaccagcagaacacccccatcggcgacggccccgtgctgc
tgcccgacaaccactacctgagcacccattccaagctgagcaaagaccccaacgagaagcgcgatcacatggtcctgctggagttc
gtgaccgccgccgggatcgacgaggtggacggcgagctgttcaccggggtggtgcccatcctggtcgagctggacggcgacgtaa
acggccacaagttcagcgtgcgcggcgagggcgagggcgatgccaccaacggcaagctgaccctgaagttcatctgcaccaccg
gcaagctgcccgtgccctggcccaccctcgtgaccaccctgacctacggcgtgcagtgcttcagccgctaccccgaccacatgaag
cagcacgacttcttcaagtccgccatgcccgaaggctacgtccaggagcgcaccatctccttcaaggacgacggcacctacaagac
ccgcgccgaggtgaagttcgagggcgacaccctggtgaaccgcatcgagctgaagggcatcgacttcaaggaggacggcaacat
cctggggcacaagctggagtacaacttcaacagccacaacgtctatatcacggccggatccgccgagtactgcctgagctacgaga
ccgagatcctgaccgtggagtacggcctgctgcctatcggcaagatcgtggagaagaggatcgagtgcaccgtgtacagcgtggac
aacaacggcaacatctacacccagcctgtggcccagtggcacgacaggggcgagcaggaggtgttcgagtactgcctggaggac
ggcagcctgatcagggccaccaaggaccacaagttcatgaccgtggacggccagatgctgcctatcgacgagatcttcgagaggg
agctggacctgatgagggtggacaacctgcctaactctagagccacgaacttctctctgttaaagcaagcaggagacgtggaagaa
aaccccggtcctgccaccatggtgagcaagggcgaggagaataacatggccatcatcaaggagttcatgcgcttcaaggtgcacat
ggagggctccgtgaacggccacgagttcgagatcgagggcgagggcgagggccgcccctacgaggcctttcagaccgctaagct
gaaggtgaccaagggtggcccctgcccttcgcctgggacatcctgtcccctcagttcatgtacggctccaaggtttacattaagcacc
cagccgacatccccgactacttcaagcagtccttccccgagggcttcaggtgggagcgcgtgatgaacttcgaggacggcggcatta
ttcacgttaaccaggactcctccctgcaggacggcgtgttcatctacaaggtgaagctgcgcggcaccaacttcccctccgacggccc
cgtaatgcagaagaagaccatgggctatgaggcctccgaggagcggatgtaccccgaggacggcgccctgaagagcgagtgtaa
ggagaggctgaagctgaaggacggcggccactacgccgccgaggtcaagaccacctacaaggccaagaagcccgtgcagctg
cccggcgcctacatcgtcgacatcaagttggacatcgtgtcccacaacgaggactacaccatcgtggaacagtacgaacgcactga
gggccgccactccaccggcggcatggacgagctgtacaagtaa

Elements:

Kozak
pH-CaspGFP
P2A
pHlorina

UAS-CharON:

ggatccaagcttgcatgcctgcaggtcggagtactgtcctccgagcggagtactgtcctccgagcggagtactgtcctccgagcggag
tactgtcctccgagcggagtactgtcctccgagcggagactctagcgagcgccggagtataaatagaggcgcttcgtctacggagcg
acaattcaattcaaacaagcaaagtgaacacgtcgctaagcgaaagctaagcaaataaacaagcgcagctgaacaagctaaac
aatctgcagtaaagtgcaagttaaagtgaatcaattaaaagtaaccagcaaccaagtaaatcaactgcaactactgaaatctgccaa
gaagtaattattgaatacaagaagagaactctgaatCaaaatgatcaagatcgccaccaggaagtacctgggcaagcagaacgtg
tacgacatcggcgtggagagggaccacaacttcgccctgaagaacggcttcatcgccagcaactgcttcaacgaattcatggacaa
gcagaagaacggcatcaaggcgaacttcaagatccgccacaacgtcgaggacggcagcgtgcagctcgccgaccactaccagc
agaacacccccatcggcgacggccccgtgctgctgcccgacaaccactacctgagcacccattccaagctgagcaaagacccca
acgagaagcgcgatcacatggtcctgctggagttcgtgaccgccgccgggatcgacgaggtggacggcgagctgttcaccggggt
ggtgcccatcctggtcgagctggacggcgacgtaaacggccacaagttcagcgtgcgcggcgagggcgagggcgatgccaccaa
cggcaagctgaccctgaagttcatctgcaccaccggcaagctgcccgtgccctggcccaccctcgtgaccaccctgacctacggcgt
gcagtgcttcagccgctaccccgaccacatgaagcagcacgacttcttcaagtccgccatgcccgaaggctacgtccaggagcgca
ccatctccttcaaggacgacggcacctacaagacccgcgccgaggtgaagttcgagggcgacaccctggtgaaccgcatcgagct
gaagggcatcgacttcaaggaggacggcaacatcctggggcacaagctggagtacaacttcaacagccacaacgtctatatcacg
gccggatccgccgagtactgcctgagctacgagaccgagatcctgaccgtggagtacggcctgctgcctatcggcaagatcgtgga
gaagaggatcgagtgcaccgtgtacagcgtggacaacaacggcaacatctacacccagcctgtggcccagtggcacgacaggg
gcgagcaggaggtgttcgagtactgcctggaggacggcagcctgatcagggccaccaaggaccacaagttcatgaccgtggacg
gccagatgctgcctatcgacgagatcttcgagagggagctggacctgatgagggtggacaacctgcctaactctagagccacgaac
ttctctctgttaaagcaagcaggagacgtggaagaaaaccccggtcctgccaccatggtgagcaagggcgaggagaataacatgg
ccatcatcaaggagttcatgcgcttcaaggtgcacatggagggctccgtgaacggccacgagttcgagatcgagggcgagggcga
gggccgcccctacgaggcctttcagaccgctaagctgaaggtgaccaagggtggccccctgcccttcgcctgggacatcctgtcccc
tcagttcatgtacggctccaaggtttacattaagcacccagccgacatccccgactacttcaagcagtccttccccgagggcttcaggtg
ggagcgcgtgatgaacttcgaggacggcggcattattcacgttaaccaggactcctccctgcaggacggcgtgttcatctacaaggtg
aagctgcgcggcaccaacttcccctccgacggccccgtaatgcagaagaagaccatgggctatgaggcctccgaggagcggatgt
accccgaggacggcgccctgaagagcgagtgtaaggagaggctgaagctgaaggacggcggccactacgccgccgaggtcaa
gaccacctacaaggccaagaagcccgtgcagctgcccggcgcctacatcgtcgacatcaagttggacatcgtgtcccacaacgag
gactacaccatcgtggaacagtacgaacgcactgagggccgccactccaccggcggcatggacgagctgtacaagtaa

Elements:
5X-UAS
Drosophila Kozak
pH-CaspGFP
P2A
pHlorina

2.5 Discussion

Although it is acknowledged that cell turnover occurs in every tissue, this has been extremely difficult to track *in vivo* [344–346] [347] [197]. While this is often attributed to rapid and efficient efferocytosis by the phagocytes, a key challenge has been the lack of probes to visualise and quantitatively determine how phagocytes find, engulf, and ultimately clear apoptotic corpses within the complex environment of a three-dimensional living organism. Here, we address this scientific challenge through the development of a novel, genetically-encoded efferocytosis reporter, CharON. As with advancements in genetically encoded tools which have illuminated questions regarding neuronal activity [348], glial cell function [288] [286] and kinase activity [278] *in vivo*, we envision CharON to be instrumental in dissecting efferocytosis *in vivo* in different contexts. Using this tool, we were able to track developmental apoptosis and efferocytosis in the *Drosophila* embryo occurring in different tissue compartments via the pH-CaspGFP and pHlorina components of CharON.

At the organismal level, CharON revealed how two distinct phagocytes (the phagocytic glia and the macrophages) co-operate to clear the developing CNS of apoptotic corpses [349]. Although both phagocyte populations act on the same wave of programmed cell death, CharON revealed differences in efferocytic dynamics.

At the population level, we found that macrophages adopt a strategy of 'eat-first, digest-later', to ensure rapid clearance of apoptotic cells. There has been speculation whether there is arrest of macrophages after they encounter or ingest an apoptotic cell[139][124][240]. However, through our ability to track the full efferocytic program with CharON, we find that efferocytic macrophages, even those with multiple corpses freely move, and conclude that engulfment and motility are not mutually exclusive. There is a concerted effort by this population of macrophages to collectively clean up the corpses quickly and efficiently. This may in part explain why it is often difficult to detect apoptotic cells even in tissues with high turnover; further, such rapid 'mop up' of emerging apoptotic cells may help avoid consequences due to secondary necrosis of the apoptotic cells.

In this work, we quantify that recruitment of macrophages to apoptotic cells can occur at as much as 8% of the embryo length. Further, by quantifying the time a macrophage spends on different steps of efferocytosis - the finding, binding, and uptake of corpses - only occupies about one fifth of the time it takes a phagocyte to digest the corpse. Macrophages appear to employ ways to retain high motility and successively ingesting apoptotic cells, i.e., two fast processes, while concurrently balancing the 'slow' digestion process of the ingested cargo. Additionally, while

elegant work from many investigators in the mammalian systems have identified organ-based genetic macrophage heterogeneity signatures[350] [351] [352], we find functional efferocytic heterogeneity among macrophages that occupy the same tissue niche. The emergence of macrophages with such extreme variation in corpse burden was striking, considering their shared environment. Despite this, we found that macrophages were remarkably robust in their ability to accommodate even very large corpse burdens, which had no effect on general motility or inflammatory chemotaxis.

In many human diseases, cells that die by different death modalities can occur in the same tissue context (e.g. apoptotic and necrotic cells seen in wounds or in atherosclerotic plaques)[353]. It is unclear whether the same macrophage can engulf cells that die by different modalities *in vivo*. After laser-induced wounding of the *Drosophila* embryonic epithelium, we found that macrophages with internalised CharON-labelled apoptotic bodies seamlessly transitioned to engulfing necrotic debris. Strikingly, phagosomes containing apoptotic and necrotic cargo sometimes fused within the same macrophage, suggesting an alternative, rapid means of phagosome acidification.

Despite their remarkable efferocytic robustness, macrophages with large apoptotic corpse burdens were impaired in clearing necrotic debris at the wound, implying functional consequences for not sharing the efferocytic burden more equally. In mathematical modelling to explore why macrophages might adopt a strategy wherein unequal corpse burden arises, simulation of developmental efferocytosis within the *Drosophila* embryo demonstrates that the speed of clearance dramatically decreases if equal corpse burden is enforced via a strict consumption limit. In contrast, allowing macrophage efferocytosis to eat freely, allows rapid clearance, in turn, introducing unequal corpse burdens. The former would undoubtedly also require additional regulatory complexity to enforce the equal sharing of corpses. Therefore, we conclude that macrophages must 'gamble' on the efferocytic compromise between rapidly clearing developmentally generated apoptotic cells and maintaining the capacity to clear necrotic debris in response to injury. While in our model, this only impaired the function of a proportion of macrophages at the wound, the vulnerability inherent to this efferocytic compromise could have profound consequences in many human disease states where macrophages are faced with overwhelming cellular debris such as atherosclerosis, lupus and diabetes [288] [354] [333] .

Chapter III

Development and evaluation of a flow cytometry based efferocytosis probe

3.1 Abstract

Efferocytosis is an essential process during development and disease, as billions of cells must be cleared in an efficient manner to prevent unchecked inflammation. In order to better define this process *in vitro* and *in vivo*, tools which facilitate the detection of cell death and cell clearance will deepen our understanding of this process. Here, we develop a genetically encoded system termed 'CharOFF', Caspase and pH Activated Reporter, Fluorescence OFF, to track both apoptosis and efferocytosis *in vitro* using both time-lapse imaging and FACS analysis. Furthermore, using CharOFF, we characterize the native ability of macrophages to enhance clearance of multiple targets in a novel co-culture system. This efferocytic priming event is time restricted, suggesting that populations of macrophages transiently enhance their ability to ingest multiple targets. These findings will support additional investigations into the mechanistic and *in vivo* relevance of efferocytic priming.

3.2 Introduction

Since Eli Metchnikoff's observation, "The extension and importance of [phagocytosis] can no longer be denied.", we have long appreciated the critical role of phagocytosis in immunity and how this intricate process is regulated at the cellular and tissue level. Despite decades of progress, we lack sufficient genetically encoded tools to study this process in a high through-put manner. It is understood that phagocytes can be presented with large quantities of apoptotic cells *in vivo* and as presented in the Drosophila embryo model with CharON in the previous chapter, phagocytes can engulf multiple corpses successively. However, determining how they are processed and to isolate them at different stages of digestion is a fascinating, yet important challenge, for us to decipher the steps of efferocytosis. To approach this question, we engineered a novel fluorescent reporter, CharOFF 'CharOFF', Caspase and pH Activated Reporter, Fluorescence OFF', to assess corpse internalization and corpse degradation via time-lapse and flow cytometry-based analysis. This probe allows a novel *in vitro* co-culture efferocytosis assay which incorporates inducible target killing and multi-target engulfment read-out to assess dynamics and kinetics of multi-cell engulfment. Using this system, we demonstrate that macrophages can individually and collectively undergo 'efferocytic priming' to eat multiple corpses upon first corpse engulfment. Furthermore, macrophage efferocytic priming, at a population level, occurs within a restricted time window after exposure to apoptotic cells. Insights from CharOFF will provide a platform to better understand efferocytic dynamics and priming response *in vitro* and *in vivo*.

3.3 Materials and Methods

3.3.1 *In vitro* cell death assays

Jurkat cells (ATCC) were treated with 150mJ of UV-C in a StrataLinker 1800 or 10 μM of ABT-737 (Abcam ab141336) in RPMI 1640 supplemented with 10% FBS and 1% Pen Strep with Glutamine. Cells were collected at indicated time points, stained 1:50 with Pacific Blue Annexin V (Biolegend #640917) and collected on an Attune Flow Cytometer (ThermoFisher). For each sample, 10,000 gated events were recorded, and data was processed in FlowJo V10. For each sample, singlet gates were used to distinguish single cells from doublets, followed by sub-gating on constitutively expressed GFP for analysis of RFP+ and Annexin V+ events. All RFP+, GFP+ and Annexin V+ event gates were set against the respective negative controls.

3.3.2 *In vitro* live cell imaging engulfment assays

UV-induced apoptotic CharOFF expressing Jurkat cells were co-cultured with mouse J774 macrophages (ATCC TIB-67) at 1:2 apoptotic cell:phagocyte ratios in 24 well plates and spun at 500rpm for 1 minute. Images were collected every 10 minutes for 24 hours on a Nikon Eclipse Ti2 scope using 40x magnification and kept under 37C and 4% CO2 for the duration of the experiment. Raw Tiff images were exported for analysis using Fiji software.

Engulfment events were manually curated through identification of apoptotic CharOFF (RFP+) cell internalization by J774 macrophages using co-localization between the apoptotic cell and the macrophage through brightfield and macrophage fluorescence (BFP+). Upon identification of engulfment events, manually drawn circular regions of interest (ROI) were placed over identified events and tracked throughout the duration of the experiment. Intensity of phagocytic events were calculated using background subtracted GFP and RFP values.

3.3.3 *In vitro* flow cytometry engulfment assays

For exogenously applied apoptotic cell engulfment assays, UV-induced apoptotic CharOFF expressing Jurkat cells were co-cultured with BFP (Addgene #122373) mouse J774 macrophages (ATCC TIB-67) at indicated apoptotic cell:phagocyte ratios in 24 well plates and spun at 500rpm for 1 minute before incubation at 37C. After 6 hours, apoptotic cells were gently washed 1x from the wells using 1x PBS before trypsinization and resuspension of cells. 10,000 macrophage events were collected per treatment on an Attune (ThermoFisher) FACS machine. Analysis of engulfment events was performed using FlowJo 10.4.2 (FlowJo LLC).

For ‘One-Dish’ engulfment assays, CharOFF-ic9 LR73, THP-1 or NIH-3T3 cells were plated the night before (12h) at indicated ratios of target : J774 macrophages. The following day, death of the target cells was induced via 20nM of AP20187 (MedChemExpress HY-13992) prior to incubation for 6 hours at 37C followed by 1x washing of wells with 1x PBS to remove unengulfed apoptotic cells and trypsinization for analysis on an Attune (ThermoFisher) FACS machine.

For ‘One-Dish’ multi-target engulfment assays, CharOFF-ic9 LR73 and miRFP720-SEP-tBid LR73 cells were plated the night before (12h) at indicated ratios of target : J774 macrophages. The following day, death of the inducible caspase-9 (ic9) and miRFP720-SEP-tBid target cells was induced via 20nM of AP20187 (MedChemExpress HY-13992) or 1ug/mL of Doxycycline (Sigma 17086-26-1), respectively, before incubation for 6 hours at 37C prior to 1x washing of wells with 1x PBS to remove unengulfed apoptotic cells and trypsinization for analysis on an Attune (ThermoFisher) FACS machine. Pretreatent of macrophages with 1 μM Cytochalasin D (Sigma 22144-77-0) was used to inhibit efferocytosis.

A detailed gating strategy for determining engulfment events is provided in Supplemental Figure 3. To begin, a singlet gate (SSC-A vs SSC-H) was created, followed by a macrophage size and fluorescence (BFP+) gate to select for macrophages (Supplemental Fig. 3A). Next, un-fed macrophages were used as a negative control gate for setting an engulfment event gate (RFP+) (Supplemental Fig. 3B). Finally, a negative acidification gate was set based upon unfed macrophages (GFP- / GFP+) to determine internalized and acidified events within fed macrophages (RFP+ / GFP-). In addition, to confirm internalized and acidified events, 50nM Bafilomycin A treated macrophages were analyzed for presence of internalized and un-acidified events (RFP+ / GFP-) (Supplemental Fig. 3C). This gating strategy was followed for all conditions and experiments.

3.3.4 Plasmid construction

In brief, all CharOFF constructs were inserted into a lentivirus backbone for expression in Jurkat cells. Gibson assembly PCR reactions using oligonucleotides (Integrated DNA Technologies) with 15bp overhangs were used to amplify and insert transgenes into restriction sites downstream of a SFFV promoter with an upstream CBX3 UCOE (UCOE-SFFV). In addition, P2A or T2A elements were used downstream of CaspRFP for bi-cistronic expression of GFP or SEP. Sanger sequencing was used to verify sequences of inserted transgenes.

For construction of CaspRFP, mScarlet-I was amplified from plasmid mSCarlet-I-mTurquoise-2 (Addgene #98839). mScarlet-I was split into N (8V-155D) and C-term (156G-224T)

segments for insertion into the split-intein scaffold, separated by a Caspase-3/7 cleaveable substrate (DEVD|G). Native *Npu* intein splice sites were maintained after NpuC (CFA) and NpuN (AEY) to ensure efficient protein trans-splicing and circularization of the mScarlet-I protein. CharOFF was constructed using pH-CaspGFP and SEP separated by a P2A site for bi-cistronic expression.

For construction of CharOFF-ic9, an inducible form of caspase-9 (Addgene #15567) was inserted downstream of CharOFF, with an upstream T2A element to ensure equimolar translation from a common promoter. For construction of miRFP720-SEP-itBID, miRFP720 (Addgene #136574) was inserted upstream of SEP, separated by a P2A site. Upon selection of miRFP720-SEP cells, cells were transduced with a dox inducible vector (Addgene #85400) encoding tBID.

3.3.5 CharOFF expressing transgenic *Drosophila* generation

The CharOFF construct was cloned downstream of UAS sequence in pUASt-ATTB, which in turn was used to generate transgenic CharOFF flies. This was recombined with daughterless GAL4 (da-gal4) to drive ubiquitous expression throughout embryo[355] (*;; da-gal4, uas-charon*) . Srp-GMA was used to label macrophages (*; srp-GMA; da-gal4, uas-charon*).

3.3.6 Lentivirus production, purification, and transduction

All lentivirus production was performed using Lenti-X HEK293T (Takara) grown in DMEM supplemented with 10% FBS and 1% Pen Strep with Glutamine. Cells were transfected at 80% confluency in 6-well plates with 2 ug total of psPAX2 packaging (Addgene #12260), pMD2.G envelope (Addgene #12259) and transfer plasmids at a 4:1:4 ratio. Supernatants were collected 48h after transfection and concentrated following the Lenti-X Concentrator (Takara) protocol.

For suspension cells like Jurkat, THP-1 and SCI cells, cells were plated in 24-well plates at 200k/well in RPMI 1640 supplemented with 10% FBS, 1% Penn Strep with Glutamine and 8µg/mL Polybrene. Purified viral supernatants were added to the wells and spun at 800g for 45min at 32 °C. After 24h, the cells were pelleted, washed in PBS and cultured in RPMI 1640 supplemented with 10% FBS and 1% Penn Strep with Glutamine. Transgene expression was assessed 72 hrs after transduction.

For adherent cells like LR73 and NIH-3T3 and, cells were plated in 24-well plates at 200k/well in alpha-MEM or DMEM supplemented with 10% FBS, 1% Penn Strep with Glutamine and 8µg/mL Polybrene. Purified viral supernatants were added to the wells and incubated for 24h. After 24h, the cells were trypsinized, lifted and washed in PBS before culturing in alpha-MEM or

DMEM supplemented with 10% FBS and 1% Penn Strep with Glutamine. Transgene expression was assessed 72 hrs after transduction.

3.4 Results

3.4.1: Generation of CharOFF for detection of apoptosis and efferocytosis *in vitro*

To complement CharON, which is much better suited for direct imaging than flow cytometry, and to obtain a more kinetic analysis of efferocytosis in both live-imaging and flow cytometry based analysis, we needed new probes. To design a reporter which detects apoptosis and corpse processing during efferocytosis, we designed a new efferocytosis reporter consisting of RFP-based apoptosis reporter and a pH sensitive GFP. To develop an RFP-based apoptosis reporter, CaspRFP, which is detectable via flow cytometry, we turned to the monomeric red fluorescent proteins mScarlet and mScarlet-I. We inserted these two fluorescent proteins into a caspase-3/7 sensitive scaffold and created stably expressing Jurkat cells for downstream analysis (*Fig. 3.1A, Figure 3.2A*). We were able to detect an RFP+ population which was in-line with Annexin V exposure. CaspRFP based upon mScarlet-I displayed improved detection of apoptotic events compared to CaspRFP T74I (mScarlet) or a previously RFP-based apoptosis reporter RC3ai (Supplemental *Figure 3.2B*). Furthermore, CaspRFP responded robustly to three apoptotic stimuli and RFP signal that correlated with Annexin V positivity and caspase activity (assessed through Q-VD inhibition) (*Fig. 3.1B, Fig. 3.2C*). Taken together, these results demonstrate the ability of CaspRFP to detect apoptotic activity.

Next, to monitor internalization of apoptotic cells and corpse acidification, we appended a pH-sensitive GFP, called SEP, to CaspRFP in a single transgene, creating the efferocytosis reporter CharOFF (**C**aspase and p**H** **A**ctivated **R**eporter, Fluorescence **OFF**), based on the previously named CharON construct. Under apoptotic conditions, CharOFF fluorescent signature is both RFP+ / GFP+, however when an apoptotic cell is internalized and acidified, the SEP based GFP signal rapidly ceases, and thus the overall signal rapidly switches to RFP+ / GFP- (*Fig. 3.1C, top)*. To determine whether CharOFF reliably detects efferocytic events, we co-cultured apoptotic CharOFF expressing Jurkat cells with mouse J774 macrophages in order to observe efferocytic events via time-lapse imaging. When an apoptotic cell is engulfed, the GFP fluorescence quenches rapidly whereas the RFP remains stable throughout the digesting period up to five hours, providing a dynamic fluorescent signature for detecting apoptotic cell resolution (*Fig. 3.1C, bottom, Fig. 3.2E, Fig 3.2F*).

To confirm whether CharOFF is able to detect efferocytic events via flow cytometry, we cocultured J774 macrophages with apoptotic CharOFF Jurkat cells and gated for RFP+ events. Convincingly, internalized apoptotic cells (RFP+) were detected in addition to internalized and acidified events (RFP+ / GFP-) (*Fig. 3.1D, left*). To further confirm the specificity of CharOFF to

detect acidified corpses, we treated macrophages with V-ATPase lysosomal inhibitor Bafilomycin A1 to decrease corpse acidification. Bafilomycin A1 treated macrophages displayed increased unprocessed (RFP+ / GFP+) events, suggesting that CharOFF is able to detect efferocytic events via flow cytometry with high signal fidelity (*Fig. 3.1D, right, Fig. 3.5A*).

Extending the ability to identify efferocytic events using a genetically encoded reporter, we developed an efferocytosis co-culture system by appending an inducible caspase-9 to CharOFF, denoted CharOFF-ic9. Using this coherent system, we could selectively kill target cells in the presence of phagocytes, preserving cell-cell interactions and secreted factors (*Fig. 3.1E, top*). To determine whether CharOFF-ic9 can induce apoptosis, we observed a significant increase in RFP+ and Annexin V+ events upon application of the inducible caspase-9 dimerizer AP20187 in three different cell lines. Importantly, this effect was inhibited by the addition of Q-VD, supporting the notion that CharOFF-ic9 can induce and detect apoptosis (*Fig, 3.2D*). Next, we co-cultured CharOFF-ic9 LR73 cells with J774 macrophages and induced apoptosis to determine if we can detect efferocytic events in a 'One-Dish' efferocytosis assay. Convincingly, in the presence of the caspase-9 inducer, we observe efferocytic events (RFP+), the majority of which are acidified (RFP+ / GFP-) (*Fig. 3.1E, bottom left*). Furthermore, the internalized and acidified signal of CharOFF-ic9 is blunted with the addition of Bafilomycin A1, increasing internalized and unacidifed events (RFP+ / GFP+) (*Fig. 3.1E, bottom right*). To further confirm the expandability of this 'One-Dish' assay, we tested CharOFF-ic9 in three cell lines, LR73 hamster fibroblasts, THP-1 monocytes and NIH-3T3 human fibroblasts. In each of these cell lines, we could observe an increase in efferocytic events with higher apoptotic cell : macrophage ratios. Importantly, macrophage efferocytosis of CharOFF-ic9 cells is significantly blunted with treatment of actin-inhibitor Cytochalasin D (*Fig. 3.1F*). In sum, these data suggest that CharOFF represents a novel RFP apoptosis reporter and a multi-functional efferocytosis reporter which includes a cohesive 'One-Dish' efferocytosis assay for facile detection of efferocytosis.

Figure 3.1: Development and evaluation of CharOFF for detection of apoptosis and efferocytosis *in vitro*

A) **Schematic of CaspRFP design and detection of caspase-3/7 activity.**

B) **CaspRFP detects multiple apoptotic stimuli.** (top) Schematic of experiment. (bottom) CaspRFP expressing Jurkat cells were exposed to UV-C, ABT-737 or Staurosporine (Stauro) apoptotic stimuli for 4h. Caspase-specific activation of RFP was evaluated by pretreatment with 50μM caspase-inhibitor Q-VD prior to exposure to apoptotic stimuli.

C) **CharOFF detects efferocytosis *in vitro*.** (top) Schematic of CharOFF fluorescent signature during efferocytosis. (bottom) Apoptotic CharOFF expressing Jurkat cells were co-cultured with BFP mouse J774 macrophages in order to detect efferocytic events. Prior to internalization, both RFP (caspase-activity) and GFP (no acidification) were detected. Upon internalization and digestion, GFP signal is lost due to pH-induced quenching in the phagolysosome while RFP signal is maintained. A.C = apoptotic cell. Mϕ = Macrophage. Scale bars = 20 μm.

D) **CharOFF detects efferocytosis via FACS.** Apoptotic CharOFF expressing Jurkat cells were co-cultured with BFP mouse J774 macrophages prior to analysis via FACS. (left) In the presence of CharOFF Jurkat cells, RFP+ events are detected. (right) CharOFF GFP signal quenching is phagolysosome dependent, as treatment of macrophages with 50nM Bafilomycin A1 increases GFP+ events.

E) **Design and evaluation of 'One-Dish' CharOFF efferocytosis assay.** (top) Schematic of 'One-Dish' CharOFF efferocytosis assay. (bottom left) Detection of efferocytosis with 'One-Dish' CharOFF efferocytosis assay. Without caspase-9 induction in LR73 CharOFF-ic9 cells, there is an absence of efferocytic (RFP+) events in J774 macrophages, however with caspase-9 induction efferocytic (RFP+) events are detected in J774 macrophages. (bottom right) CharOFF GFP+ signal is phagolysosome dependent. Inducer = AP20187. BafA1 = Bafilomycin A1.

F) **CharOFF detects efferocytosis of different targets.** (top left) Apoptotic CharOFF-ic9 LR73, (top right) apoptotic CharOFF-ic9 THP-1, (bottom) and apoptotic CharOFF-ic9 NIH-3T3 cells were co-cultured with mouse J774 macrophages are varying apoptotic cell : macrophage ratios.

Pretreatment of macrophages with 1 μM Cytochalasin D was used to inhibit efferocytosis to determine specificity of CharOFF signal. A.C = apoptotic cell.

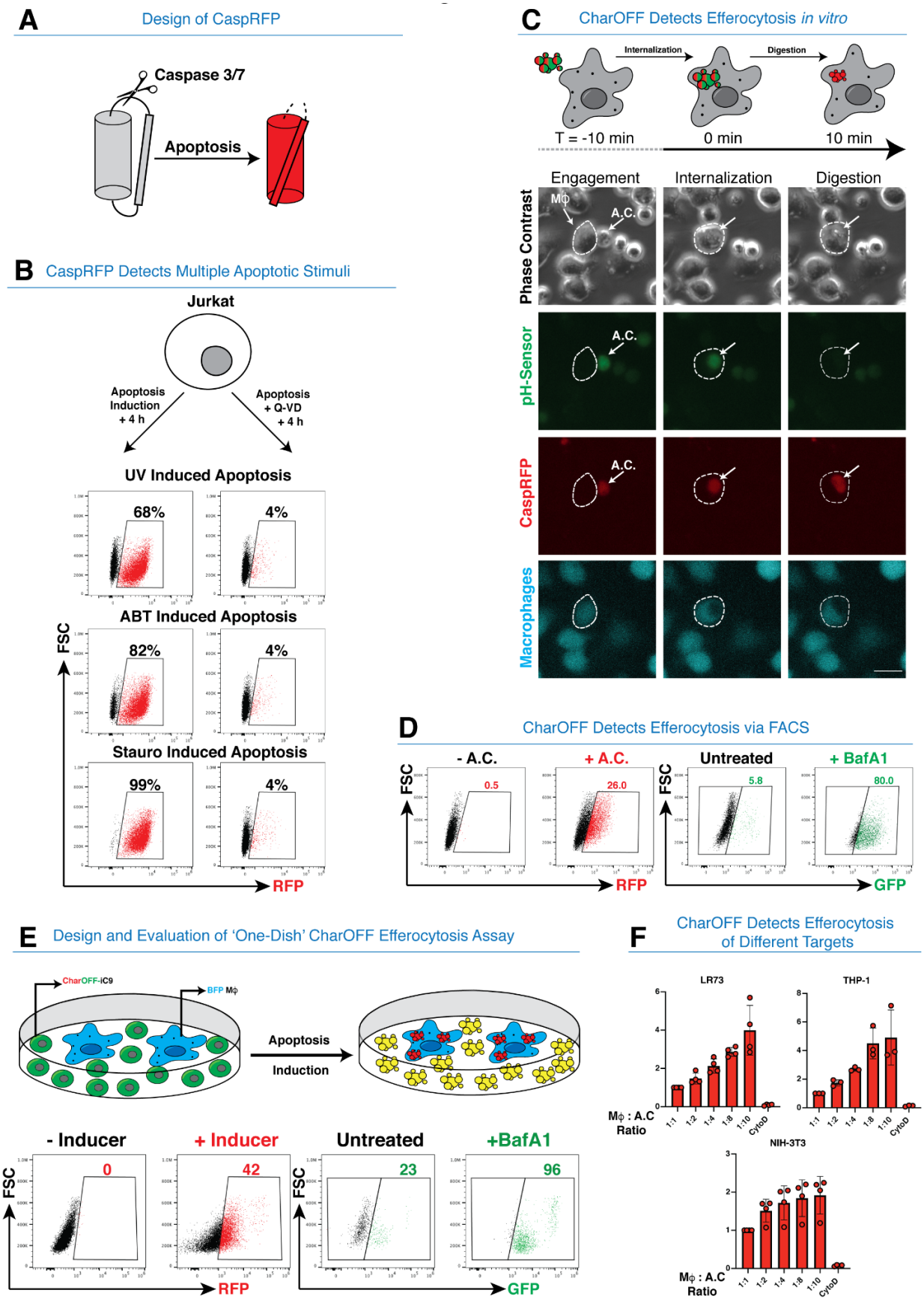
A
Design of CaspRFP
Caspase 3/7
Apoptosis
B
CaspRFP Detects Multiple Apoptotic Stimuli
Jurkat
Apoptosis Induction + 4 h
Apoptosis + Q-VD + 4 h
UV Induced Apoptosis
68%
4%
ABT Induced Apoptosis
82%
4%
Stauro Induced Apoptosis
99%
4%
FSC
RFP
C
CharOFF Detects Efferocytosis in vitro
Internalization
Digestion
T = -10 min
0 min
10 min
Engagement
Internalization
Digestion
Phase Contrast
MΦ
A.C.
pH-Sensor
CaspRFP
Macrophages
D
CharOFF Detects Efferocytosis via FACS
- A.C.
+ A.C.
Untreated
+ BafA1
0.5
26.0
5.8
80.0
FSC
RFP
GFP
E
Design and Evaluation of 'One-Dish' CharOFF Efferocytosis Assay
CharOFF-iC9
BFP MΦ
Apoptosis Induction
- Inducer
+ Inducer
Untreated
+BafA1
0
42
23
96
FSC
RFP
GFP
F
CharOFF Detects Efferocytosis of Different Targets
LR73
THP-1
NIH-3T3
MΦ : A.C Ratio
1:1
1:2
1:4
1:8
1:10
CytoD

Figure 3.2: Evaluation of RFP-based apoptosis sensors, CaspRFP, and CharOFF fluorescent signature during efferocytosis

A) **Design of RFP apoptosis reporters.** Plasmid vector design of RFP-based apoptosis reporters. (top) CaspRFP vector design, (middle) RC3ai vector design and (bottom) CaspRFP T74I vector design. 2A = p2a site. pA = polyA.

B) **CaspRFP Accurately Detects Apoptosis**. Jurkat cells stably expressing CaspRFP (red circle), CaspRFP T74I (magenta triangle) or RC3ai (purple square) were subjected to UV-C induced apoptosis and assayed at 1 hour increments for Annexin V+ and RFP+ double-positive events to confirm RFP signal fidelity. One-Way ANOVA,*= p<=.0332,** = p<=.0021, **** =p<.0001. N=3

C) **Time course of CaspRFP apoptosis detection through several stimuli.** CaspRFP Jurkat cells were subjected to UV-C, ABT-737 or Staurosporine induced apoptosis and assayed at 1 hour increments for presence of Annexin V+ (grey square) and RFP+ (red circle) events. To confirm caspase-3/7 specific RFP signal, Jurkat cells were pretreated with caspase inhibitor Q-VD and checked for Annexin V+ and RFP+ events (red and grey triangles). N=3

D) **CharOFF ic9 induces apoptosis in several cell lines**. THP-1, NIH-3T3 and LR73 cells stably expressing CharOFF-ic9 were subjected to induction of caspase-9 and monitored at 1 hour increments for presence of Annexin V+ (grey square) and RFP+ (red circle) events. To determine specificity of caspase-3/7 RFP signal, Jurkat cells were pretreated with caspase inhibitor Q-VD and checked for Annexin V+ and RFP+ events (red and grey triangles). N=3

E) **CharOFF fluorescent signature during *in vitro* efferocytosis.** (left) RFP and GFP signal of CharOFF was tracked during *in vitro* efferocytosis time lapse imaging of J774 macrophages phagocytosing apoptotic Jurkat CharOFF cells. (right) Fold change of CharOFF GFP signal after 10 minutes post internalization. N=20

F) **CharOFF RFP signal maintains in the phagosome.** J774 macrophages were co-cultured with apoptotic Jurkat CharOFF cells. RFP fluorescence was tracked upon internalization for 5 hours. N=17

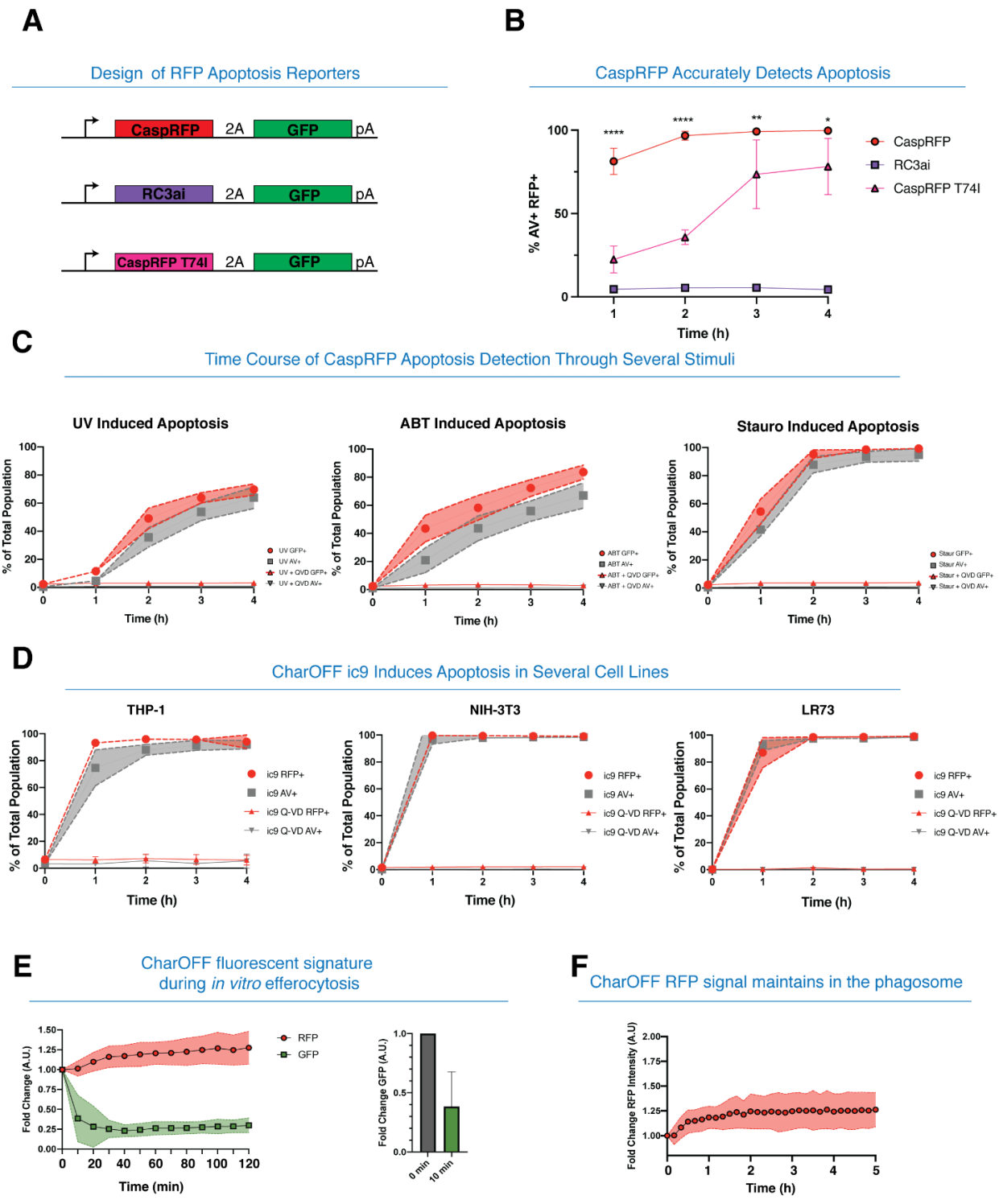
A
Design of RFP Apoptosis Reporters
CaspRFP
2A
GFP
pA
RC3ai
2A
GFP
pA
CaspRFP T74I
2A
GFP
pA
B
CaspRFP Accurately Detects Apoptosis
% AV+ RFP+
Time (h)
CaspRFP
RC3ai
CaspRFP T74I
C
Time Course of CaspRFP Apoptosis Detection Through Several Stimuli
UV Induced Apoptosis
ABT Induced Apoptosis
Stauro Induced Apoptosis
% of Total Population
Time (h)
D
CharOFF ic9 Induces Apoptosis in Several Cell Lines
THP-1
NIH-3T3
LR73
% of Total Population
Time (h)
ic9 RFP+
ic9 AV+
ic9 Q-VD RFP+
ic9 Q-VD AV+
E
CharOFF fluorescent signature during in vitro efferocytosis
Fold Change (A.U.)
Time (min)
RFP
GFP
Fold Change GFP (A.U.)
0 min
10 min
F
CharOFF RFP signal maintains in the phagosome
Fold Change RFP Intensity (A.U)
Time (h)

3.4.2 Macrophage corpse-priming occurs in a time dependent manner

It has long been assumed that macrophages maintain a heightened ability to engulf apoptotic cells, however whether there is any longitudinal variation in their efferocytic capacity remains to be elucidated. To begin to understand macrophage efferocytic fitness, we developed an assay in which we can pulse two unique fluorescent targets to determine single and multi corpse engulfment capacity.

The 'Dubbel' system incorporates two spectrally unique fluorescent targets with inducible caspase-9 for target killing. Dubbel includes: 1) a far-red fluorescent protein, miRFP720 (720), which is paired in a single transgene with pH-quenchable GFP, SEP, to permit detection of internalized and acidified corpses and 2) CharOFF-ic9 (*Fig. 3.3A, 3.4A, 3.4B*). Upon induction of cell death, engulfment of unique target types are able to be resolved via FACS using the Dubbel system (*Fig 3.3B, Fig. 3.4D*) To ascertain whether prior corpse engulfment influences additional corpse engulfment, termed corpse priming, macrophages which were 720+ had higher percentages of RFP+ compared to single-target engulfers alone. This phenomena was true for the inverse as well, RFP+ macrophages displayed significantly higher engulfment percentages of 720 targets compared to 720 single-target engulfers (Fig. 3.3C). To determine whether duration of corpse priming had an effect on macrophages at the population level to engulf multiple targets, we developed an assay with orthogonal death switches, inducible caspase 9 and inducible tBID, to permit time-dependent pulses of apoptotic targets (Fig. 3.3D, Fig. 3.4C). Remarkably, corpse priming only occured after 24 hours of first corpse exposure, and was observed at three different macrophage : apoptotic cell ratios, suggesting a time-dependent element for macrophage corpse priming at the population level (*Fig. 3.3E*).

Figure 3.3: Macrophage corpse-priming enhances efferocytosis in a time dependent manner

A) **Design of 'Dubbel' Multi-Corpse 'One-Dish' Efferocytosis Assay.** (top) To detect multi-corpse engulfment in a contained system, termed Dubbel, CharOFF-ic9 and miRFP720-ic9 expressing LR73 cells were co-cultured with mouse J774 macrophages at varying macrophage : target ratios. Analysis of single (RFP+/720-, RFP-/720+) or multi-corpse (RFP+/720+) engulfment was determined by FACS.

B) **Dubbel detects unique target engulfment.** Upon induction of death in Dubbel, engulfment of CharOFF-ic9 (top) and miRFP720-ic9 (bottom) was detected in J774 macrophages.

C) **Prior corpse engulfment enhances second corpse engulfment.** Engulfment percentage of macrophages which have eaten a single corpse (represented as a single-color red or purple dot) were compared to those which have eaten at least two corpses (double colored dots). Macrophages which had eaten only RFP (CharOFF-ic9) corpses or had eaten both 720 (miRFP720-ic9) and RFP targets were compared across three different macrophage : apoptotic cell ratios. Unpaired t-test, * = p<=.0332, ** = p<=.0021.

D) **Macrophage corpse-priming longitudinal assay**. To determine the time period in which corpse-priming occurs, CharOFF-ic9 LR73 cells were killed in the presence of macrophages for 6, 24 or 48 hours prior to exposure to miRFP720-itBID LR73 cells serving as a second target.

E) **Macrophage corpse-priming is time dependent**. Macrophages were exposed to apoptotic LR73 cells (CharOFF-ic9) for 6, 24 or 48 hours before induction of second target (miRFP72-itBID) death. Engulfment percentages of second target alone (grey bar) or corpse-primed macrophages (red bars) were determined across different macrophage : apoptotic cell ratios. One-Way ANOVA,*= p<=.0332,*** = p<=.0002, **** =p<.0001.

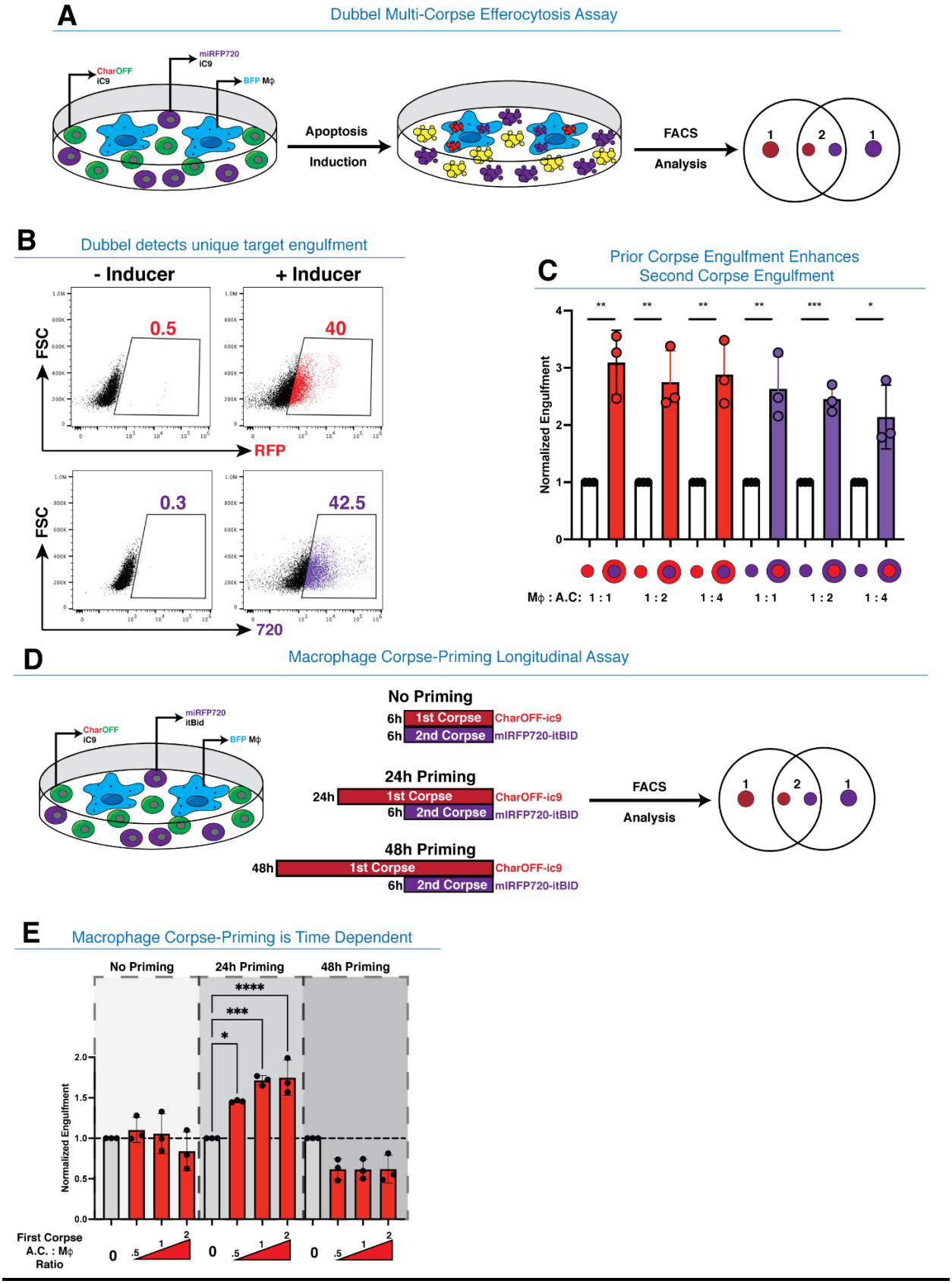
A
Dubbel Multi-Corpse Efferocytosis Assay
CharOFF iC9
miRFP720 iC9
BFP Mϕ
Apoptosis Induction
FACS Analysis
1
2
1
B
Dubbel detects unique target engulfment
- Inducer
+ Inducer
FSC
0.5
40
RFP
0.3
42.5
720
C
Prior Corpse Engulfment Enhances Second Corpse Engulfment
Normalized Engulfment
Mϕ : A.C: 1 : 1 1 : 2 1 : 4 1 : 1 1 : 2 1 : 4
D
Macrophage Corpse-Priming Longitudinal Assay
CharOFF iC9
miRFP720 itBid
BFP Mϕ
No Priming
6h 1st Corpse CharOFF-ic9
6h 2nd Corpse mIRFP720-itBID
24h Priming
24h 1st Corpse CharOFF-ic9
6h 2nd Corpse mIRFP720-itBID
48h Priming
48h 1st Corpse CharOFF-ic9
6h 2nd Corpse mIRFP720-itBID
FACS Analysis
1
2
1
E
Macrophage Corpse-Priming is Time Dependent
No Priming
24h Priming
48h Priming
Normalized Engulfment
First Corpse A.C. : Mϕ Ratio
0 .5 1 2 0 .5 1 2 0 .5 1 2

Figure 3.4: Evaluation of miRFP720-SEP engulfment and itBID induction of apoptosis.

A) **miRFP720-SEP detects efferocytic events *in vitro*.** Apoptotic stably expressing miRFP720-SEP LR73 cells were incubated with J774 macrophages to determine fluorescent signature upon engulfment. After internalization, SEP (pH-sensitive GFP) is quenched while miRFP720 fluorescence is maintained. Mϕ = Macrophage. A.C = apoptotic cell. Scale bar = 20 μm.

B) **CharOFF, CharOFF-ic9 and Dubbel Constructs**. Vector designs for CharOFF, CharOFF inducible caspase 9 (ic9), miRFP720-SEP inducible caspase 9 (ic9) and miRFP720-SEP inducible tBID (itBID). Dubbel incorporates cells expressing CharOFF-ic9 and miRFP720-SEP-ic9 or CharOFF-ic9 and miRFP720-SEP-itBID depending on whether a single or double death trigger is required, respectively.

C) **Inducible tBid (itBID) rapidly induces apoptosis**. Stably expressing miRFP720-SEP-itBID LR73 cells were treated with 1μM doxycycline and assayed for Annexin V+ events every hour.

D) **miRFP720 is detected during *in vitro* engulfment**. J774 macrophages were incubated with stably expressing miRFP720-SEP-ic9 cells and death was induced to detect efferocytic events. After 6 hours, internalized and acidified (720+ / GFP-) events (right panel) were analyzed via flow cytometry compared to a J774 macrophage alone control (left panel).

Supplemental Figure 2

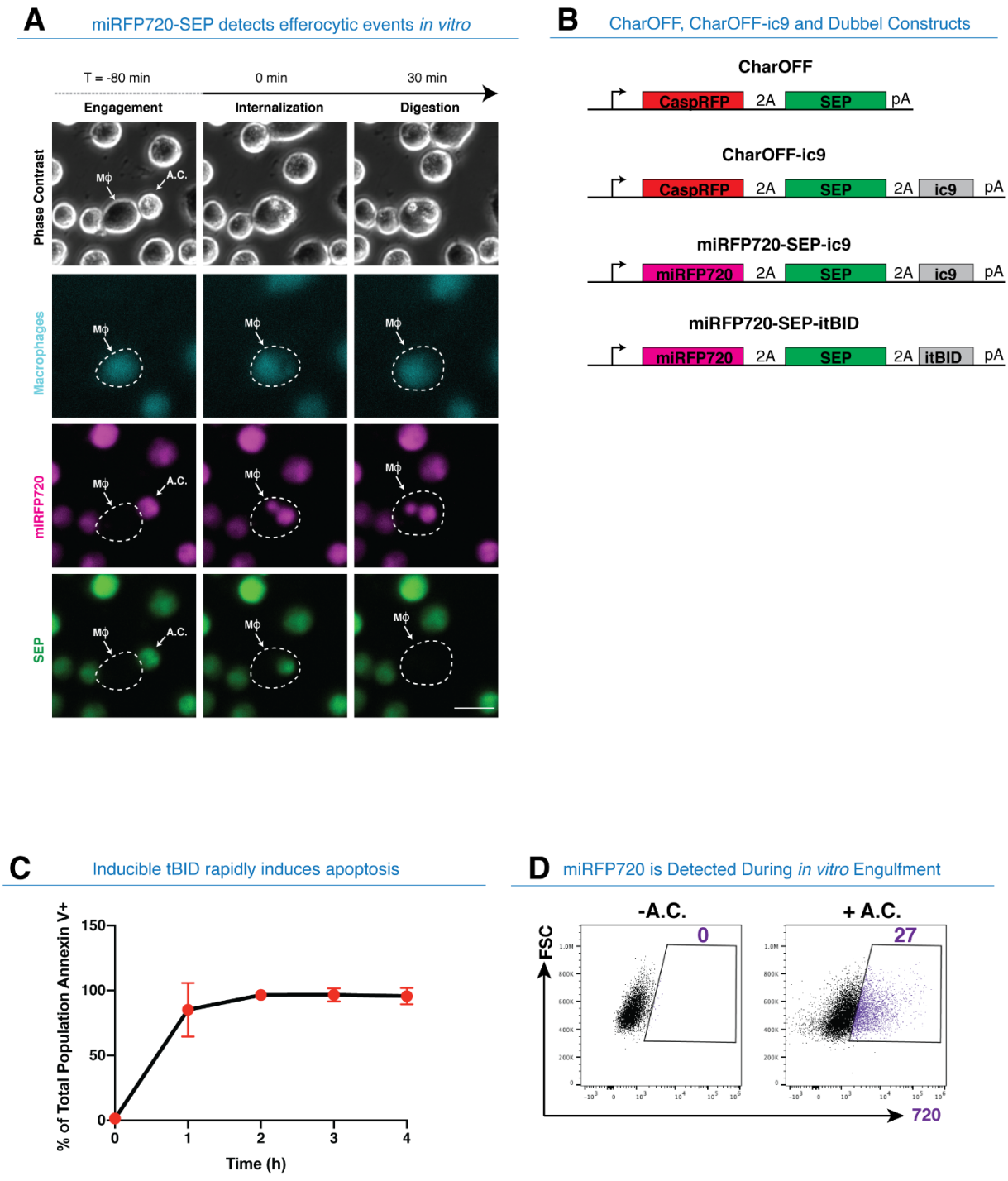

Figure 3.5: Flow cytometry gating strategy for CharOFF *in vitro* efferocytosis assays

A) **Macrophage gating strategy**. Singlets (SSC-H vs SSC-A), followed by size exclusion (FSC vs SSC) and finally J774 BFP+ gating (FSC vs BFP) are used to select macrophages in CharOFF efferocytosis assays.

B) **Efferocytic event gating strategy**. (left) No apoptotic cell (RFP-) gates are used to determine efferocytic events (right).

C) **Internalization and acidification gating strategy**. (left) No apoptotic cell (GFP- / GFP+) gates are set to determine acidified (GFP-) and unacidified (GFP+) RFP+ events within macrophages. (right) Bafilomycin A1 is used as a control to confirm internalized and unacidified (GFP+ / RFP+) efferocytic events.

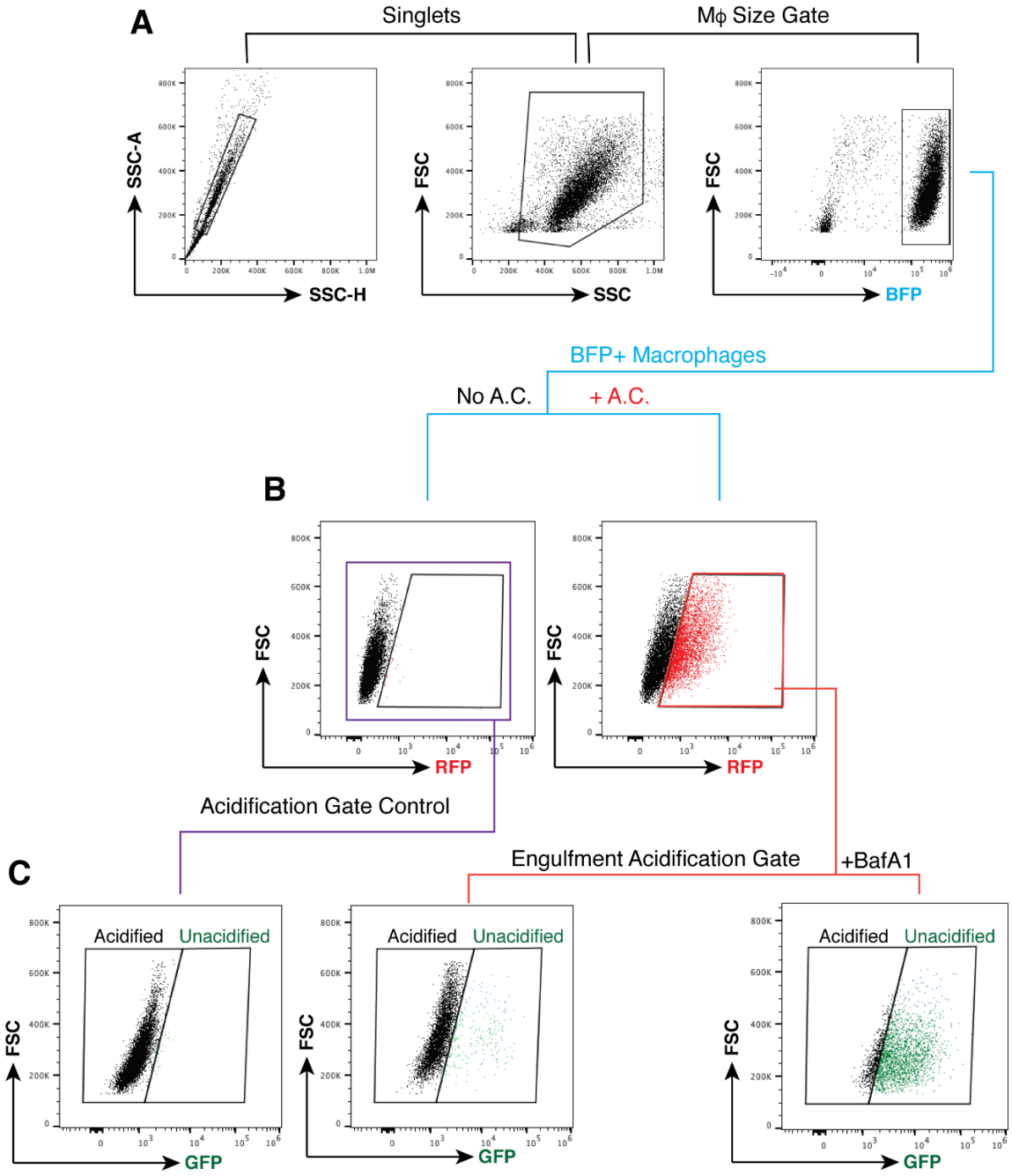
A
Singlets
Mϕ Size Gate
SSC-A
SSC-H
FSC
SSC
FSC
BFP
BFP+ Macrophages
No A.C.
+ A.C.
B
FSC
RFP
FSC
RFP
Acidification Gate Control
Engulfment Acidification Gate
+BafA1
C
Acidified
Unacidified
FSC
GFP
Acidified
Unacidified
FSC
GFP
Acidified
Unacidified
FSC
GFP

Table 3.1: CharOFF, CharOFF-ic9, CharOFF-itBID sequences

CharOFF

Gccaccatgatcaagatcgccaccaggaagtacctgggcaagcagaacgtgtacgacatcggcgtggagagggaccacaacttc
gccctgaagaacggcttcatcgccagcaactgcttcaacgaattcggcgtgctgaagggcgacattaagatggccctgcgcctgaag
gacggcggccgctacctggcggacttcaagaccacctacaaggccaagaagcccgtgcagatgcccggcgcctacaacgtcgac
cgcaagttggacatcacctcccacaacgaggactacaccgtggtggaacagtacgaacgctccgagggccgccactccaccgac
gaggtggacggcgtgatcaaggagttcatgcggttcaaggtgcacatggagggctccatgaacggccacgagttcgagatcgagg
gcgagggcgagggccgcccctacgagggcacccagaccgccaagctgaaggtgaccaagggtggcccccctgcccttctcctggg
acatcctgtcccctcagttcatgtacggctccagggccttcatcaagcaccccgccgacatccccgactactataagcagtccttcccc
gagggcttcaagtgggagcgcgtgatgaacttcgaggacggcggcgccgtgaccgtgacccaggacacctccctggaggacggc
accctgatctacaaggtgaagctccgcggcaccaacttccctcctgacggccccgtaatgcagaagaagacaatgggctgggaag
cgtccaccgagcggttgtaccccgaggacggatccgccgagtactgcctgagctacgagaccgagatcctgaccgtggagtacgg
cctgctgcctatcggcaagatcgtggagaagaggatcgagtgcaccgtgtacagcgtggacaacaacggcaacatctacacccag
cctgtggcccagtggcacgacaggggcgagcaggaggtgttcgagtactgcctggaggacggcagcctgatcagggccaccaag
gaccacaagttcatgaccgtggacggccagatgctgcctatcgacgagatcttcgagagggagctggacctgatgagggtggacaa
cctgcctaactctagaggctccggcgccacgaacttctctctgttaaagcaagcaggagacgtggaagaaaaccccggtcctgcca
ccatgagtaaaggagaagaacttttcactggagttgtcccaattcttgttgaattagatggtgatgttaatgggcacaaattttctgtcagtg
gagagggtgaaggtgatgcaacatacggaaaacttacccttaaatttatttgcactactggaaaactacctgttccatggccaacactt
gtcactacgttaacttatggtgttcaatgcttttcaagatacccagatcatatgaaacggcatgactttttcaagagtgccatgcccgaagg
ttacgtacaggaaagaactatatttttcaaagatgacgggaactacaagacacgtgctgaagtcaagtttgaaggtgatacccttgtta
atagaatcgagttaaaaggtattgattttaaagaagatggaaacattcttggacacaaattggaatacaactataacgatcaccaggtg
tacatcatggcagacaaacaaaagaatggaatcaaagctaacttcaaaattagacacaacattgaagatggaggcgttcaactagc
agaccattatcaacaaaatactccaattggcgatgggcccgtccttttaccagacaaccattacctgtttacaacttctactctttcgaaag
atcccaacgaaaagagagaccacatggtccttcttgagtttgtaacagctgctgggattacacatggcatggatgaactatacaaata
a

Elements
Kozak
CaspRFP
P2A
SEP

CharOFF-ic9

Gccaccatgatcaagatcgccaccaggaagtacctgggcaagcagaacgtgtacgacatcggcgtggagagggaccacaacttc
gccctgaagaacggcttcatcgccagcaactgcttcaacgaattcggcgtgctgaagggcgacattaagatggccctgcgcctgaag
gacggcggccgctacctggcggacttcaagaccacctacaaggccaagaagcccgtgcagatgcccggcgcctacaacgtcgac
cgcaagttggacatcacctcccacaacgaggactacaccgtggtggaacagtacgaacgctccgagggccgccactccaccgac
gaggtggacggcgtgatcaaggagttcatgcggttcaaggtgcacatggagggctccatgaacggccacgagttcgagatcgagg
gcgagggcgagggccgcccctacgagggcacccagaccgccaagctgaaggtgaccaagggtggcccccctgcccttctcctggg
acatcctgtcccctcagttcatgtacggctccagggccttcatcaagcaccccgccgacatccccgactactataagcagtccttcccc
gagggcttcaagtgggagcgcgtgatgaacttcgaggacggcggcgccgtgaccgtgacccaggacacctccctggaggacggc

accctgatctacaaggtgaagctccgcggcaccaacttccctcctgacggccccgtaatgcagaagaagacaatgggctgggaag
cgtccaccgagcggttgtaccccgaggacggatccgccgagtactgcctgagctacgagaccgagatcctgaccgtggagtacgg
cctgctgcctatcggcaagatcgtggagaagaggatcgagtgcaccgtgtacagcgtggacaacaacggcaacatctacacccag
cctgtggcccagtggcacgacaggggcgagcaggaggtgttcgagtactgcctggaggacggcagcctgatcagggccaccaag
gaccacaagttcatgaccgtggacggccagatgctgcctatcgacgagatcttcgagagggagctggacctgatgagggtggacaa
cctgcctaactctagaggctccggcgccacgaacttctctctgttaaagcaagcaggagacgtggaagaaaaccccggtcctgcca
ccatgagtaaaggagaagaacttttcactggagttgtcccaattcttgttgaattagatggtgatgttaatgggcacaaattttctgtcagtg
gagagggtgaaggtgatgcaacatacggaaaacttacccttaaatttatttgcactactggaaaactacctgttccatggccaacactt
gtcactacgttaacttatggtgttcaatgcttttcaagatacccagatcatatgaaacggcatgactttttcaagagtgccatgcccgaagg
ttacgtacaggaaagaactatatttttcaaagatgacgggaactacaagacacgtgctgaagtcaagtttgaaggtgatacccttgtta
atagaatcgagttaaaaggtattgattttaaagaagatggaaacattcttggacacaaattggaatacaactataacgatcaccaggtg
tacatcatggcagacaaacaaaagaatggaatcaaagctaacttcaaaattagacacaacattgaagatggaggcgttcaactagc
agaccattatcaacaaaatactccaattggcgatgggcccgtccttttaccagacaaccattacctgtttacaacttctactctttcgaaag
atcccaacgaaaagagagaccacatggtccttcttgagtttgtaacagctgctgggattacacatggcatggatgaactatacaaata
aggctccggcgagggcagaggaagtctgctaacatgcggtgacgtcgaggagaatcctggcccagccaccatgggagtgcaggt
ggagactatctccccaggagacgggcgcaccttccccaagcgcggccagacctgcgtggtgcactacaccgggatgcttgaagat
ggaaagaaagttgattcctcccgggacagaaacaagccctttaagtttatgctaggcaagcaggaggtgatccgaggctgggaaga
aggggttgcccagatgagtgtgggtcagagagccaaactgactatatctccagattatgcctatggtgccactgggcacccaggcatc
atcccaccacatgccactctcgtcttcgatgtggagcttctaaaactggaatctggcggtggatccggagtcgacggatttggtgatgtc
ggtgctcttgagagtttgaggggaaatgcagatttggcttacatcctgagcatggagccctgtggccactgcctcattatcaacaatgtg
aacttctgccgtgagtccgggctccgcacccgcactggctccaacatcgactgtgagaagttgcggcgtcgcttctcctcgctgcatttc
atggtggaggtgaagggcgacctgactgccaagaaaatggtgctggctttgctggagctggcgcggcaggaccacggtgctctgga
ctgctgcgtggtggtcattctctctcacggctgtcaggccagccacctgcagttcccaggggctgtctacggcacagatggatgccctgt
gtcggtcgagaagattgtgaacatcttcaatgggaccagctgccccagcctgggagggaagcccaagctctttttcatccaggcctgt
ggtggggagcagaaagaccatgggtttgaggtggcctccacttcccctgaagacgagtcccctggcagtaaccccgagccagatgc
caccccgttccaggaaggtttgaggaccttcgaccagctggacgccatatctagtttgcccacacccagtgacatctttgtgtcctactct
actttcccaggttttgtttcctggagggaccccaagagtggctcctggtacgttgagaccctggacgacatctttgagcagtgggctcact
ctgaagacctgcagtccctcctgcttagggtcgctaatgctgtttcggtgaaagggatttataaacagatgcctggttgctttaatttcctcc
ggaaaaaactttttctttaaaacatcagtcgactatccgtacgacgtaccagactacgcactcgactaa

Elements

Kozak

CaspRFP

P2A

SEP

T2A

Inducible Caspase-9

Inducible tBID:

Gccaccatgggcagccaggccagccgctccttcaaccaaggaagaatagagccagattctgaaagtcaggaagaaatcatccac
aacattgccagacatctcgcccaaataggcgatgagatggaccacaacatccagcccacactggtgagacagctagccgcacagt
tcatgaatggcagcctgtcggaggaagacaaaaggaactgcctggccaaagcccttgatgaggtgaagacagccttccccagaga

catggagaacgacaaggccatgctgataatgacaatgctgttggccaaaaaagtggccagtcacgcaccatctttgctccgtgatgtc
ttccacacgactgtcaactttattaaccagaacctattctcctatgtgaggaacttggttagaaacgagatggacgaattcggatccggta
cctag

Elements

Kozak

tBID

3.5 Discussion

Macrophages are highly dynamic and adaptable to their environment. We have uncovered much about their responses in health and disease, where they serve as the mediators of tissue homeostasis. In this work we develop a novel *in vitro* system, CharOFF, which permits induction and detection of single and multi corpse macrophage efferocytosis in a closed loop system. Using this platform, we demonstrate that macrophages undergo corpse-induced priming to collectively increase their ability to engulf multiple targets in a time dependent manner.

To begin with our technical innovations, we first designed a novel RFP-based apoptosis reporter, CaspRFP, which outperforms previously reported RFP-based apoptosis reporters. Second, we paired CaspRFP with a pH-sensitive GFP in a single transgene to create CharOFF, an efferocytosis reporter which functions in both imaging and FACS settings. Third, we designed and tested a 'One-Dish' efferocytosis assay which uses an inducible apoptosis system tethered to CharOFF, providing on-demand killing of target cells in a contained *in vitro* system. Fourth, to monitor multi-corpse engulfment, we designed and tested 'Dubbel', which permits detection of single and multiple corpse engulfment via FACS in a coherent system. Fifth, we generated an orthogonal, dual inducible death Dubbel engulfment system to monitor macrophage response to first and second waves of corpses at specified time points.

Insights from Dubbel prompted us to study the effect of macrophage corpse priming, which we observed *in vivo* during our CharON studies. To further define this phenomena, we demonstrate that previous corpse engulfment augments the ability of macrophages to eat subsequent corpses, and this phenomena occurs within a defined time window. Corpse priming has broad ranging implications with regards to innate immune memory, developmental and disease states such as CNS development, atherosclerosis and wounding where macrophages are subjected to waves of dying cells [350] [351] [356]. Furthermore, understanding the transcriptional and metabolic landscape of corpse primed macrophages will further our understanding of macrophage efferocytosis and provide a basis for manipulating these circuits for therapeutic benefit.

3.6 Future Directions

We are arriving at an exciting time in the efferocytosis field where the nexus of novel technologies, model organisms and understanding of the efferocytic process are beginning to merge and strengthen our ability to manipulate and potentially harness efferocytosis for amelioration of disease. This section will focus on key areas which are notable for future investigation. Namely, generation of novel transgenics, application of tools for understanding of development and disease, and potential application of knowledge derived from these efforts will be discussed.

3.6.1 Generation of CharON transgenics

CharON is in its infancy for applications beyond *in vitro* and *Drosophila* developmental work. To begin, CharON would benefit from wide adoption and creation of transgenics in such model organisms as *C. elegans*, Zebrafish and mice. *C. elegans* are similar in their plethora of genetic drivers and amenability to generation of transgenics. Furthermore, *C. elegans* offer many of the same optical benefits as *Drosophila*, such as a high degree of optical transparency during development and compact size. In addition, *C. elegans* have a well defined cell death and cell clearance atlas, providing a template for location of cell death and cell clearance during development. These properties make *C. elegans* a great candidate for studying cell death and cell clearance using CharON.

Zebrafish offer many of the same beneficial optical qualities as both *C. elegans* and *Drosophila*, in addition to sharing many conserved immune cells with mammals. While genetic drivers are not as robust as previously described model organisms, Zebrafish have several well established immune cell reporters and protocols for generation of transgenics. In particular, creation of a Cre-dependent CharON Zebrafish would allow expression of CharON in many neuronal tissues, which have been demonstrated to undergo cell death during development. Using this system, we could track the fate of individual neuronal populations and identify phagocytes which mediate their removal. Insights from these studies could help build an understanding of phagocyte behavior and targets during development.

There are many benefits to *C. elegans*, *Drosophila* and Zebrafish, however mice assume a unique status with regards to disease modeling and understanding of shared biology with humans. While not as extensive as *Drosophila*, mice have many well established Cre-based systems which could be used in conjunction with a Cre-dependent CharON mouse. To gain insights at the tissue and single-cell level, optical windows and other minimally invasive

techniques such as *ex utero* culture could be used to provide an avenue for observing cell death and cell clearance during development and disease [357]. In sum, these three efforts would permit the study and comparative analysis of cell death and cell clearance in three well established model organisms. It would be interesting to compare and contrast the modes in which phagocytes clear apoptotic corpses across species, perhaps uncovering conserved and unique aspects to the efferocytic process.

3.6.2 Generation of CharOFF transgenics

As CharON relies primarily on imaging techniques, CharOFF has an inherent advantage is its ability to detect apoptosis and efferocytosis via imaging and flow cytometry. In addition to the previously described CharON transgenics, generation of CharOFF in a similar manner would permit a high-throughput approach to cataloging cell death and cell clearance during organismal growth.

For instance, many tissues in mice are not easily accessible for live-imaging or require invasive techniques in order to gain the required temporal and spatial resolution. While CharOFF can certainly be used in imaging campaigns, a Cre-based CharOFF transgenic would permit additional analysis. For instance, using a Cre-based CharOFF transgenic mouse, tissue could be excised, processed and run through a flow cytometer in order to determine the quantity of cell death and cell clearance. Additional layers of information could be added using immunostaining, RNA-seq analysis and proteomics of efferocytic phagocytes during development or in disease models. These approaches could assist with defining the efferocytic landscape and means by which phagocytes maintain tissue homeostasis.

Finally, the flexibility of CharOFF in the mouse system would be an advantage for the field where instrumentation or expertise are limiting factors. Many of the proposed imaging techniques are esoteric and require extensive training, limiting the accessibility of this technology. The flexibility of CharOFF would help in collective efforts to create, share and evaluate cell death and cell clearance, which is needed for substantial progress in the field.

3.6.4 Additional applications of CharON

Generation of CharON *Drosophila* resulted in several key insights into the kinetics and qualities of efferocytosis at the single-cell and tissue wide level. While there are many exciting avenues to explore, three areas of future investigation will be discussed.

First, the identity of cells which undergo apoptosis during *Drosophila* embryonic development are not fully characterized. In order to discern which cells and lineages undergo extensive cell death during CNS development, different UAS drivers could be used to express CharON in specific cellular subsets, such as neuroblasts, which give rise to many neuron and glial cells [358]. By driving CharON in these different subsets, the quantity of cell death could be evaluated with regards to lineage. Furthermore, the identity of phagocytes which clear the apoptotic cells could be tracked, providing information on location and kinetics of cell clearance. These detailed studies would assist in systematically defining the means by which an organism shapes a rapidly growing tissue.

Second, while much of our *Drosophila* work focused on macrophages, additional phagocyte populations are prime candidates for future exploration. Specifically, phagocytic glia within the developing embryo exhibit high levels of phagocytosis, however their targets and kinetics have not been fully evaluated. In order to better characterize these cells, glial specific repo Gal4 could be used in conjunction with a blue or far-red fluorescent protein to mark these cells. Once established, these lines could be used in conjunction with CharON to determine the location of cell clearance and the kinetics by which these cells maintain homeostasis within the CNS. Furthermore, it would be interesting to evaluate whether similarities exist between macrophage and glial mediated efferocytosis.

Third, there have been many exciting developments within the *Drosophila* macrophage field with regards to distinct subsets of macrophages during development. What was once thought of as a homogenous population is now being re-examined, as several unique subsets have been identified [359]. To better understand the efferocytic qualities and contributions of these subpopulations, CharON could be used to determine whether they are similar in their target cells, cargo processing and capacity. Insights from these collective studies would provide a detailed view into the *Drosophila* efferocytic network.

3.6.5 Additional applications of CharOFF

Use and analysis of CharOFF transgenics in a high-throughput, unbiased manner has the potential to transform our understanding of efferocytosis *in vivo*. Three approaches to better characterize efferocytosis *in vivo* will be explored.

First, using mice which express a Cre-dependent CharOFF, neuronal drivers could be used to express CharOFF in the developing CNS. Next, during CNS development, dissected tissues could be prepared and run through a FACS machine in order to sort out phagocytes

which had internalized and digested apoptotic neurons. After collecting the phagocytes which have phagocytosed neurons, these cells could be prepared for single cell RNAseq. This unbiased approach would have the potential to elucidate the identity of known and unknown efferocytic players during CNS development. Furthermore, information from such studies would help build a cellular atlas of efferocytes during development, which could be contrasted with one during disease states.

Second, design and generation of a Cre-dependent CharOFF AAV would be beneficial for *in vivo* analysis of specific tissue compartments in a focal manner. One such effort that would benefit from the use of CharOFF AAV would be evaluation of efferocytosis during spinal cord injury and recovery. Through use of CharOFF AAV within the spinal column after focal injury, apoptotic cell death and cell clearance could be studied at the tissue level through FACS based analysis, and additional RNAseq profiling. Insights from this effort would help us define the clearance repertoire within an injury setting.

Third, an alternative means to assess apoptotic cell clearance *in vivo* using CharOFF, is through the creation of CharOFF expressing allogeneic cells, such as primary HoxB8 hematopoietic cell lines [360] [361]. HoxB8 cells are generated by immortalization of bone marrow precursors from mice using a ER-fused HoxB8 construct, which allow a ready supply of allogeneic cells for differentiation into many progenitors *in vitro* and use within *in vivo* bone-marrow chimera settings. Creation of stably expressing HoxB8 CharOFF cells with an inducible death switch, such as diphtheria toxin, would permit *in vivo* analysis of monocyte or macrophage clearance through bone marrow chimera experiments. One interesting application would be to evaluate the identity of phagocytes which clear infiltrating monocytes during injury, such as EAE where there is a large influx of monocytes. This could provide insights into disease course, and the role of efferocytosis in EAE disease progression. Taken together, these three proposals survey the landscape of cell death and cell clearance in different settings and using different methods, highlighting the utility of CharOFF.

3.6.6 Extending our understanding of efferocytic compromise and coordination

Additional investigations into the coordination and compromise of macrophages during efferocytosis has broad ranging applications for disease states where there is a mix of apoptotic and necrotic targets. First, branching from our findings to study efferocytic dynamics during development and the ways in which macrophages prioritize and compromise their collective efforts, it will be important to determine whether these findings extend to other model organisms and tissues. For instance, do macrophages in different tissue compartments experience

efferocytic burden and do they display different distributions of efferocytic burden? Likewise, does efferocytic burden shape their response to inflammatory insults? Insights from these focused studies would help us further understand the similarities and differences among efferocytic macrophages.

One possible avenue of research would be to create CharOFF-ic9 or CharOFF-DTR mouse transgenics to determine whether generation of additional apoptotic cells during development results in macrophage adaptation to corpse burden and if this has any impact on tissue health, inflammatory state or ability to clear necrotic debris. An approach to answer these outstanding questions within the peripheral nervous system would be to subject mice to spinal cord injury after induction of apoptotic cell death using CharOFF-ic9 or CharOFF-DTR. It is known that monocytes and microglia are important for clearance of apoptotic and myelin debris post-injury, however using this experimental approach would further our understanding between corpse burden and resolution of injury. Second, as we demonstrated that glia and macrophages display unique efferocytic properties, it will be important to perform longitudinal studies during organismal development to determine which efferocytes are present and the extent to which they are similar or different in their phagocytic capacity. These two points would serve as important extensions of our findings in order to better define the landscape of cell death and cell clearance *in vivo*.

References

1. Gordon, S. Elie Metchnikoff: father of natural immunity. (2008) doi:10.1002/eji.200838855.

2. Tauber, A. I. Metchnikoff and the phagocytosis theory. *Nat Rev Mol Cell Bio* **4**, 897–901 (2003).

3. deCathelineau, A. M. & Henson, P. M. The final step in programmed cell death: phagocytes carry apoptotic cells to the grave. *Essays in biochemistry* 105–17 (2003) doi:10.1042/bse0390105.

4. Gordon, S. Phagocytosis: An Immunobiologic Process. *Immunity* **44**, 463–475 (20**16**).

5. Kerr, J., Wyllie, A. & Currie, A. *Apoptosis*: A Basic Biological Phenomenon with Wideranging Implications in Tissue Kinetics. *Brit J Cancer* **26**, 239–257 (1972).

6. Green, D. R. & Fitzgerald, P. Just So Stories about the Evolution of Apoptosis. *Current Biology* **26**, R620–R627 (2016).

7. Roos, W. P., Thomas, A. D. & Kaina, B. DNA damage and the balance between survival and death in cancer biology. *Nature Reviews Cancer* 20–33 (2016) doi:10.1038/nrc.2015.2.

8. Hata, A. N., Engelman, J. A. & Faber, A. C. The BCL2 Family: Key Mediators of the Apoptotic Response to Targeted Anticancer Therapeutics. *Cancer Discovery* 475–487 (2015) doi:10.1158/2159-8290.CD-15-0011.

9. Aluvila, S. *et al.* Organization of the Mitochondrial Apoptotic BAK Pore. *Journal of Biological Chemistry* **289**, 2537–2551 (2014).

10. Shamas-Din, A., Kale, J., Leber, B. & Andrews, D. W. Mechanisms of Action of Bcl-2 Family Proteins. *Cold Spring Harbor Perspectives in Biology* a008714 (2013) doi:10.1101/cshperspect.a008714.

11. Hardwick, J. & biology, S.-L. perspectives in. Multiple functions of BCL-2 family proteins. (2013) doi:10.1101/cshperspect.a008722.

12. Tait, S. W. & Green, D. R. Mitochondria and cell death: outer membrane permeabilization and beyond. *Nature Reviews Molecular Cell Biology* **11**, 621 (2010).

1**3**. Salvesen, G. S. & Duckett, C. S. IAP proteins: blocking the road to death's door. Nature Reviews Molecular Cell Biology 3, 401–410 (2002).

14. Galluzzi, L. et al. Essential versus accessory aspects of cell death: recommendations of the NCCD 2015. *Cell Death & Differentiation* **22**, 58–73 (2015).

15. Scott, F. L. et al. The Fas–FADD death domain complex structure unravels signalling by receptor clustering. Nature **457**, 1019–1022 (2009).

16. Brenner, D., Blaser, H. & Mak, T. W. Regulation of tumour necrosis factor signalling: live or let die. *Nature Reviews Immunology* **15**, 362–374 (2015).
17. Ting, A. T. & Bertrand, M. More to Life than NF-κB in TNFR1 Signaling. *Trends in Immunology* **37**, 535–**545** (2016).
18. Reilly, L. A. et al. Membrane-bound Fas ligand only is essential for Fas-induced apoptosis. Nature 659–663 (2009) doi:10.1038/nature08402.
19. Oberst, A. et al. Inducible Dimerization and Inducible Cleavage Reveal a Requirement for Both Processes in Caspase-8 Activation. Journal of Biological Chemistry **285**, 166**32**–16642 (2010).
20. Jost, P. J. et al. XIAP discriminates between type I and type II FAS-induced apoptosis. Nature **460**, 1035–1039 (2009).
21. Fadok, V. A. et al. Macrophages that have ingested apoptotic cells in vitro inhibit proinflammatory cytokine production through autocrine/paracrine mechanisms involving TGF-beta, PGE2, and PAF. *The Journal of clinical investigation* **101**, 890–8 (1998).
22. Huynh, M.-L. N. L., Fadok, V. A. & Henson, P. M. Phosphatidylserine-dependent ingestion of apoptotic cells promotes TGF-beta1 secretion and the resolution of inflammation. The Journal of clinical investigation **109**, 41–**50** (2002).
23. Wyllie, A., Morris, R., Smith, A. & Dunlop, D. Chromatin cleavage in apoptosis: Association with condensed chromatin morphology and dependence on macromolecular synthesis. *The Journal of Pathology* 67–77 (1984) doi:10.1002/path.**171**1420112.
24. Yuste, V. J. et al. The Contribution of Apoptosis-inducing Factor, Caspase-activated DNase, and Inhibitor of Caspase-activated DNase to the Nuclear Phenotype and DNA Degradation during Apoptosis*. Journal of Biological Chemistry 35670–35683 (2005) doi:10.1074/jbc.M**504**01**52**00.
25. Coleman, M. L. et al. Membrane blebbing during apoptosis results from caspase-mediated activation of ROCK I. *Nature Cell Biology* 339–345 (2001) doi:10.1038/3**507**0009.
26. Peter, C. et al. Migration to apoptotic “find-me” signals is mediated via the phagocyte receptor G2A. *The Journal of biological chemistry* **283**, 5296–305 (2008).
27. Kern, K. et al. The G2A Receptor Controls Polarization of Macrophage by Determining Their Localization Within the Inflamed Tissue. *Frontiers in Immunology* **9**, (2018).
28. Lee, H.-J., Ko, H.-J., Song, D.-K. & Jung, Y.-J. Lysophosphatidylcholine Promotes Phagosome Maturation and Regulates Inflammatory Mediator Production Through the Protein Kinase A–Phosphatidylinositol 3 Kinase–p38 Mitogen-Activated Protein Kinase Signaling Pathway During Mycobacterium tuberculosis Infection in Mouse Macrophages. Frontiers in

Immunology 9, (2018).
29. Knies, U. E. et al. Regulation of endothelial monocyte-activating polypeptide II release by apoptosis. *Proceedings of the National Academy of Sciences* **123**22–12327 (1998) doi:10.1073/pnas.95.21.12322.
30. Lauber, K. et al. Apoptotic Cells Induce Migration of Phagocytes via Caspase-3-Mediated Release of a Lipid Attraction Signal. Cell 717–730 (2003) doi:10.1016/S0092-8674(03)00422-7.
31. Behrensdorf, H. A., Craen, M. van de, Knies, U. E., Vandenabeele, P. & Clauss, M. The endothelial monocyte-activating polypeptide II (EMAP II) is a substrate for caspase-7. *FEBS letters* **466**, 143–7 (2000).
32. Hou, Y. et al. Endothelial-monocyte-activating polypeptide II induces migration of endothelial progenitor cells via the chemokine receptor CXCR3. *Experimental hematology* **34**, 1125–32 (2006).
33. Shalak, V. et al. Characterization of p43(ARF), a Derivative of the p43 Component of Multiaminoacyl-tRNA Synthetase Complex Released during Apoptosis*. Journal of Biological Chemistry 10935–10943 (2007) doi:10.1074/jbc.M611737200.
34. Ko, Y.-G. et al. A Cofactor of tRNA Synthetase, p43, Is Secreted to Up-regulate Proinflammatory Genes*. Journal of Biological Chemistry 23028–23033 (2001) doi:10.1074/jbc.M101544200.
35. Truman, L. A. et al. CX3CL1/fractalkine is released from apoptotic lymphocytes to stimulate macrophage chemotaxis. *Blood* **112**, 5026–36 (2008).
36. Elliott, M. R. et al. Nucleotides released by apoptotic cells act as a find-me signal to promote phagocytic clearance. Nature **461**, 282–6 (2009).
37. Chekeni, F. B. et al. Pannexin 1 channels mediate 'find-me' signal release and membrane permeability during apoptosis. Nature 863–867 (2010) doi:10.1038/nature094**13**.
38. Idzko, M., Ferrari, D. & Eltzschig, H. K. Nucleotide signalling during inflammation. Nature **509**, 310–7 (2014).
39. Medina, C. B. et al. Metabolites released from apoptotic cells act as tissue messengers. Nature 130–135 (2020) doi:10.1038/s41586-020-2121-3.
40. Silva, M. T. Secondary necrosis: the natural outcome of the complete apoptotic program. FEBS letters **584**, 4491–9 (2010).
41. Wang, Y. et al. Chemotherapy drugs induce pyroptosis through caspase-3 cleavage of a gasdermin. Nature 99–103 (2017) doi:10.1038/nature22393.
42. Sender, R. & Milo, R. The distribution of cellular turnover in the human body. *Nat Med* **27**, 45–48 (2021).

43. Fadok, V. A., Bratton, D. L., Frasch, C. S., Warner, M. L. & Henson, P. M. The role of phosphatidylserine in recognition of apoptotic cells by phagocytes. Cell Death & Differentiation 551–562 (1998) doi:10.1038/sj.cdd.4400404.
44. Balasubramanian, K. & Schroit, A. J. Aminophospholipid Asymmetry: A Matter of Life and Death. *Annual Review of Physiology* 701–734 (2003) doi:10.1146/annurev.physiol.65.092101.142459.
45. Lemke, G. How macrophages deal with death. Nature Reviews Immunology 1–11 (2019) doi:10.1038/s41577-019-0167-y.
46. CYTOLOGICAL AND CYTOCHEMICAL STUDIES ON CELL DEATH AND DIGESTION IN THE FOETAL RAT FOOT: THE ROLE OF MACRO- PHAGES AND HYDROLYTIC ENZYMES. (n.d.).
47. Park, D. et al. BAI1 is an engulfment receptor for apoptotic cells upstream of the ELMO/Dock180/Rac module. Nature 430–434 (2007) doi:10.1038/nature06329.
48. Rodriguez-Manzanet, R. & the …, S.-M. of. T and B cell hyperactivity and autoimmunity associated with niche-specific defects in apoptotic body clearance in TIM-4-deficient mice. (2010) doi:10.**107**3/pnas.0910359107.
49. Lemke, G. & Rothlin, C. V. Immunobiology of the TAM receptors. *Nature reviews. Immunology* **8**, 327–36 (2008).
50. Schledzewski, K. et al. Deficiency of liver sinusoidal scavenger receptors stabilin-1 and -2 in mice causes glomerulofibrotic nephropathy via impaired hepatic clearance of noxious blood factors. *Journal of Clinical Investigation* 703–714 (2011) doi:10.1**172**/JCI44740.
51. Lee, C. S. et al. Boosting Apoptotic Cell Clearance by Colonic Epithelial Cells Attenuates Inflammation In Vivo. *Immunity* **44**, 807–20 (2016).
52. Das, S. et al. Brain angiogenesis inhibitor 1 is expressed by gastric phagocytes during infection with Helicobacter pylori and mediates the recognition and engulfment of human apoptotic gastric epithelial cells. *The FASEB Journal* 2214–22**24** (2014) doi:10.1096/fj.13-243238.
53. Mazaheri, F. et al. Distinct roles for BAI1 and TIM-4 in the engulfment of dying neurons by microglia. *Nature communications* **5**, 4046 (2014).
54. Miyanishi, M. et al. Identification of Tim4 as a phosphatidylserine receptor. Nature 435–439 (2007) doi:10.1038/nature06307.
55. Wong, K., Valdez, P., Tan, C. & the …, Y.-S. of. Phosphatidylserine receptor Tim-4 is essential for the maintenance of the homeostatic state of resident peritoneal macrophages. (2010) doi:10.1073/pnas.0910929107.

56. Miyanishi, M., Segawa, K. & Nagata, S. Synergistic effect of Tim4 and MFG-E8 null mutations on the development of autoimmunity. *International Immunology* 551–559 (2012) doi:10.1093/intimm/dxs064.
57. Park, S.-Y. Y. et al. Rapid cell corpse clearance by stabilin-2, a membrane phosphatidylserine receptor. *Cell death and differentiation* **15**, 192–201 (2008).
58. Park, S.-Y. et al. Requirement of Adaptor Protein GULP during Stabilin-2-mediated Cell Corpse Engulfment*. Journal of Biological Chemistry 10**593**–10600 (2008) doi:10.1074/jbc.M709105200.
59. Lee, G. et al. Molecular targeting of atherosclerotic plaques by a stabilin-2-specific peptide ligand. *Journal of Controlled Release* 211–217 (2011) doi:10.1016/j.jconrel.2011.07.010.
60. Brugnera, E. et al. Unconventional Rac-GEF activity is mediated through the Dock180–ELMO complex. Nature Cell Biology **574**–582 (2002) doi:10.1038/ncb824.
61. Devitt, A. et al. Human CD14 mediates recognition and phagocytosis of apoptotic cells. Nature 505–509 (1998) doi:10.1038/33**169**.
62. Schlegel, R. A., Krahling, S., Callahan, M. K. & Williamson, P. CD14 is a component of multiple recognition systems used by macrophages to phagocytose apoptotic lymphocytes. Cell Death & Differentiation 583–592 (1999) doi:10.1038/sj.cdd.4400529.
63. Fadok, V., Warner, M., Bratton, D. & Henson, P. CD36 is required for phagocytosis of apoptotic cells by human macrophages that use either a phosphatidylserine receptor or the vitronectin receptor (alpha v beta 3). *Journal of immunology (Baltimore, Md. : 1950)* 6250–7 (1998).
64. Moffatt, O., Devitt, A., Bell, E., Simmons, D. & Gregory, C. Macrophage recognition of ICAM-3 on apoptotic leukocytes. Journal of immunology (Baltimore, Md. : 1950) 6800–10 (1999).
65. Lemke, G. Biology of the TAM receptors. *Cold Spring Harbor perspectives in biology* **5**, a009076 (2013).
66. Anderson, H. A. et al. Serum-derived protein S binds to phosphatidylserine and stimulates the phagocytosis of apoptotic cells. *Nature Immunology* 87–91 (**20**03) doi:10.1038/ni871.
67. Ishimoto, Y., Ohashi, K., Mizuno, K. & Nakano, T. Promotion of the Uptake of PS Liposomes and Apoptotic Cells by a Product of Growth Arrest-Specific Gene, gas6. *Journal of Biochemistry* 411–417 (2000) doi:10.1093/oxfordjournals.jbchem.a022622.
68. Zagórska, A., Través, P. G., Lew, E. D., Dransfield, I. & Lemke, G. Diversification of TAM receptor tyrosine kinase function. *Nature immunology* **15**, 920–8 (2014).
69. Lu, Q. et al. Tyro-3 family receptors are essential regulators of mammalian

spermatogenesis. Nature **398**, 723–8 (**19**99).
70. Cohen, P. L. et al. Delayed Apoptotic Cell Clearance and Lupus-like Autoimmunity in Mice Lacking the c-mer Membrane Tyrosine Kinase. *The Journal of Experimental Medicine* 135–140 (2002) doi:10.1084/jem.20012094.
71. Duncan, J. L. et al. An RCS-Like Retinal Dystrophy Phenotype in Mer Knockout Mice. *Investigative Ophthalmology & Visual Science* 826–838 (2003) doi:10.1167/iovs.02-0438.
72. Burstyn-Cohen, T. et al. Genetic Dissection of TAM Receptor-Ligand Interaction in Retinal Pigment Epithelial Cell Phagocytosis. *Neuron* **76**, 1123–1132 (2012).
73. Fourgeaud, L. et al. TAM receptors regulate multiple features of microglial physiology. Nature **532**, 240–4 (2016).
74. Chung, W.-S. S. et al. Astrocytes mediate synapse elimination through MEGF10 and MERTK pathways. Nature 504, 394–400 (2013).
75. Lee, J.-H. et al. Astrocytes phagocytose adult hippocampal synapses for circuit homeostasis. Nature 612–617 (2021) doi:10.**103**8/s**41**586-020-03060-3.
76. Miksa, M. et al. Fractalkine-Induced MFG-E8 Leads to Enhanced Apoptotic Cell Clearance by Macrophages. *Mol Med* **13**, 553–560 (2007).
77. Ogden, C. et al. C1q and Mannose Binding Lectin Engagement of Cell Surface Calreticulin and Cd91 Initiates Macropinocytosis and Uptake of Apoptotic Cells. The Journal of Experimental Medicine 781–796 (2001) doi:10.1084/jem.194.6.781.
78. Albert, M. L., Kim, J.-I. & Birge, R. B. αvβ5 integrin recruits the CrkII–Dock180–Rac1 complex for phagocytosis of apoptotic cells. *Nat Cell Biol* **2**, 899–905 (2000).
79. Akakura, S. et al. The opsonin MFG-E8 is a ligand for the αvβ5 integrin and triggers DOCK180-dependent Rac1 activation for the phagocytosis of apoptotic cells. *Experimental Cell Research* **4**03–416 (2004) doi:10.**101**6/j.yexcr.2003.09.011.
80. Ostrowski, P. P., Grinstein, S. & Freeman, S. A. Diffusion Barriers, Mechanical Forces, and the Biophysics of Phagocytosis. *Dev Cell* **38**, 135–146 (2016).
81. Freeman, S. A. et al. Transmembrane Pickets Connect Cyto- and Pericellular Skeletons Forming Barriers to Receptor Engagement. Cell 172, 305-317.e10 (n.d.).
82. Barclay, A. N. & Berg, T. K. van den. The Interaction Between Signal Regulatory Protein Alpha (SIRPα) and CD**47**: Structure, Function, and Therapeutic Target. Immunology 32, 25–50 (2014).
83. Lv, Z. et al. Loss of Cell Surface CD47 Clustering Formation and Binding Avidity to SIRPα Facilitate Apoptotic Cell Clearance by Macrophages. *J Immunol* **195**, 661–671 (2015).
84. Lehrman, E. K. et al. CD47 Protects Synapses from Excess Microglia-Mediated Pruning

during *Development*. Neuron **100**, 120-134.e6 (2018).
85. Kristiansen, G. et al. CD24 expression is a new prognostic marker in breast cancer. *Clin Cancer Res Official J Am Assoc Cancer Res* **9**, 4906–13 (2003).
86. Voll, R. E. et al. Immunosuppressive effects of apoptotic cells. Nature 350–351 (19**97**) doi:10.1038/37022.
87. Barkal, A. A. et al. CD24 signalling through macrophage Siglec-10 is a target for cancer immunotherapy. Nature **572**, 392–396 (2019).
88. Fanger, N. A. et al. The MHC class I binding proteins LIR-1 and LIR-2 inhibit Fc receptor-mediated signaling in monocytes. *Eur J Immunol* **28**, 3423–3434 (1998).
89. Barkal, A. A. et al. Engagement of MHC class I by the inhibitory receptor LILRB1 suppresses macrophages and is a target of cancer immunotherapy. Nature immunology (2017) doi:10.1038/s41590-017-0004-z.
90. Brown, S. et al. Apoptosis disables CD31-mediated cell detachment from phagocytes promoting binding and engulfment. Nature **418**, 200–203 (2002).
91. Varki, A. & Angata, T. Siglecs—the major subfamily of I-type lectins. *Glycobiology* **16**, 1R-27R (2006).
92. Nomura, K., Vilalta, A., Allendorf, D. H., Hornik, T. C. & Brown, G. C. Activated Microglia Desialylate and Phagocytose Cells via Neuraminidase, Galectin-3, and Mer Tyrosine Kinase. J Immunol **198**, 4792–**48**01 (2017).
93. Klaus, C. et al. Reduced sialylation triggers homeostatic synapse and neuronal loss in middle-aged mice. *Neurobiol Aging* **88**, 91–107 (2020).
94. Linnartz, B., Kopatz, J., Tenner, A. J. & Neumann, H. Sialic Acid on the Neuronal Glycocalyx Prevents Complement C1 Binding and Complement Receptor-3-Mediated Removal by Microglia. *J Neurosci* **32**, 946–952 (2012).
95. Imbert, P. R. C. et al. An Acquired and Endogenous Glycocalyx Forms a Bidirectional “Don’t Eat” and “Don’t Eat Me” Barrier to Phagocytosis. *Curr Biol* **31**, 77-89.e5 (2021).
96. Païdassi, H. et al. C1q Binds Phosphatidylserine and Likely Acts as a Multiligand-Bridging Molecule in Apoptotic Cell Recognition. J Immunol **180**, 2329–2338 (2008).
97. Bode, K. et al. Dectin-1 Binding to Annexins on Apoptotic Cells Induces Peripheral Immune Tolerance via NADPH Oxidase-2. *Cell Reports* **29**, 44**35**-4446.e9 (2019).
9**8**. Hanayama, R., Miyasaka, K., Nakaya, M. & Nagata, S. MFG-E8-Dependent Clearance of Apoptotic Cells, and Autoimmunity Caused by Its Failure. *Curr Dir Autoimmun* **9**, 162–172 (2005).
99. Hanayama, R. et al. Autoimmune Disease and Impaired Uptake of Apoptotic Cells in MFG-

E8-Deficient Mice. Science **304**, 1**14**7–1150 (2004).
100. Gardai, S. J. et al. Cell-Surface Calreticulin Initiates Clearance of Viable or Apoptotic Cells through trans-Activation of LRP on the Phagocyte. Cell 123, 321–3**34** (2005).
101. Blackburn, J. W. D. et al. Soluble CD93 is an apoptotic cell opsonin recognized by αxβ2. Eur J Immunol **49**, 600–610 (2019).
102. Caberoy, N. B., Alvarado, G., Bigcas, J. & Li, W. Galectin-3 is a new MerTK-specific eat-me signal. *J Cell Physiol* **227**, **40**1–407 (2012).
103. Moodley, Y. et al. Macrophage Recognition and Phagocytosis of Apoptotic Fibroblasts Is Critically Dependent on Fibroblast-Derived Thrombospondin 1 and CD**36**. *Am J Pathology* **162**, 771–779 (2003).
104. MacPherson, M., Lek, H. S., Prescott, A. & Fagerholm, S. C. A Systemic Lupus Erythematosus-associated R77H Substitution in the CD11b Chain of the Mac-1 Integrin Compromises Leukocyte Adhesion and Phagocytosis*. *J Biol Chem* **286**, 17303–17**31**0 (2011).
105. Ramirez-Ortiz, Z. G. et al. The scavenger receptor SCARF1 mediates the clearance of apoptotic cells and prevents autoimmunity. *Nat Immunol* **14**, 9**17**–926 (2013).
106. Tao, H. et al. Macrophage SR-BI mediates efferocytosis via Src/PI3K/Rac1 signaling and reduces atherosclerotic lesion necrosis[S]. *J Lipid Res* **56**, **144**9–**146**0 (2015).
107. Kourtzelis, I. et al. DEL-1 promotes macrophage efferocytosis and clearance of inflammation. Nature Immunology 20, 40–49 (2019).
108. Ren, Y., Silverstein, R. L., Allen, J. & Savill, J. CD36 gene transfer confers capacity for phagocytosis of cells undergoing apoptosis. *J Exp Medicine* **181**, 1857–**186**2 (1995).
109. Greenberg, M. E. et al. Oxidized phosphatidylserine–CD36 interactions play an essential role in macrophage-dependent phagocytosis of apoptotic cells. J Exp Medicine **203**, 2613–26**25** (2006).
110. Oka, K. et al. Lectin-like oxidized low-density lipoprotein receptor 1 mediates phagocytosis of aged/apoptotic cells in endothelial cells. *Proc National Acad Sci* **95**, 9535–9**54**0 (1998).
111. Friggeri, A. et al. Participation of the Receptor for Advanced Glycation End Products in Efferocytosis. J Immunol 186, 6191–6198 (2011).
112. Kojima, Y. et al. CD47-blocking antibodies restore phagocytosis and prevent atherosclerosis. Nature **536**, 86 (2016).
113. Gordon, S. R. et al. PD-1 expression by tumour-associated macrophages inhibits phagocytosis and tumour immunity. Nature 545, 495–**499** (2017).
114. Su, S. et al. Immune Checkpoint Inhibition Overcomes ADCP-Induced Immunosuppression by Macrophages. Cell **175**, 442-457.e23 (2018).

115. Sambrano, G. R. & Steinberg, D. Recognition of oxidatively damaged and apoptotic cells by an oxidized low density lipoprotein receptor on mouse peritoneal macrophages: role of membrane phosphatidylserine. Proc National Acad Sci **92**, 1396–1400 (1995).
116. Suter, E. C. et al. Antibody:CD47 ratio regulates macrophage phagocytosis through competitive receptor phosphorylation. Cell Reports 36, 109587 (2021).
117. Hochreiter-Hufford, A. & Ravichandran, K. S. Clearing the Dead: Apoptotic Cell Sensing, Recognition, Engulfment, and Digestion. Cold Spring Harbor Perspectives in Biology a008748 (2013) doi:10.**110**1/cshperspect.a008748.
118. Mao, Y. & Finnemann, S. C. Regulation of phagocytosis by Rho GTPases. *Small GTPases* **6**, 89–99 (2015).
119. Kim, S.-Y. et al. Coordinated balance of Rac1 and RhoA plays key roles in determining phagocytic appetite. *Plos One* **12**, e0174603 (2017).
120. Wu, Y., Singh, S., Georgescu, M. & Birge, R. A role for Mer tyrosine kinase in αvβ5 integrin-mediated phagocytosis of apoptotic cells. (2005) doi:10.1242/jcs.01632.
121. Nishi, C., Yanagihashi, Y., Segawa, K. & Nagata, S. MERTK tyrosine kinase receptor together with TIM4 phosphatidylserine receptor mediates distinct signal transduction pathways for efferocytosis and cell proliferation. J Biol Chem **294**, 7221–7230 (2019).
122. Ishibe, S., Joly, D., Liu, Z.-X. & Cantley, L. G. Paxillin Serves as an ERK-Regulated Scaffold for Coordinating FAK and Rac Activation in Epithelial Morphogenesis. Mol Cell 16, 257–267 (2004).
123. Mahajan, N. P. & Earp, S. H. An SH2 Domain-dependent, Phosphotyrosine-independent Interaction between Vav1 and the Mer Receptor Tyrosine Kinase A MECHANISM FOR LOCALIZING GUANINE NUCLEOTIDE-EXCHANGE FACTOR ACTION. Journal of Biological Chemistry **278**, 42596–42603 (2003).
124. Kinchen, J. M. & Ravichandran, K. S. Phagosome maturation: going through the acid test. *Nature reviews. Molecular cell biology* **9**, 781–95 (2008).
125. Kinchen, J. M. et al. A pathway for phagosome maturation during engulfment of apoptotic cells. *Nature cell biology* **10**, 556–66 (2008).
126. Yin, C., Kim, Y., Argintaru, D. & Heit, B. Rab17 mediates differential antigen sorting following efferocytosis and phagocytosis. *Cell Death Dis* **7**, e252**9**–e2529 (2016).
127. Martinez, J. et al. Noncanonical autophagy inhibits the autoinflammatory, lupus-like response to dying cells. Nature **533**, 115–9 (2016).
128. Martinez, J. et al. Microtubule-associated protein 1 light chain 3 alpha (LC3)-associated phagocytosis is required for the efficient clearance of dead cells. Proc National Acad Sci **108**,

17396–17401 (2011).
129. Cunha, L., Yang, M., Carter, R., Guy, C. & Cell, H.-L. LC3-associated phagocytosis in myeloid cells promotes tumor immune tolerance. (2018).
130. Wu, Y. et al. Microglial lysosome dysfunction contributes to white matter pathology and TDP-43 proteinopathy in GRN-associated FTD. Cell Reports 36, 109581 (2021).
131. Aflaki, E. et al. Efferocytosis is impaired in Gaucher macrophages. *Haematologica* **102**, 656–665 (2017).
132. Keller, S., Berghoff, K. & Kress, H. Phagosomal transport depends strongly on phagosome size. *Scientific Reports* **7**, 170**68** (2017).
133. Yvan-Charvet, L. et al. ABCA1 and ABCG1 Protect Against Oxidative Stress–Induced Macrophage Apoptosis During Efferocytosis. *Circ Res* **106**, 1861–1869 (2010).
134. Fond, A. M. & Ravichandran, K. S. Clearance of Dying Cells by Phagocytes: Mechanisms and Implications for Disease Pathogenesis. *Advances in experimental medicine and biology* **930**, 25–49 (2016).
135. Morioka, S. et al. Efferocytosis induces a novel SLC program to promote glucose uptake and lactate release. Nature **563**, 714–718 (2018).
136. A-Gonzalez, N. et al. Apoptotic Cells Promote Their Own Clearance and Immune Tolerance through Activation of the Nuclear Receptor LXR. Immunity 245–258 (2009) doi:10.1016/j.immuni.2009.06.018.
137. Zhang, S. et al. Efferocytosis Fuels Requirements of Fatty Acid Oxidation and the Electron Transport Chain to Polarize Macrophages for Tissue Repair. *Cell Metab* **29**, 443-456.e5 (2019).
138. Wang, Y. et al. Mitochondrial Fission Promotes the Continued Clearance of Apoptotic Cells by Macrophages. Cell 171, 331-345.e22 (2017).
139. Park, D. et al. Continued clearance of apoptotic cells critically depends on the phagocyte Ucp2 protein. Nature **477**, 220–224 (2011).
140. Yurdagul, A. et al. Macrophage Metabolism of Apoptotic Cell-Derived Arginine Promotes Continual Efferocytosis and Resolution of Injury. *Cell Metabolism* (2020) doi:10.1016/j.cmet.2020.01.001.
141. Wang, Z. A., Hsu, W. & Liu, W. R. Handbook of Nutrition, Diet, and Epigenetics. 311–329 (2019) doi:10.1007/978-3-319-55530-0_1.
142. Noda, M., Doi, Y., Liang, J. & Biological …, K.-J. of. Fractalkine attenuates excito-neurotoxicity via microglial clearance of damaged neurons and antioxidant enzyme heme oxygenase-1 expression. (2011).
143. Engel, D., Krause, T. & of …, S.-S. CX3CR1 reduces kidney fibrosis by inhibiting local

proliferation of profibrotic macrophages. (2015) doi:10.4049/jimmunol.1402149.
144. Köröskényi, K. et al. Involvement of Adenosine A2A Receptors in Engulfment-Dependent Apoptotic Cell Suppression of Inflammation. *The Journal of Immunology* 7144–7155 (2011) doi:10.4049/jimmunol.1002284.
145. Yamaguchi, H., Maruyama, T., Urade, Y. & Nagata, S. Immunosuppression via adenosine receptor activation by adenosine monophosphate released from apoptotic cells. *eLife* e02172 (2014) doi:10.7554/eLife.02172.
146. Cekic, C. & Immunology, L.-J. Purinergic regulation of the immune system. (2016) doi:10.1038/nri.2016.4.
147. Poon, I. K. et al. Unexpected link between an antibiotic, pannexin channels and apoptosis. Nature 507, 329–34 (2014).
148. Ma, C., Martin, C., Ma, Z., Hafiane, A. & Biological …, D.-M. of. Engulfment protein GULP is regulator of transforming growth factor-β response in ovarian cells. (2012).
149. Sen, P., Wallet, M., Yi, Z., Huang, Y. & Blood, H.-M. Apoptotic cells induce Mer tyrosine kinase–dependent blockade of NF-κB activation in dendritic cells. (2007).
150. Rothlin, C. V., Ghosh, S., Zuniga, E. I., Oldstone, M. B. & Lemke, G. TAM receptors are pleiotropic inhibitors of the innate immune response. Cell 131, 1124–36 (2007).
151. Murakami, Y. et al. CD300b regulates the phagocytosis of apoptotic cells via phosphatidylserine recognition. Cell Death & Differentiation 1746–1757 (2014) doi:10.1038/cdd.2014.86.
152. Voss, O., Murakami, Y., Pena, M., Lee, H. & Immunity, T.-L. Lipopolysaccharide-induced CD300b receptor binding to toll-like receptor 4 alters signaling to drive cytokine responses that enhance septic shock. (2016).
153. Nakahashi-Oda, C. & Experimental …, T.-H.-S. of. Apoptotic cells suppress mast cell inflammatory responses via the CD300a immunoreceptor. (2012) doi:10.1084/jem.20120096.
154. McWhorter, F. Y., Wang, T., Nguyen, P., Chung, T. & Liu, W. F. Modulation of macrophage phenotype by cell shape. Proc National Acad Sci 110, 17253–17258 (2013).
155. Castrillo, A. & Tontonoz, P. NUCLEAR RECEPTORS IN MACROPHAGE BIOLOGY: At the Crossroads of Lipid Metabolism and Inflammation. *Annual Review of Cell and Developmental Biology* 455–480 (2004) doi:10.1146/annurev.cellbio.20.012103.134432.
156. Xu, W. et al. IL-10–producing macrophages preferentially clear early apoptotic cells. Blood 107, 4930–4937 (2006).
157. Snodgrass, R. G. et al. Efferocytosis potentiates the expression of arachidonate 15-lipoxygenase (ALOX15) in alternatively activated human macrophages through LXR activation.

Cell Death Differ 1–16 (2020) doi:10.1038/s41418-020-00652-4.
158. Roberts, A. W. et al. Tissue-Resident Macrophages Are Locally Programmed for Silent Clearance of Apoptotic Cells. Immunity 47, 913-927.e6 (2017).
159. Mukundan, L. et al. PPAR-δ senses and orchestrates clearance of apoptotic cells to promote tolerance. *Nature Medicine* 1266–1272 (2009) doi:10.1038/nm.2048.
160. Rőszer, T. et al. Autoimmune Kidney Disease and Impaired Engulfment of Apoptotic Cells in Mice with Macrophage Peroxisome Proliferator-Activated Receptor γ or Retinoid X Receptor α Deficiency. The Journal of Immunology 621–631 (2011) doi:10.4049/jimmunol.1002230.
161. Fouda, A. Y. et al. Arginase 1 promotes retinal neurovascular protection from ischemia through suppression of macrophage inflammatory responses. Cell Death Dis 9, 1001 (2018).
162. Shen, K., Sidik, H. & Talbot, W. S. The Rag-Ragulator Complex Regulates Lysosome Function and Phagocytic Flux in Microglia. Cell Reports 14, 547–559 (2016).
163. Diaz-Aparicio, I. et al. Microglia actively remodels adult hippocampal neurogenesis through the phagocytosis secretome. *bioRxiv* 583849 (2019) doi:10.1101/583849.
164. Nimmerjahn, A., Kirchhoff, F. & Helmchen, F. Resting Microglial Cells Are Highly Dynamic Surveillants of Brain Parenchyma in Vivo. Science **308**, 1314–1318 (2005).
165. Ginhoux, F. et al. Fate mapping analysis reveals that adult microglia derive from primitive macrophages. *Science (New York, N.Y.)* **330**, 841–5 (2010).
166. Matcovitch-Natan, O. et al. Microglia development follows a stepwise program to regulate brain homeostasis. Science **353**, aad8670 (2016).
167. Miller, F. D. & Gauthier, A. S. Timing Is Everything: Making Neurons versus *Glia* in the Developing Cortex. Neuron 54, 357–369 (2007).
168. Hammond, T. R., Marsh, S. E. & Stevens, B. Immune Signaling in Neurodegeneration. Immunity 50, 9**55**–974 (2019).
169. Masuda, T. et al. Spatial and temporal heterogeneity of mouse and human microglia at single-cell resolution. Nature 1–5 (2019) doi:10.1038/s41586-019-0924-x.
170. Peri, F. & Nüsslein-Volhard, C. Live Imaging of Neuronal Degradation by Microglia Reveals a Role for v0-ATPase a1 in Phagosomal Fusion In Vivo. Cell 133, 916–927 (2008).
171. Kurant, E., Axelrod, S., Leaman, D. & Gaul, U. Six-Microns-Under Acts Upstream of Draper in the Glial Phagocytosis of Apoptotic Neurons. Cell 133, 498–509 (2008).
172. Sierra, A. et al. Microglia Shape Adult Hippocampal Neurogenesis through Apoptosis-Coupled Phagocytosis. *Cell Stem Cell* **7**, 483–495 (2010).
173. Anderson, S. R. et al. Developmental Apoptosis Promotes a Disease-Related Gene Signature and Independence from CSF1R Signaling in Retinal Microglia. Cell Reports 27, 2002-

2013.e5 (2019).
174. Casano, A. M., Albert, M. & Peri, F. Developmental Apoptosis Mediates Entry and Positioning of Microglia in the Zebrafish Brain. *Cell reports* **16**, 897–906 (2016).
175. Squarzoni, P. et al. Microglia Modulate Wiring of the Embryonic Forebrain. Cell Reports 8, 1271–1279 (2014).
176. Cunningham, C. L., Martínez-Cerdeño, V. & Noctor, S. C. Microglia regulate the number of neural precursor cells in the developing cerebral cortex. *The Journal of neuroscience : the official journal of the Society for Neuroscience* **33**, 4216–33 (2013).
177. Rice, R. A. et al. Elimination of Microglia Improves Functional Outcomes Following Extensive Neuronal Loss in the Hippocampus. J Neurosci 35, 9977–9989 (2015).
178. Ayata, P. et al. Epigenetic regulation of brain region-specific microglia clearance activity. *Nature neuroscience* (2018) doi:10.1038/s415**9**3-018-0192-3.
179. Li, Q. et al. Developmental Heterogeneity of Microglia and Brain Myeloid Cells Revealed by Deep Single-Cell RNA Sequencing. Neuron 101, 207-223.e10 (2018).
180. Marín-Teva, J. L. et al. Microglia Promote the Death of Developing Purkinje Cells. Neuron 41, 535–547 (2004).
181. Wakselman, S. et al. Developmental Neuronal Death in Hippocampus Requires the Microglial CD11b Integrin and DAP12 Immunoreceptor. *The Journal of Neuroscience* **28**, 8138–8143 (2008).
182. Weinhard, L. et al. Microglia remodel synapses by presynaptic trogocytosis and spine head filopodia induction. *Nature Communications* **9**, 1228 (2018).
183. Butovsky, O. et al. Microglia activated by IL-**4** or IFN-γ differentially induce neurogenesis and oligodendrogenesis from adult stem/progenitor cells. *Mol Cell Neurosci* **31**, 149–160 (2006).
184. Ueno, M. et al. Layer V cortical neurons require microglial support for survival during postnatal development. *Nat Neurosci* **16**, 543–551 (**20**13).
185. Xavier, A. L., Kress, B. T., Goldman, S. A., Menezes, J. R. de & Nedergaard, M. A Distinct Population of Microglia Supports Adult Neurogenesis in the Subventricular Zone. The Journal of Neuroscience **35**, 11848–118**61** (2015).
186. Diaz-Aparicio, I. et al. Microglia actively remodel adult hippocampal neurogenesis through the phagocytosis secretome. J Neurosci 40, 0993–19 (2020).
187. Villani, A. et al. Clearance by Microglia Depends on Packaging of Phagosomes into a Unique Cellular Compartment. *Developmental Cell* (2019) doi:**10**.1016/j.devcel.2019.02.0**14**.
188. Dorman, L. C. et al. A type I interferon response defines a conserved microglial state required for effective phagocytosis. *Biorxiv* 2021.04.29.441889 (2021)

doi:10.1101/2021.04.29.441889.
189. Prinz, M., Priller, J., Sisodia, S. S. & Ransohoff, R. M. Heterogeneity of CNS myeloid cells and their roles in neurodegeneration. Nat Neurosci 14, 1227–1235 (2011).
190. Hove, H. et al. A single-cell atlas of mouse brain macrophages reveals unique transcriptional identities shaped by ontogeny and tissue environment. *Nature Neuroscience* 1 (2019) doi:10.1038/s41593-019-0393-4.
191. Mrdjen, D. et al. High-Dimensional Single-Cell Mapping of Central Nervous System Immune Cells Reveals Distinct Myeloid Subsets in Health, Aging, and Disease. Immunity 48, 599 (2018).
192. Goldmann, T. et al. Origin, fate and dynamics of macrophages at central nervous system interfaces. Nat Immunol 17, 797–805 (20**16**).
193. Mildner, A. et al. Microglia in the adult brain arise from Ly-6ChiCCR2+ monocytes only under defined host conditions. Nat Neurosci 10, 1544–1553 (2007).
194. Askew, K. et al. Coupled Proliferation and Apoptosis Maintain the Rapid Turnover of Microglia in the Adult Brain. Cell Reports 18, 391–405 (2017).
195. Cronk, J. C. et al. Peripherally derived macrophages can engraft the brain independent of irradiation and maintain an identity distinct from microglia. *The Journal of experimental medicine* **215**, 1627–1647 (2018).
196. Lund, H. et al. Competitive repopulation of an empty microglial niche yields functionally distinct subsets of microglia-like cells. Nature Communications 9, 4845 (2018).
197. Chen, H.-R. et al. Fate mapping via CCR2-CreER mice reveals monocyte-to-microglia transition in development and neonatal stroke. *Sci Adv* **6**, eabb2119 (2020).
198. Cugurra, A. et al. Skull and vertebral bone marrow are myeloid cell reservoirs for the meninges and CNS parenchyma. Science **373**, eabf7844 (2021).
199. Wohleb, E. S., McKim, D. B., Sheridan, J. F. & Godbout, J. P. Monocyte trafficking to the brain with stress and inflammation: a novel axis of immune-to-brain communication that influences mood and behavior. *Front Neurosci-switz* **8**, 447 (2015).
200. Zhang, W. et al. Macrophages reprogram after ischemic stroke and promote efferocytosis and inflammation resolution in the mouse brain. *Cns Neurosci Ther* **25**, 1329–1342 (2019).
201. Chang, C.-F. et al. Erythrocyte efferocytosis modulates macrophages towards recovery after intracerebral hemorrhage. *J Clin Invest* **128**, 607–624 (2017).
202. Ritzel, R. M. et al. Functional differences between microglia and monocytes after ischemic stroke. *J Neuroinflamm* **12**, 106 (2015).
203. Cai, W. et al. STAT6/Arg1 promotes microglia/macrophage efferocytosis and inflammation

resolution in stroke mice. *Jci Insight* **4**, e131355 (2019).
204. Tsai, H.-H. et al. Regional Astrocyte Allocation Regulates CNS Synaptogenesis and Repair. Science **337**, **358**–**36**2 (2012).
205. DeWitt, D. A., Perry, G., Cohen, M., Doller, C. & Silver, J. Astrocytes Regulate Microglial Phagocytosis of Senile Plaque Cores of Alzheimer's Disease. *Exp Neurol* **149**, 329–340 (1998).
206. Lööv, C., Mitchell, C. H., Simonsson, M. & Erlandsson, A. Slow degradation in phagocytic astrocytes can be enhanced by lysosomal acidification. Glia **63**, 1997–2009 (2015).
207. Iram, T. et al. Megf10 Is a Receptor for C1Q That Mediates Clearance of Apoptotic Cells by Astrocytes. Journal of Neuroscience 36, 5185–5192 (2016).
208. Pringle, N. & Richardson, W. A singularity of PDGF alpha-receptor expression in the dorsoventral axis of the neural tube may define the origin of the oligodendrocyte lineage. *Dev Camb Engl* **117**, 525–33 (1993).
209. Buchanan, J. et al. Oligodendrocyte precursor cells prune axons in the mouse neocortex. Biorxiv 2021.05.29.446047 (2021) doi:10.1101/2021.05.29.446047.
210. Nguyen, K. & Pender, M. Phagocytosis of apoptotic lymphocytes by oligodendrocytes in experimental autoimmune encephalomyelitis. *Acta Neuropathologica* **95**, 40–46 (1997).
211. Damisah, E. C. et al. Astrocytes and microglia play orchestrated roles and respect phagocytic territories during neuronal corpse removal in vivo. Sci Adv 6, eaba3239 (2020).
212. Lu, Z. et al. Phagocytic activity of neuronal progenitors regulates adult neurogenesis. Nature Cell Biology 13, 1076–1083 (2011).
213. Zhu, Y. et al. Migratory Neural Crest Cells Phagocytose Dead Cells in the Developing Nervous System. Cell 179, 74-89.e10 (2019).
214. Prasad, D. et al. TAM receptor function in the retinal pigment epithelium. *Molecular and Cellular Neuroscience* **33**, 96–108 (2006).
215. Finnemann, S. C. & Rodriguez-Boulan, E. Macrophage and Retinal Pigment Epithelium Phagocytosis. J Exp Medicine 190, 861–874 (1999).
216. Ruggiero, L., Connor, M. & the …, C. J. of. Diurnal, localized exposure of phosphatidylserine by rod outer segment tips in wild-type but not Itgb5−/− or Mfge8−/− mouse retina. (2012) doi:10.1073/pnas.1121101109.
217. Penberthy, K. K. et al. Context-dependent compensation among phosphatidylserine-recognition receptors. *Scientific reports* **7**, 14623 (2017).
218. Penberthy, K. K., Lysiak, J. J. & Ravichandran, K. S. Rethinking Phagocytes: Clues from the Retina and Testes. *Trends in cell biology* (2018) doi:10.1016/j.tcb.2018.01.004.
219. Müller, C. & Finnemann, S. C. Retinal Pigment Epithelium in Health and Disease. 47–63

(2020) doi:10.1007/978-3-030-28384-1_3.
220. Bertram, L., Lill, C. M. & Tanzi, R. E. The Genetics of Alzheimer Disease: Back to the Future. Neuron 68, 270–281 (2010).
221. Rohn, T. T. Caspase-cleaved TAR DNA-binding protein-43 is a major pathological finding in Alzheimer's disease. *Brain Res* **1228**, 189–198 (2008).
222. Radi, E., Formichi, P., Battisti, C. & Federico, A. Apoptosis and Oxidative Stress in Neurodegenerative Diseases. *J Alzheimer's Dis* **42**, S125–S152 (2014).
223. Naj, A. C., Schellenberg, G. D. & (ADGC), A. Genomic variants, genes, and pathways of Alzheimer's disease: An overview. *Am J Medical Genetics Part B Neuropsychiatric Genetics* **174**, 5–26 (2017).
224. Su, J. H., Kesslak, P. J., Head, E. & Cotman, C. W. Caspase-cleaved amyloid precursor protein and activated caspase-3 are co-localized in the granules of granulovacuolar degeneration in Alzheimer's disease and Down's syndrome brain. Acta Neuropathol **104**, 1–6 (2002).
225. Rissman, R. A. et al. Caspase-cleavage of tau is an early event in Alzheimer disease tangle pathology. J Clin Invest **114**, 121–130 (2004).
226. Caccamo, A. et al. Necroptosis activation in Alzheimer's disease. Nat Neurosci 20, 1236–1246 (2017).
227. Derecki, N. C., Katzmarski, N., Kipnis, J. & Meyer-Luehmann, M. Microglia as a critical player in both developmental and late-life CNS pathologies. Acta Neuropathologica **128**, 333–345 (2014).
228. Frost, J. & Schafer, D. Microglia: architects of the developing nervous system. (2016).
229. Colonna, M. & Butovsky, O. Microglia Function in the Central Nervous System During Health and Neurodegeneration. *Annual Review of Immunology* **35**, 1–28 (2016).
230. Hong, S. et al. Complement and microglia mediate early synapse loss in Alzheimer mouse models. Science (New York, N.Y.) **352**, 712–6 (2016).
231. Krabbe, G. et al. Functional Impairment of Microglia Coincides with Beta-Amyloid Deposition in Mice with Alzheimer-Like Pathology. *PLoS ONE* **8**, e60**9**21 (2013).
232. Huang, K., Marcora, E., Pimenova, A. & Nature …, D. A. A common haplotype lowers PU. 1 expression in myeloid cells and delays onset of Alzheimer's disease. (2017) doi:10.1038/nn.4587.
233. Jonsson, T., Stefansson, H. & of …, S.-S. Variant of TREM2 Associated with the Risk of Alzheimer's Disease. (2013) doi:10.**105**6/NEJMoa1211103.
234. Zhou, Y., Ulland, T. & neuroscience, C.-M. in aging. TREM2-dependent effects on

microglia in Alzheimer's disease. (2018).
235. Wang, Y., Cella, M., Mallinson, K., Ulrich, J. & Cell, Y.-K. TREM2 lipid sensing sustains the microglial response in an Alzheimer's disease model. (2015).
236. Cantoni, C., Bollman, B., Licastro, D., Xie, M. & Acta …, M.-R. TREM2 regulates microglial cell activation in response to demyelination in vivo. (2015).
237. Lee, C. Y. D. et al. Elevated TREM2 Gene Dosage Reprograms Microglia Responsivity and Ameliorates Pathological Phenotypes in Alzheimer's Disease Models. Neuron 97, 1032-1048.e5 (2018).
238. Garcia-Reitboeck, P., Phillips, A. & reports, P.-T. Human induced pluripotent stem cell-derived microglia-like cells harboring TREM2 missense mutations show specific deficits in phagocytosis. (2018).
239. Yuan, P., Condello, C., Keene, C., Wang, Y. & Neuron, B.-T. TREM2 haplodeficiency in mice and humans impairs the microglia barrier function leading to decreased amyloid compaction and severe axonal dystrophy. (2016).
240. Keren-Shaul, H. et al. A Unique Microglia Type Associated with Restricting Development of Alzheimer's Disease. Cell 169, 1276-1290.e17 (2017).
241. Song, W. M. & Colonna, M. The identity and function of microglia in neurodegeneration. Nature Immunology 19, 1048–1058 (2018).
242. Krasemann, S. et al. The TREM2-APOE Pathway Drives the Transcriptional Phenotype of Dysfunctional Microglia in Neurodegenerative Diseases. Immunity 47, 566-581.e9 (2017).
243. Jay, T. R. et al. TREM2 deficiency eliminates TREM2+ inflammatory macrophages and ameliorates pathology in Alzheimer's disease mouse models. J Exp Med 212, 287–295 (2015).
244. Estus, S. et al. Evaluation of CD33 as a genetic risk factor for Alzheimer's disease. *Acta neuropathologica* **138**, 187–199 (2019).
245. Hollingworth, P. et al. Common variants at ABCA7, MS4A6A/MS4A4E, EPHA1, CD33 and CD2AP are associated with Alzheimer's disease. *Nature genetics* **43**, 429–35 (2011).
246. Schwarz, F. et al. Human-specific derived alleles of CD33 and other genes protect against postreproductive cognitive decline. *Proceedings of the National Academy of Sciences of the United States of America* **113**, 74–9 (2016).
247. Son, M. et al. Evidence for C1q-mediated crosslinking of CD33/LAIR-1 inhibitory immunoreceptors and biological control of CD33/LAIR-1 expression. *Sci Rep-uk* **7**, **2**70 (2017).
24**8**. Griciuc, A. et al. TREM2 Acts Downstream of CD33 in Modulating Microglial Pathology in Alzheimer's Disease. Neuron 103, 820-835.e7 (2019).
249. Hickman, S. E. et al. The microglial sensome revealed by direct RNA sequencing. Nature

Neuroscience 16, 1896–1905 (2013).
250. Bhattacherjee, A., Rodrigues, E. & Communications …, J.-J. Repression of phagocytosis by human CD33 is not conserved with mouse CD33. (2019) doi:10.1038/s42003-019-0698-6.
251. Estes, M. L. & McAllister, K. A. Immune mediators in the brain and peripheral tissues in autism spectrum disorder. *Nat Rev Neurosci* **16**, 469–486 (2015).
252. Sidorov, M. S., Auerbach, B. D. & Bear, M. F. Fragile X mental retardation protein and synaptic plasticity. *Mol Brain* **6**, 15 (2013).
253. Cheng, Y., Corbin, J. G. & Levy, R. J. Programmed Cell Death Is Impaired in the Developing Brain of Fmr1 Mutants. *Dev Neurosci-basel* **35**, 347–358 (2013).
254. O'Connor, R. M. et al. A Drosophila model of Fragile X syndrome exhibits defects in phagocytosis by innate immune cells. *J Cell Biol* jcb.201607093 (2017) doi:10.1083/jcb.201607093.
255. Tessier, C. R. & Broadie, K. Drosophila fragile X mental retardation protein developmentally regulates activity-dependent axon pruning. Development 135, 1547–1557 (2008).
256. Gholizadeh, S., Halder, S. K. & Hampson, D. R. Expression of fragile X mental retardation protein in neurons and glia of the developing and adult mouse brain. Brain Res **1596**, 22–30 (2015).
257. Pacey, L. K. K. & Doering, L. C. Developmental expression of FMRP in the astrocyte lineage: Implications for fragile X syndrome. Glia 55, 1601–1609 (2007).
258. Lee, F. H. F., Lai, T. K. Y., Su, P. & Liu, F. Altered cortical Cytoarchitecture in the Fmr1 knockout mouse. Mol Brain **12**, 56 (2019).
259. Dickson, D. W. Parkinson's Disease and Parkinsonism: Neuropathology. *Csh Perspect Med* **2**, a009258 (2012).
260. Poewe, W. et al. Parkinson disease. *Nat Rev Dis Primers* **3**, 17013 (2017).
261. Bodea, L.-G. et al. Neurodegeneration by Activation of the Microglial Complement–Phagosome Pathway. J Neurosci 34, 8546–8556 (2014).
262. Stefanova, N. et al. Toll-Like Receptor 4 Promotes α-Synuclein Clearance and Survival of Nigral Dopaminergic Neurons. Am J Pathology 179, 954–963 (2011).
263. Luk, K. C. et al. Intracerebral inoculation of pathological α-synuclein initiates a rapidly progressive neurodegenerative α-synucleinopathy in mice. J Exp Med 209, 975–986 (2012).
264. Gustafsson, G. et al. Secretion and Uptake of α-Synuclein Via Extracellular Vesicles in Cultured Cells. *Cell Mol Neurobiol* **38**, 1**539**–1550 (2018).
265. Haenseler, W. et al. Excess α-synuclein compromises phagocytosis in iPSC-derived

macrophages. Sci Rep-uk 7, 9003 (2017).
266. Liddelow, S. A. et al. Neurotoxic reactive astrocytes are induced by activated microglia. Nature **541**, 481–487 (2017).
267. Morales, I., Sanchez, A., Rodriguez-Sabate, C. & Rodriguez, M. Striatal astrocytes engulf dopaminergic debris in Parkinson's disease: A study in an animal model. Plos One 12, e0185989 (2017).
268. Fricker, M., Oliva-Martín, M. & Brown, G. C. Primary phagocytosis of viable neurons by microglia activated with LPS or Aβ is dependent on calreticulin/LRP phagocytic signalling. *Journal of Neuroinflammation* **9**, 1–12 (2012).
269. Emmrich, J. V., Hornik, T. C., Neher, J. J. & Brown, G. C. Rotenone induces neuronal death by microglial phagocytosis of neurons. *Febs J* **280**, 5030–5038 (2013).
270. Barcia, C. et al. ROCK/Cdc42-mediated microglial motility and gliapse formation lead to phagocytosis of degenerating dopaminergic neurons in vivo. Sci Rep-uk 2, 809 (2012).
271. Virgone-Carlotta, A. et al. Mapping and kinetics of microglia/neuron cell-to-cell contacts in the 6-OHDA murine model of Parkinson's disease. Glia 61, 1645–1658 (2013).
272. Wijeyekoon, R. S. et al. Monocyte Function in Parkinson's Disease and the Impact of Autologous Serum on Phagocytosis. *Front Neurol* **9**, 870 (2018).
273. Markow, T. The secret lives of Drosophila flies. *Elife* **4**, e06793 (2015).
274. Sonnenfeld, M. & Jacobs, J. Apoptosis of the midline glia during Drosophila embryogenesis: a correlation with axon contact. *Development (Cambridge, England)* 569–78 (1995).
275. Tepass, U., Fessler, L., Aziz, A. & Hartenstein, V. Embryonic origin of hemocytes and their relationship to cell death in Drosophila. Development (Cambridge, England) 1829–37 (1994).
276. Pritchett, T. L., Tanner, E. A. & McCall, K. Cracking open cell death in the Drosophila ovary. Apoptosis 969 (2009) doi:**10**.1007/s10495-009-0369-z.
277. Freeman, M. R. Drosophila Central Nervous System Glia. *Csh Perspect Biol* **7**, a020552 (2015).
278. Davidson, A. J. & Wood, W. Phagocyte Responses to Cell Death in Flies. Csh Perspect Biol **12**, a036350 (2020).
279. Moreira, S., Stramer, B., Evans, I., Wood, W. & Martin, P. Prioritization of Competing Damage and Developmental Signals by Migrating Macrophages in the Drosophila Embryo. Current Biology 464–470 (2010) doi:10.1016/j.cub.2010.01.047.
280. Evans, I. R., Rodrigues, F. S. L. M., Armitage, E. L. & Wood, W. Draper/CED-1 Mediates an Ancient Damage Response to Control Inflammatory Blood Cell Migration In Vivo. Curr Biol

25, 1606–1612 (2015).
281. Davidson, A. J. & Wood, W. Macrophages Use Distinct Actin Regulators to Switch Engulfment Strategies and Ensure Phagocytic Plasticity In Vivo. Cell Reports 31, 107692 (2020).
282. Franc, N. C., Dimarcq, J.-L., Lagueux, M., Hoffmann, J. & Ezekowitz, R. A. B. Croquemort, A Novel Drosophila Hemocyte/Macrophage Receptor that Recognizes Apoptotic Cells. Immunity 431–443 (1996) doi:10.1016/S1074-7613(00)80410-0.
283. Franc, N. C., Heitzler, P., R., A. B., Ezekowitz & White, K. Requirement for Croquemort in Phagocytosis of Apoptotic Cells in Drosophila. Science 1991–1994 (1999) doi:10.1126/science.284.5422.1991.
284. Guillou, A., Troha, K., Wang, H., Franc, N. C. & Buchon, N. The Drosophila CD36 Homologue croquemort Is Required to Maintain Immune and Gut Homeostasis during Development and Aging. *PLOS Pathogens* e1005961 (2016) doi:10.1371/journal.ppat.1005961.
285. Nagaosa, K. et al. Integrin βv-mediated Phagocytosis of Apoptotic Cells in Drosophila Embryos*. Journal of Biological Chemistry 25770–25777 (2011) doi:10.1074/jbc.M110.204503.
286. Freeman, M. R., Delrow, J., Kim, J., Johnson, E. & Doe, C. Q. Unwrapping Glial Biology Gcm Target Genes Regulating Glial Development, Diversification, and Function. Neuron 567–580 (2003) doi:10.1016/S0896-6273(03)00289-7.
287. Awasaki, T. et al. Essential Role of the Apoptotic Cell Engulfment Genes draper and ced-6 in Programmed Axon Pruning during Drosophila Metamorphosis. Neuron 855–867 (2006) doi:10.1016/j.neuron.2006.04.027.
288. Roddie, H. G., Armitage, E. L., Coates, J. A., Johnston, S. A. & Evans, I. R. Simu-dependent clearance of dying cells regulates macrophage function and inflammation resolution. *PLOS Biology* **17**, e2006741 (2019).
289. Williams, D. W., Kondo, S., Krzyzanowska, A., Hiromi, Y. & Truman, J. W. Local caspase activity directs engulfment of dendrites during pruning. Nature neuroscience 9, 1234–6 (2006).
290. Ziegenfuss, J. S., Doherty, J. & Freeman, M. R. Distinct molecular pathways mediate glial activation and engulfment of axonal debris after axotomy. Nature Neuroscience 979–987 (2012) doi:10.1038/nn.3135.
291. Logan, M. A. et al. Negative regulation of glial engulfment activity by Draper terminates glial responses to axon injury. Nature Neuroscience 722–730 (2012) doi:10.1038/nn.3066.
292. Nakano, R. et al. Cortex glia clear dead young neurons via Drpr/dCed-6/Shark and Crk/Mbc/dCed-12 signaling pathways in the developing Drosophila optic lobe. Developmental Biology 68–85 (2019) doi:10.1016/j.ydbio.2019.05.003.

293. Santoso, C. S. et al. The ABC Transporter Eato Promotes Cell Clearance in the Drosophila melanogaster Ovary. *G3: Genes, Genomes, Genetics* g3.300427.2017 (2018) doi:10.1534/g3.117.300427.
294. Rogulja-Ortmann, A., Lüer, K., Seibert, J., Rickert, C. & Technau, G. M. Programmed cell death in the embryonic central nervous system of Drosophila melanogaster. Dev Camb Engl **134**, 105–16 (2007).
295. Wood, W., Faria, C. & Jacinto, A. Distinct mechanisms regulate hemocyte chemotaxis during development and wound healing in Drosophila melanogaster. J Cell Biol **173**, 405–416 (2006).
296. Bangs, P. & White, K. Regulation and execution of apoptosis during Drosophila development. *Developmental Dynamics* 68–79 (2000) doi:10.1002/(SICI)1097-0177(200005)218:1<68::AID-DVDY6>3.0.CO;2-9.
297. Defaye, A. et al. Genetic Ablation of Drosophila Phagocytes Reveals Their Contribution to Both Development and Resistance to Bacterial Infection. *Journal of Innate Immunity* 322–334 (2009) doi:10.1159/000210264.
298. Evans, I. R. & Wood, W. Understanding in vivo blood cell migration—Drosophila hemocytes lead the way: Drosophila hemocytes lead the way. *Fly* 110–114 (2011) doi:10.4161/fly.5.2.14055.
299. Cho, N. K. et al. Developmental Control of Blood Cell Migration by the Drosophila VEGF Pathway. Cell 865–876 (2002) doi:10.1016/S0092-8674(02)00676-1.
300. Weavers, H., Evans, I. R., Martin, P. & Wood, W. Corpse Engulfment Generates a Molecular Memory that Primes the Macrophage Inflammatory Response. Cell 165, 1658–71 (2016).
301. Yildirim, K., Petri, J., Kottmeier, R. & Klämbt, C. Drosophila glia: Few cell types and many conserved functions. Glia 5–26 (2019) doi:10.1002/glia.23459.
302. Etchegaray, J. et al. Defective Phagocytic Corpse Processing Results in Neurodegeneration and Can Be Rescued by TORC1 Activation. The Journal of Neuroscience 3170–3183 (2016) doi:10.1523/JNEUROSCI.1912-15.2016.
303. Hilu-Dadia, R., Hakim-Mishnaevski, K., Levy-Adam, F. & Kurant, E. Draper-mediated JNK signaling is required for glial phagocytosis of apoptotic neurons during Drosophila metamorphosis. Glia 1520–1532 (2018) doi:10.1002/glia.23322.
304. Piston, D. W. & Kremers, G.-J. Fluorescent protein FRET: the good, the bad and the ugly. *Trends Biochem Sci* **32**, 407–414 (2007).
305. Mayer, C. T. et al. The microanatomic segregation of selection by apoptosis in the germinal

center. Science 358, eaao2602 (2017).
306. Takemoto, K., Nagai, T., Miyawaki, A. & Miura, M. Spatio-temporal activation of caspase revealed by indicator that is insensitive to environmental effects. *The Journal of Cell Biology* **160**, 235–243 (2003).
307. Nicholls, S. B., Chu, J., Abbruzzese, G., Tremblay, K. D. & Hardy, J. A. Mechanism of a Genetically Encoded Dark-to-Bright Reporter for Caspase Activity. Journal of Biological Chemistry 286, 24977–24986 (2011).
308. Zhang, J. et al. Visualization of caspase-3-like activity in cells using a genetically encoded fluorescent biosensor activated by protein cleavage. Nature Communications 4, 2157 (2013).
309. Schott, S. et al. A fluorescent toolkit for spatiotemporal tracking of apoptotic cells in living Drosophila tissues. Development 144, dev.149807 (2017).
310. To, T.-L. L. et al. Rational Design of a GFP-Based Fluorogenic Caspase Reporter for Imaging Apoptosis In Vivo. *Cell chemical biology* **23**, 875–82 (2016).
311. Zhang, Q. et al. Designing a Green Fluorogenic Protease Reporter by Flipping a Beta Strand of GFP for Imaging Apoptosis in Animals. *Journal of the American Chemical Society* (2019) doi:10.1021/jacs.8b13042.
312. Ham, T. J. van, Mapes, J., Kokel, D. & Peterson, R. T. Live imaging of apoptotic cells in zebrafish. The FASEB Journal 24, 4336–4342 (2010).
313. Martínez-Lagunas, K. et al. In vivo detection of programmed cell death during mouse heart development. Cell Death Differ 1–17 (2019) doi:10.1038/s41418-019-0426-2.
314. Nasu, Y. et al. Genetically Encoded Fluorescent Probe for Imaging Apoptosis in Vivo with Spontaneous GFP Complementation. *Analytical Chemistry* **88**, 838–44 (2016).
315. Bardet, P.-L. et al. A fluorescent reporter of caspase activity for live imaging. Proc National Acad Sci 105, 13901–13905 (2008).
316. Tang, H. L., Tang, H. M., Fung, M. C. & Hardwick, J. In Vivo Biosensor Tracks Non-apoptotic Caspase Activity in Drosophila. *Journal of visualized experiments : JoVE* (2016) doi:10.3791/53992.
317. Shinoda, H., Shannon, M. & Nagai, T. Fluorescent Proteins for Investigating Biological Events in Acidic Environments. *International Journal of Molecular Sciences* **19**, 1548 (2018).
318. Tanida, I., Ueno, T. & Uchiyama, Y. A Super-Ecliptic, pHluorin-mKate2, Tandem Fluorescent Protein-Tagged Human LC3 for the Monitoring of Mammalian Autophagy. PLoS ONE 9, e110600 (2014).
319. Violot, S., Carpentier, P., Blanchoin, L. & Bourgeois, D. Reverse pH-Dependence of Chromophore Protonation Explains the Large Stokes Shift of the Red Fluorescent Protein

mKeima. Journal of the American Chemical Society **131**, 10356–10357 (2009).
320. Tantama, M., Hung, Y. & Yellen, G. Imaging Intracellular pH in Live Cells with a Genetically Encoded Red Fluorescent Protein Sensor. Journal of the American Chemical Society **133**, 10034–10037 (2011).
321. Hess, K. L., Babcock, G. F., Askew, D. S. & Cook-Mills, J. M. A novel flow cytometric method for quantifying phagocytosis of apoptotic cells. *Cytometry* 145–152 (1997) doi:10.1002/(SICI)1097-0320(19970201)27:2<145::AID-CYTO6>3.0.CO;2-F.
322. Adie, E. et al. A pH-Sensitive Fluor, CypHer TM 5, Used to Monitor Agonist-Induced G Protein-Coupled Receptor Internalization in Live Cells. *BioTechniques* 1152–1157 (2002) doi:10.2144/02335dd10.
323. Norris, G. T. et al. Neuronal integrity and complement control synaptic material clearance by microglia after CNS injury. J Exp Med jem.20172244 (2018) doi:10.1084/jem.20172244.
324. Smith, B. A. et al. In Vivo Optical Imaging of Acute Cell Death Using a Near-Infrared Fluorescent Zinc−Dipicolylamine Probe. *Molecular Pharmaceutics* 583–590 (2011) doi:10.1021/mp100395u.
325. Tufail, Y. et al. Phosphatidylserine Exposure Controls Viral Innate Immune Responses by Microglia. Neuron 574-586.e8 (2017) doi:10.1016/j.neuron.2016.12.021.
326. Kim, Y. E., Chen, J., Langen, R. & Chan, J. R. Monitoring apoptosis and neuronal degeneration by real-time detection of phosphatidylserine externalization using a polarity-sensitive indicator of viability and apoptosis. *Nature Protocols* 1396–1405 (2010) doi:10.1038/nprot.2010.101.
327. Shklyar, B., Shklover, J. & Kurant, E. Live Imaging of Apoptotic Cell Clearance during Drosophila Embryogenesis. *Journal of Visualized Experiments* (2013) doi:10.3791/50151.
328. Hu, B., Sonstein, J., Christensen, P. J., Punturieri, A. & Curtis, J. L. Deficient In Vitro and In Vivo Phagocytosis of Apoptotic T Cells by Resident Murine Alveolar Macrophages. The Journal of Immunology 2124–2133 (2000) doi:10.4049/jimmunol.165.4.2124.
329. Miksa, M., Komura, H., Wu, R., Shah, K. G. & Wang, P. A novel method to determine the engulfment of apoptotic cells by macrophages using pHrodo succinimidyl ester. *Journal of Immunological Methods* 71–77 (2009) doi:10.1016/j.jim.2008.11.019.
330. Stöhr, R., Deckers, N., Schurgers, L., Marx, N. & Reutelingsperger, C. P. AnnexinA5-pHrodo: a new molecular probe for measuring efferocytosis. Sci Rep-uk 8, 17731 (2018).
331. Esmann, L. et al. Phagocytosis of Apoptotic Cells by Neutrophil Granulocytes: Diminished Proinflammatory Neutrophil Functions in the Presence of Apoptotic Cells. The Journal of

Immunology 391–400 (2010) doi:10.4049/jimmunol.0900564.
332. Roberts, T. et al. Identification and Characterisation of a pH-stable GFP. Scientific Reports 6, 28166 (2016).
333. Wood, W. et al. Wound healing recapitulates morphogenesis in Drosophila embryos. Nat Cell Biol 4, 907–912 (2002).
334. Carmody, W. R. Easily prepared wide range buffer series. *J Chem Educ* **38**, 559 (1961).
335. Tisue, S. & Wilenski, U. NetLogo: A Simple Environment for Modeling Complexity. *International Conference on Complex Systems* (2004).
336. Galluzzi, L. et al. Molecular mechanisms of cell death: recommendations of the Nomenclature Committee on Cell Death 2018. Cell Death & Differentiation 25, 486–541 (2018).
337. Shaner, N. C. et al. Improving the photostability of bright monomeric orange and red fluorescent proteins. *Nat Methods* **5**, 545–551 (2008).
338. Liu, Z. et al. Systematic comparison of 2A peptides for cloning multi-genes in a polycistronic vector. Scientific Reports 7, 2193 (2017).
339. Abrams, J. M., White, K., Fessler, L. I. & Steller, H. Programmed cell death during Drosophila embryogenesis. Dev Camb Engl 117, 29–43 (1993).
340. Harteinstein, V. Atlas of Drosophila Development . *Cold Spring Harbor Laboratory Press* (1993).
341. Cummings, R. J. et al. Different tissue phagocytes sample apoptotic cells to direct distinct homeostasis programs. Nature 539, 565–569 (2016).
342. MARKOW, T. A., BEALL, S. & MATZKIN, L. M. Egg size, embryonic development time and ovoviviparity in Drosophila species: Ovoviviparity in Drosophila species. *J Evolution Biol* **22**, 430–434 (2008).
343. Herzog, C. et al. Rapid clearance of cellular debris by microglia limits secondary neuronal cell death after brain injury in vivo. Development 146, dev174698 (2019).
344. Chen, T.-W. et al. Ultrasensitive fluorescent proteins for imaging neuronal activity. Nature 499, 295–300 (2013).
345. Abdelfattah, A. S. et al. Bright and photostable chemigenetic indicators for extended in vivo voltage imaging. Science (New York, N.Y.) **365**, 699–704 (2019).
346. Piatkevich, K. D. et al. Population imaging of neural activity in awake behaving mice. Nature 574, 413–417 (2019).
347. Kaiser, T. & Feng, G. Tmem119-EGFP and Tmem119-CreERT2 transgenic mice for labeling and manipulating microglia. *Eneuro* **6**, ENEURO.0448-18.2019 (2019).
348. Zhang, J.-F. et al. An ultrasensitive biosensor for high-resolution kinase activity imaging in

awake mice. *Nat Chem Biol* **17**, 39–46 (2021).
349. Guilliams, M., Thierry, G. R., Bonnardel, J. & Bajenoff, M. Establishment and Maintenance of the Macrophage Niche. Immunity 52, 434–451 (2020).
350. Yurdagul, A., Doran, A. C., Cai, B., Fredman, G. & Tabas, I. A. Mechanisms and Consequences of Defective Efferocytosis in Atherosclerosis. *Frontiers in Cardiovascular Medicine* 86 (2018) doi:**10**.3389/fcvm.2017.00086.
351. Doran, A. C., Yurdagul, A. & Tabas, I. Efferocytosis in health and disease. Nature Reviews Immunology 1–14 (2019) doi:10.1038/s41577-019-0240-6.
352. Ogden, C. A. & Elkon, K. B. Role of Complement and Other Innate Immune Mechanisms in the Removal of Apoptotic Cells. Curr Dir Autoimmun 9, 120–142 (2005).
353. O'Brien, B. A. et al. A deficiency in the in vivo clearance of apoptotic cells is a feature of the NOD mouse. *J Autoimmun* **26**, 104–115 (2006).
354. Evans, I. R., Zanet, J., Wood, W. & Stramer, B. M. Live Imaging Of Drosophila melanogaster Embryonic Hemocyte Migrations. *J Vis Exp Jove* 1696 (2010) doi:10.3791/1696.
355. Boraschi, D. & Italiani, P. Innate Immune Memory: Time for Adopting a Correct Terminology. *Front Immunol* **9**, 799 (2018).
356. Aguilera-Castrejon, A. et al. Ex utero mouse embryogenesis from pre-gastrulation to late organogenesis. Nature 593, 119–124 (2021).
357. Redecke, V. et al. Hematopoietic progenitor cell lines with myeloid and lymphoid potential. Nat Methods 10, 795–803 (2013).
358. Álvarez, J.-A. & Díaz-Benjumea, F. J. Origin and specification of type II neuroblasts in the Drosophila embryo. Development dev158394 (2018) doi:10.1242/dev.158394.
359. Coates, J. A. et al. Identification of functionally distinct macrophage subpopulations in Drosophila. Elife 10, e58686 (2021).
360. Wang, G. G. et al. Quantitative production of macrophages or neutrophils ex vivo using conditional Hoxb8. Nat Methods 3, 287–293 (2006).
361. Jiang, Z., Jiang, J. X. & Zhang, G.-X. Macrophages: A double-edged sword in experimental autoimmune encephalomyelitis. *Immunology Letters* **160**, 17–22 (2014).